THE FLORIDA STATE UNIVERSITY

COLLEGE OF ARTS AND SCIENCES

AN INGREDIENTS-BASED EXAMINATION OF U.S. SEVERE TORNADO ALLEYS USING REANALYSIS DATA

By

GRAYUM VICKERS

A Master's Thesis submitted to the
College of Arts and Sciences
in partial fulfillment of the
requirements for the degree of
Master's of Science

Degree Awarded:
Summer Semester, 2012

Grayum Vickers defended this thesis on June, 1 2012.

The members of the supervisory committee were:

Eric Chassignet
Professor Directing Thesis

Robert Hart
Professor Directing Thesis

Mark Bourassa
Committee Member

The Graduate School has verified and approved the above-named committee members, and certifies that the thesis has been approved in accordance with university requirements.

This work is dedicated to all those scientists who have spent countless hours working towards the advancement of the atmospheric sciences with the overarching goal of improving forecasts and saving people's lives.

ACKNOWLEDGEMENTS

I would like to acknowledge the following people and institutions for contributions, aid and generally making this work possible: Dr. Robert Hart, Dr. Eric Chassignet, Dr. Mark Bourassa, Josh Cossuth, Dr. Pieter Groenemeijer, COAPS and the FSU Department of Earth, Ocean Atmospheric Sciences.

TABLE OF CONTENTS

LIST OF TABLES

LIST OF FIGURES

ABSTRACT

A new metric for identifying severe tornado (F3+) alleys is presented. Regions are distinguished by average F-scale values with a minimum of 15 severe tornado events within 200km. Five distinct "severe tornado alleys" are described across the United States: 1) the Carolinas, 2) "Dixie Alley," 3) Kansas and Oklahoma, 4) Iowa and Nebraska, and 5) Wisconsin, Illinois, Indiana and Michigan. These regions are evaluated using CFSR global reanalysis data to determine the presence of atmospheric variables relating to tornadogenesis (as described by prior work) in the pre-tornadic environments. Composite CFSR soundings and composite field charts are created for severe tornado events within each region. A robust comparison of pre-tornadic atmospheric conditions among regions is conducted using a Student t-test at 95% confidence.. An evaluation of the Sigtor parameter, a commonly used significant tornado forecast parameter developed by the Storm Prediction Center, is also conducted to identify regional variability. It is found that each region significantly differs at 95% confidence from each other in terms of many atmospheric variables from pre-tornadic environments, with the most significant differences existing between the two more eastern and two mid-western regions. SigTor values and the individual components, are calculated for severe tornado events and for every time-step for every grid-point within each region over a "peak severe tornado season" for U.S. severe tornadoes in order to compare the event cases to a background mean state. It is shown using linear correlations and covariances of the individual terms of the Sigtor parameter to the Sigtor value that not only is there discrepancy in Sigtor values between regions, but the different components of SigTor contribute to the value of Sigtor in different ways between regions. Some regions show background values of Sigtor terms to be favorable for tornadogenesis even when tornadoes have not occurred. Regional biases in presence of atmospheric variables preceding severe tornado events between regions are described.

CHAPTER ONE

MOTIVATION AND PREVIOUS WORK

1.1 Introduction and Motivation

As technology advances, new methods of studying tornadoes and their behavior emerge. In the past, climatological analysis of tornado occurrence could only be accomplished using sparse data from upper air observations, surface observations, and photographs. As recent as 60 years ago, no reliable record of tornado occurrence was available anywhere in the world. It wasn't until 1973 that a metric for rating tornadoes was developed. Today, with the U.S. radar network, satellites, relatively dense sounding network, reanalysis data, and most of all a reliable record of tornado occurrence and damage assessment, we are able to look at tornadoes and the climatology of tornadoes from myriad angles.

Since tornadoes have been assigned ratings via the Fujita scale, research has been done into spatial and temporal trends of strong versus weak tornadoes (Doswell and Burgess, 1988; Grazulis, 1993; Brooks and Doswell, 2000, Concannon et al. 2000). One of the goals of this work is to continue analysis of specifically strong tornadoes in the United States by using a reliable record (1979-2009) to uncover trends in spatial distribution and frequency of strong tornadoes. Using data starting in 1979 avoids many of the caveats noted by Doswell and Burgess (1988) and Broyles and Crosbie (2004) relating to population biases since these works examine the tornado record starting much earlier. Moreover, Concannon et al. (2000) and Passe-Smith (2006) include extra criteria for path length and width of the tornadoes examined to avoid said caveats. However, this limits the number of tornadoes that can be included in the study.

From work identifying trends in tornado frequency and occurrence, studies of tornadoes within specific geographic regions began to emerge in the mid 1970's and have evolved since. David (1976) and Williams (1976) both distinguished trends in presence of atmospheric variables with tornadoes in different regions. However, the definitions of the examined regions in these studies were based on coarse geographic connections and state borders. Advances in data collection have lead to more sophisticated examinations of atmospheric variables in pre-tornadic environments in different regions. Another goal of this work is to present a metric for robust identification of regions of high frequency of severe tornadoes; and hence provide better spatial boundaries for this study.

Reanalysis data has allowed tornado researchers to examine environments associated with tornadoes at finer spatial and temporal scales (Brooks et al. 2003; Gensini and Brooks, 2008). Advances in reanalysis data in terms of resolution and incorporation of observations have allowed scientists to get more realistic data from tornado environments (Tippet, 2012). Using reanalysis data, this work will focus on how atmospheric variables vary between geographic regions during and just preceding severe tornado events. Prior work has advanced our understanding of how different atmospheric variables relate to the likelihood of severe tornado events. Further, forecasting parameters have been developed using this understanding in order to benefit real-time forecasting of tornado events (Rasmussen and Blanchard, 1998; Thompson et al. 2002). Building on developments in identifying atmospheric variables which can distinguish between tornadic and non-tornadic environments, this work aims to quantify the presence of these variables and the applicability of a tornado forecast parameter within different regions of high severe tornado frequency. Differences in applicability of forecasting parameters due to regional biases can lead to misinterpretations of parameter values for severe tornado events.

1.2 Studies of Atmospheric Processes Relating to Tornadogenesis

Given the innumerable complexities involved with tornadogenesis both local to the tornado, and in the broader environment of the tornado, a look at some of the work leading to our current understanding of tornadogenesis and the atmospheric variables associated with it is warranted. While the body of research on the specific topic of this work is small, many facets of previous work on observational, numerical modeling, and reanalysis studies are utilized.

Both observation based studies and studies involving numerical models have led to our current understanding of how certain atmospheric variables relate to general convection and tornadogenesis. Lemon and Doswell (1979) presents a model of supercell interaction with different atmospheric currents (specifically updrafts and downdrafts) resulting in tornadogenesis (Fig. 1.2). Our current understanding of the roles of updrafts and downdrafts in supercells is based on this model. Markowski et al. (1998) describes how atmospheric boundaries are crucial in most cases for severe tornadogenesis. From accrued past research, Markowski and Richardson (2009) encompasses a summation of known processes involved in tornado formation. Understanding of tornadogenesis mechanisms and studies from a more ingredients perspective have evolved in tandem over the years. For example, numerous studies involving tornado proximity soundings have led to our understanding of the association of atmospheric ingredients with tornadogenesis (Schaefer and Livingston, 1988; Johns et al. 1993; Potvin et al. 2010). Numerical modeling studies like Davies-Jones et al. (2001) and Wicker and Wilhelmson (1995) and statistical modeling studies like Feuerstein et al. (2005) have also advanced toward similar ends.

From the many studies on atmospheric variables and tornadogenesis some variables have been shown to be essential for tornado formation. Johns et al. (1993) identifies convective available potential energy (CAPE) and 0-2km vertical wind shear as two variables which are associated with strong and violent tornadoes. Edwards et al. (2003) shows how parameters involving low-level moisture and vertical shear can distinguish between different classes of supercells. 0-6km vertical wind shear, specific humidity in the low levels, CAPE, and LCL (lifted condensation level) height are shown to also factor in to formation of tornadoes in an important way (Brooks et al. 2003a). Romero et al. (2005) identifies mid-troposhperic lapse rates, and helicity in the lower troposphere as crucial for tornadogenesis. CAPE, CIN, mid-troposphere lapse-rate, storm-relative helicity, and specific humidity were also used to look for temporal trends in tornadogenesis by Tippett (2012). Eventually, as understanding of atmospheric variables increased, parameters were developed to combine and weight the usefulness of certain variables as predictive entities (Rasmussen and Blanchard, 1998; Craven et al. 2002; Edwards et al. 2003).

In summary of the previous works on atmospheric processes relating to tornadogenesis, elaboration of some of the relevant variables used to approximate these processes is prudent. Specifically, the importance of LCL, CAPE, and helicity as variables which have been shown to pertain to processes relevant to the formation of tornadoes cannot be understated in this work. LCL, which is indicative of the height of the cloud base, is a crucial factor in determining whether tornadogenesis is likely to occur or not. Typically, lower values of LCL support tornadogenesis since the region of CAPE will be lower to the surface with lower values of LCL height. CAPE, as introduced earlier, is a proxy for vertical velocity in the atmosphere and a measure of instability if realized. Realized CAPE values are important indicators of an

atmosphere favorable for tornadogenesis, with higher values indicating increased instability and vertical velocity in the atmosphere. CAPE which is unrealized, or inhibited, is known as CIN. Helicity is the measure of the potential for helical flow in the atmosphere. Values of helicity are proportional to the strength of the stream-wise component of the wind, the amount of vertical wind shear, and the amount of turning in the flow as described in the tilting and twisting terms of the vorticity equation. High values of helicity in the lower levels of the atmosphere are crucial for tornadogenesis as helical motion- the vertical displacement of vorticity- describes the motion of the mesocyclone. These variables among other less complicated ones mentioned above (lapse rates, vertical wind shear, and low-level moisture) are commonly used by forecasters as indicators of the potential for tornadogenesis in certain environments (see chapter 2).

1.3 Studies Examining Tornado Alleys

Much work has been done on examining spatial and temporal trends in tornado occurrence providing the basis for our current understanding of regionalization of tornadoes in the U.S. Several limitations from these works though, are left for future examination. Kelly et al. (1978) elucidates varying spatial frequencies of strong, weak, and violent tornadoes (Fig. 1.3a) as well as describing three general regions of quasi-homogeneous geographical influences on tornado characteristics. Here, the general record of tornado occurrence up to 1978 is elucidated, yet the boundaries of these geographic regions are not robust. Further, the geographic influences on tornadogenesis are at too large a scale to be relevant to any analysis of atmospheric variables present in the pre-tornadic atmosphere. Broyles and Crosbie (2004) further identifies smaller regions of high tornado frequency (Fig. 1.3b). In that study, the occurrence of F3 and greater tornadoes is examined over the 1880-2003 period (though only those with a 25 mile and greater

track are included). The data record extending back to 1880 is unreliable (Doswell and Burgess 1988) and hence, the caveat of only including tornadoes with 25 mile and greater path lengths is implemented. While this caveat surely verifies that the tornadoes actually occurred, it forces the exclusion of F3 and greater tornadoes with paths less than 25 miles. Broyles and Crosbie (2004) begs further examination of the atmospheric conditions which drive tornadogenesis in specific regions and, moreover, leaves the definitions of tornado regions open to be modified based on specific criteria such as frequency of tornadoes of certain intensities.

Further, Brooks et al. (2003b) indentifies regional threat for tornadoes in the U.S. by examining tornado days, or a climatological record of days where a tornado has occurred (Fig. 1.3c). Brooks et al. (2003b) identifies conditions favorable for tornadogenesis in reanalysis data as compared with observations, thus permitting the identification of potential tornado environments in observation sparse regions. However, it should be noted that Brooks et al. (2003b) analyzes only a small period (1997-1999) and uses a reanalysis dataset with relatively coarse grid spacing and many known biases (see chapter 2). The use of reanalysis data to examine tornado environments is paramount to this work and the importance of such prior work will be addressed in later sections.

Other relevant prior work includes Passe-Smith (2006) which also looks at local tornado alleys, evaluating terrain and land cover as predictive parameters for severe tornadogenesis. Brooks and Doswell (2000) suggest that a discrepancy between favoring supercell tornadoes and non-supercell tornadoes exists between the mid-west United States and the Eastern United States. Finally, different regions of significant tornado occurrence are identified by Grams et al. (2011) using geographic features such as mountain ranges and seasonal trends in flow regimes as

criteria. These works contribute to the larger body of regional examination of tornado occurrence but exhibit many of the same caveats as the earlier mentioned work.

In summary, prior works relating to regionalization of tornadoes provide a solid foundation for expansion but leave several distinct limitations to be addressed; occurrence and intensity of tornadoes are not addressed in tandem, some work uses unreliable or very small data records, some work uses coarse reanalysis data, and general classification of regions is done using limited metrics. The following chapter will address each of these limitations. It is a key goal of this work to present an objective metric to identify regional maxima of tornadoes in the U.S.

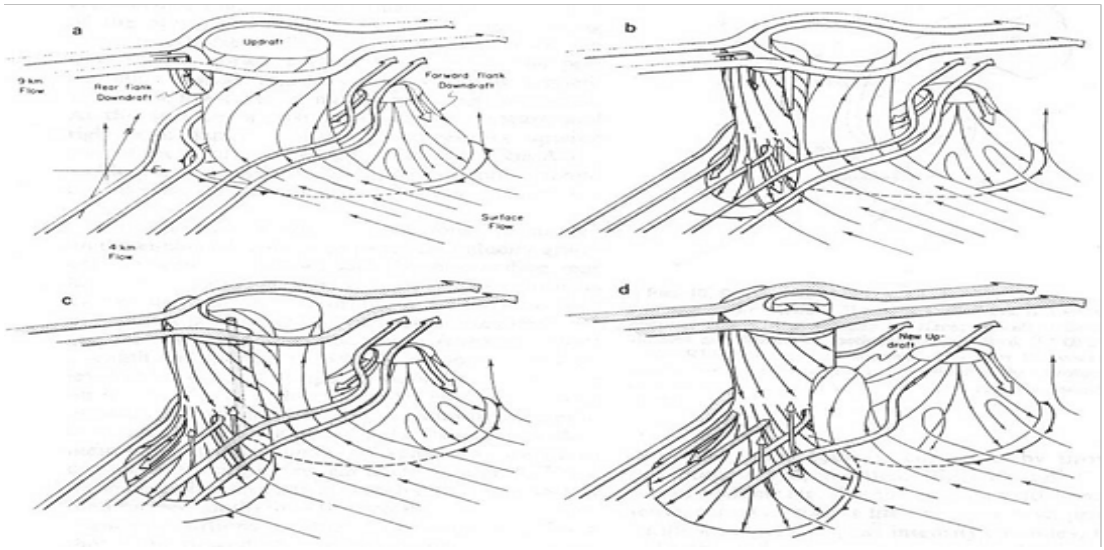

Figure 1.2: From Lemon and Doswell, (1979). Figure shows how updrafts and downdrafts relate to supercells and tornadogenesis. A-D shows the evolution of the supercell and TVS (tornado vortex signature) which id denoted by the stippling. Boundaries are denoted by frontal symbols.

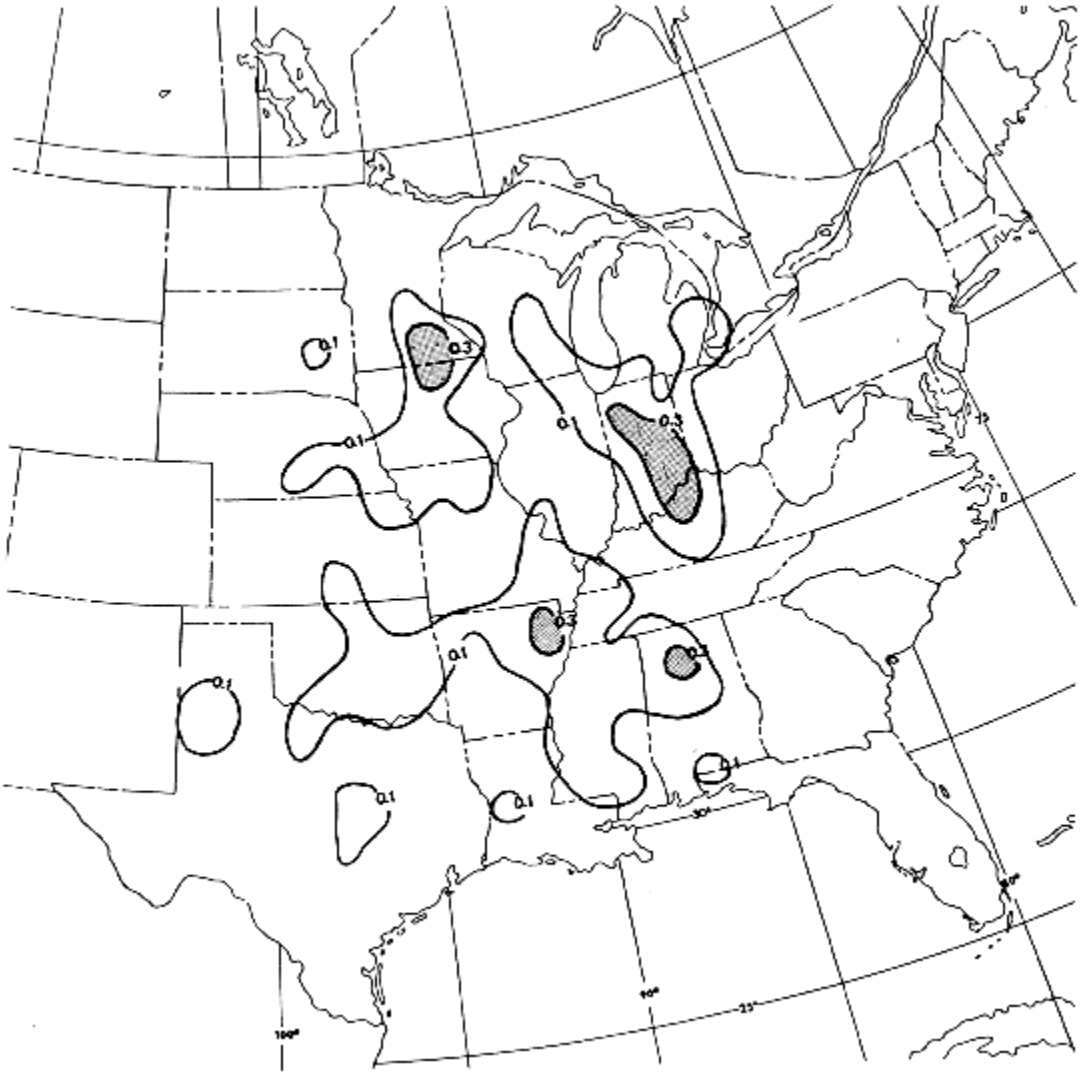

Figure 1.3a: From Kelly et al. (1978). Frequency per 2º overlapping square for (a) weak, (b) strong and (c) violent tornadoes normalized to 10,000 sq. mi area per year (1950-76).

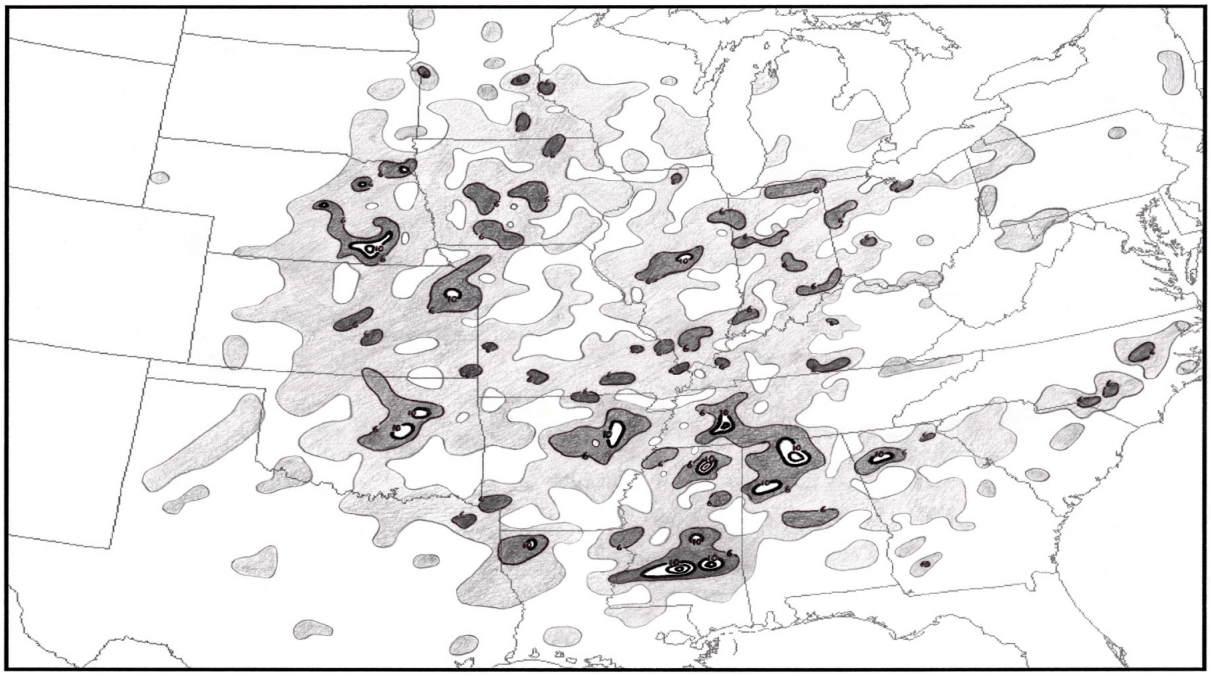

Figure 1.3b: From Broyles and Crosby (2004). A map showing the frequency of F3 to F5 tornadoes with at least 25 mile tracks from 1880 to 2003 normalized to 1,000 square miles. Contours are 2, 6, 10, 14 and 18

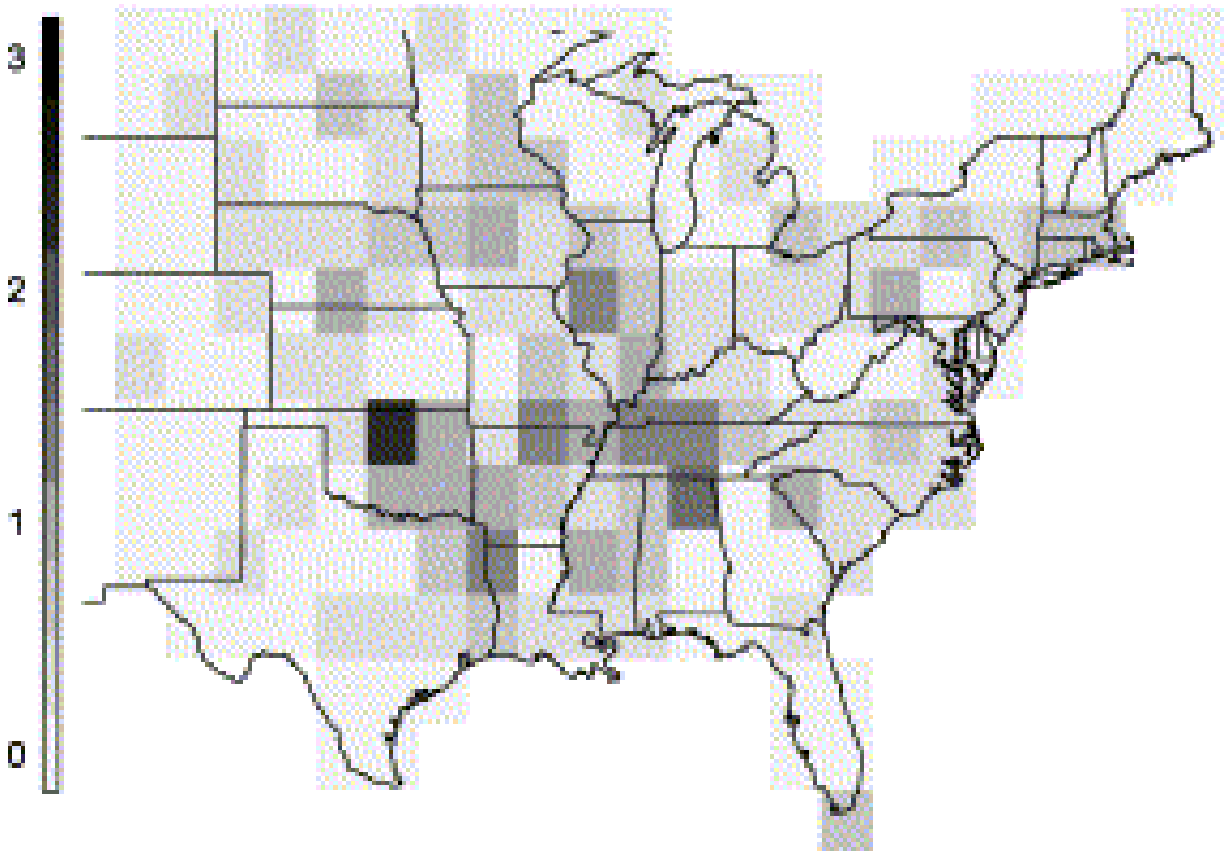

Figure 1.3c: From Brooks et al. (2003). Number of reanalysis soundings associated with significant Tornadoes in US, based on 1997–1999 period.

CHAPTER TWO

DATA AND METHODOLOGY

2.1 The SPC Tornado Dataset

Tornado events in the United States are officially recognized only through the National Climatic Data Center's (NCDC) *Storm Data* publication. However, this tornado data is not recorded for entire tornado events, rather by county segments of the tornado tracks. The Storm Prediction Center (SPC) has repackaged this data into a different dataset which is centered on individual tornado events and not county-specific. As this work focuses on individual tornadoes, the SPC dataset is as the basis for tornado data in this work. SPC tornado data includes every verified tornado from 1950-present and features the event date, approximate latitude and longitude of touchdown and liftoff/dissipation, path length and width, F/EF scale ranking, and various other fields such as loss of life and property damage (Shaefer and Edwards, 1999).

Many caveats exist in tornado data collection and assessment. In-situ data is virtually non-existent for tornadoes due to their extremely violent and ephemeral nature. Further, in order for a tornado to be reported and included in a dataset it must either be witnessed by a human or indicated on radar and have its path subsequently examined. This issue raises the problem of unreported tornadoes. This is a problem which becomes increasingly less important as population density increases in tornado-prone areas and tornado awareness amongst citizens increases. Doswell and Burgess (1988) have also documented problems with under reporting of tornadoes. Although it is possible that some tornadoes in the United States to this day go undocumented and unreported, these are likely to be insignificant in number (Doswell and Burgess, 1988). Moreover, any tornadoes that are unreported are likely to be very weak and/or

short-lived since any damage caused by it would have to go unnoticed or mistaken for straight-line wind damage (Grazulis, 1993).

Another important facet of tornado data is the intensity classification of the tornado. A tornado is ranked posthumously by the magnitude of the damage done in its path as prescribed by the Enhanced-Fujita (EF) scale which was modified from the original Fujita (F) scale in 2007 (National Weather Service, 2006). The EF-scale ranks tornadoes from 0 to 5 with 0 being the least destructive and 5 being the most destructive. Table 2.1 shows the breakdown of estimated wind speed according to the original F-scale. Also included in Table 2.1 is a description of typical damage associated with such events. It is a common misconception that tornadoes are ranked by their maximum wind speed when, in fact, the winds in a tornado are only estimated by the severity of damage caused (Brooks and Doswell, 2000). Some tornadoes have path lengths of several miles and path widths of a mile or more. At different points along a tornado's path it may strengthen or weaken, resulting in different EF scale damage along a single path. Given these potential problems, incorrect ranking of tornado events can also be a concern in tornado datasets (Brooks and Doswell, 2000). However, the National Weather Service tornado damage assessment teams in the United States in recent years have yielded what can be considered the best available estimate of tornado damage assessment. Note that in many other countries which experience tornadoes, these issues are drastically more problematic (Dotzek, 2000).

2.2 Focus on Severe Tornado Events

Only EF3 and higher ranked tornadoes are examined in this work, and while this has the caveat of eliminating a significant portion (about 85%) of the available tornado dataset, there are several benefits that lend weight to a more focused study. The primary reason that EF3 and

higher tornadoes were chosen to be the focus of this work is that these tornadoes, despite being the fewest in frequency, account for the majority of loss of life and property damages. Because these tornadoes have, in that sense, the biggest impact on human life, it follows that exclusive studies of them are beneficial. Further, any improvements in understanding, and thus forecasting, of these specific types of tornado events is the most likely to prevent loss of life. Figure 2.2 shows the percent of tornado related deaths from 1950 to 1994 broken down by weak (F0-F1), strong (F2-F3), and violent (F4-F5) tornadoes. It can clearly be seen that severe tornadoes cause the overwhelming majority of loss of life.

Another reason for choosing to exclusively look at "severe" tornadoes (EF3 and stronger) relates to the previous section where the possibility of missing tornado data is discussed. In the SPC tornado dataset EF3 and greater tornadoes are the least likely to have been missed since they leave the most damage, even to forested areas. This follows the metric of Passe-Smith (2006) and Broyles and Crosbie (2004). Also, according to the criteria for damage assessment in the Enhanced Fujita scale, EF3 is the threshold at which structures begin to be destroyed. Therefore any severe tornado is unlikely to be ranked lower than EF3 when this type of damage occurs.

Furthermore, focusing on only EF3 and greater tornadoes guarantees that the tornadoes being studied were originated in mesocyclones. While tornadoes which have been spawned from mesocyclones can do any amount of damage, and therefore be associated with any rank on the damage scale. A non-mesocyclone tornado has never been observed to do EF3 or greater damage (Wakimoto and Wilson, 1989). Though it is also uncommon, tornadoes not originating from mesocyclonic systems have done EF2 damage (Wakimoto and Wilson, 1989). The reason why looking at only mesocyclone tornadoes is specifically useful in this work is that tornado

environments are examined using reanalysis data (chapter 3.3) which has too course a resolution to see actual tornadoes but should be able to resolve to meso-beta scale, which is the scale at which supercells (thunderstorms with mesocyclones) exist. Hence, it is insured that all tornado environments examined in this work are well reported to the reanalysis data.

2.3 CFSR Data

The National Centers for Environmental Prediction's (NCEP) Climate Forecast System Reanalysis (CFSR) is utilized to examine atmospheric environments associated with the tornado events in the SPC dataset. CFSR is the sequel to the NCEP/NCAR (National Center for Atmospheric Research) reanalysis versions 1 and 2 or R1 and R2 for short (Saha et al. 2010). The older R1 and R2 cover a period from 1948 through 2002 at a global horizontal resolution of approximately 210km and a 6 hour temporal resolution. CFSR spans the period 1979 through 2009 with a global horizontal resolution of approximately 38km and a temporal resolution of 6 hours. Some of the main reasons for CFSR's genesis were to establish initial conditions for NCEP's CFS version 2 model as well as to correct many known errors and biases in the previous reanalysis packages. CFSR is unique in its incorporation of raw observed satellite radiances, which is why it begins in 1979 – the modern satellite era. The atmospheric component of CFSR is the NCEP Global Forecast System which has vertical sigma-pressure hybrid coordinate with 64 atmospheric levels up to 0.266hPa (Saha et al. 2010).

It is important to note here that the main caveat in using reanalysis data is that reanalysis is not observations; reanalysis data is a synthesis of observations and short-term model forecasts. Brooks et al. (2003b) and Lee (2002) have demonstrated the usefulness of using reanalysis data for the study of the atmospheric environments of tornado events. Typically the atmospheric

conditions of tornado events are assessed with proximity soundings, or soundings from weather stations which lie in close proximity to the area in which the tornado occurred (Craven, 2001). However, the advent of reanalysis datasets allows for the possibly of obtaining data at a much closer proximity to tornadoes. These studies utilize the NCEP/NCAR reanalysis (hereafter NNR) data to create CFSR-proximity soundings (soundings created from reanalysis) and to show that reanalysis can provide a good approximation of important atmospheric variables germane to tornadogenesis. With the increased spatial and temporal resolution of the CFSR it may be possible to obtain more accurate representations of these same environments and variables.

Kounkou et al. (2009) also used NNR as well the ERA-40 reanalysis (created by the European Center for Medium-range Weather Forecasting) to examine tornado environments, and to create a climatology for tornadoes over southern Australia. Gensini and Brooks (2008) show that reanalysis data is also useful in elucidating deep wind shear and CAPE environments in different global regions. These two studies provide precedence to some of the methodology of this work, namely to use reanalysis data to compare pre-tornadic atmospheric conditions in regions of severe tornado maxima. Using CFSR, with its many improvements, in place of NNR though is likely to provide a more accurate depiction of the environmental conditions of tornado events.

Toward examining the advantages of CFSR over NNR, Higgins et al. (2010) shows that CFSR does a better job than NNR in capturing spatial details and magnitudes of daily precipitation data. While tornado events are certainly not always associated with precipitation, they often are, and it follows that a better representation of precipitation weather systems would overlap somewhat with a better representation of tornadic systems. Lileo and Petrik (2010) demonstrates how CFSR better represents observed wind data at various heights in the lower

atmosphere compared to NNR. Winds in the lowest parts of the atmosphere are crucial for tornadogenesis and therefore CFSR should better be able to see this aspect of tornado formation as opposed to the NNR.

One study by Tippet et al. (2012) specifically uses CFSR in examining environmental parameters associated with tornadogenesis such as storm-relative helicity (SRH), CAPE, and convective inhibition (CIN) with the goal of associating these reanalysis parameters with tornado occurrence. The spatial compositing of data, as well as demonstrated in Brooks et al. (2003a), is similar to that done in the following chapters. While using the CFSR for atmospheric analysis comes with the caveat of having to begin the data set in 1979, this may actually serve as an advantage since as time increases, the reliability of tornado data sets also increases. It is more likely that any years with incomplete tornado data would fall in the older portions of the SPC dataset.

2.4.1 Severe Tornado Alleys

As mentioned earlier, this work aims to identify and compare U.S. regions of high occurrence of EF3 and stronger tornadoes or "severe tornado alleys." First, a metric must be established to classify a region as a severe tornado alley. From the limitations of prior work identified in chapter 1, it follows that determining regions of high severe tornado occurrence should involve plots of actual occurrence in tandem with plots of intensity. Further, any regional analysis should incorporate and be limited to a reliable data record (see earlier in chapter 2) and the metric of classification should be objective and well defined. Considering these factors, determining of severe tornado alleys is accomplished in two approaches: the first examining

occurrence of F3 and greater tornadoes, and the second examining average intensity of tornadoes.

The first approach in determining severe tornado alleys is to examine plots of tornado occurrence. Figure 2.4.1a shows every F2 (since the EF scale was not adopted until 2007, tornadoes will hereafter be generalized with the F-scale and not the EF-scale unless specifically applicable) and higher tornado touchdown point which has occurred in the U.S. over the 1979-2009 period. Note that this specific record length is different from those in previous works, and is somewhat biased to large outbreaks which have occurred over that period. In order to determine information about the pre-tornadic atmosphere, the area where the tornadoes originate is the most important to consider. From this figure it is clear that severe tornadoes can occur in a wide range of areas of the United States.

Occurrence of F3 and greater tornadoes within 200km is shaded over the 1979-2009 period (Fig. 2.4.1b). Several areas stand out as maxima of severe tornado frequency. The reason for using the 200km threshold is that since severe tornadoes do not often occur in close proximity to each other, a radius this large is necessary to visualize trends on a plot. Figure 2.4.1c is similar to this figure but instead shows only F4 and greater tornado frequency. It can be seen that while the frequency of tornadoes in fig 2.4.1c is reduced compared to fig 2.4.1b, the local maxima are generally collocated meaning that these areas are not spatially biased by large numbers of only F3 tornadoes. The reduction in frequency is to be expected since F4 and F5 tornadoes are exceedingly less common than F3 tornadoes. There are several areas in this figure where more than five, in a few areas more than eight, tornadoes of F4 or F5 have touched down per 200km which is anomalously high against the rest of the United States.

Plots of the density of tornado touchdowns though, do not lend insight into the average intensity of tornadoes which have occurred in a specific area. For this reason, approach 2 examines average intensity (F-scale) of severe tornadoes. Figure 2.4.1d is a graph of the number of tornadoes in the U.S. F3 and greater from 1979 to 2009. Here, we can see that the large majority of these tornadoes are F3 tornadoes, with a small percentage of the total number being F4 and an even smaller percentage being F5. This should lead us to conclude that any areas which experience higher percentages of F4 and F5 tornadoes to F3 tornadoes are apart from the norm for the U.S. Figure 2.4.1e shows the average F-scale value of tornadoes equal to or above the threshold of F3. Data in this figure is only plotted when there are more than 15 F3 and greater tornadoes per 200km area. These criteria were chosen in order to be consistent with figures 2.4.1b and 2.4.1c. Here, we observe that the local maxima are still relatively collocated with those in figures 2.4.1b and 2.4.1c, although with the magnitudes of the maxima diminished slightly in some regions such as near Tennessee and slightly greater in other areas such as near Chicago. The largest average F-scale value is 3.45 near South-central Iowa and near Chicago, while some areas have values of only F3. In other words, these latter areas have experienced near zero F4 or F5 tornadoes over the past 30 years even though they have experienced at least 15 F3 tornado events. Further, the regions which have higher average F-scale values of F3 and greater tornadoes experience a significant number of severe tornado events on the higher end of the F-scale as F4s or F5s.

It is important to note here that areas in figure 2.4.1e which are mostly purple (value of 3) have high occurrence of F3 tornadoes but have zero or close to zero cases of F4 or F5 tornadoes. On the other hand, regions like parts of Wisconsin and Iowa, which are pink (values of 3.45) have not only a high occurrence of severe tornadoes, but experience almost as many F4s and F5s

as F3s. Regions such as these are well above the mean average F-scale of severe tornadoes for the U.S.

For the entire United States over the 30 year period the average F-scale value for F3 and greater tornadoes is 3.186 which suggest 1 F4 or F5 for every 5 F3s on average. Figure 2.4.1f shows this value contoured over the U.S. and it becomes clear that several regions stick out as being well above normal for tornado intensity. These regions experience a high number of severe tornado events and they also experience a higher than average number of these events in the violent tornado class (F4 and F5). It is that criterion that serves as the metric for identifying severe tornado alleys in this work. Five such regions which are either within closed contours, or within contours that are almost cut-off, and which also possess strong local maxima of tornado count and intensity are apparent and thus boxed in figure 2.4.1g. The dimensions of the boxes encapsulating the regions of local maxima are slightly larger than the exact contours, partly to account for spatial biases in the plotting criteria and partly to include some areas known to have experienced relatively high volumes of violent tornadoes just prior to the 30 year period chosen. It is possible that some of the regions examined as distinct are in fact indistinct in terms of pre-tornadic atmospheric environments (see chapter 4).

2.4.2 Description of Chosen Regions

In order to visualize the regions examined in this work, it is important to give some background information and to describe some characteristics of each region. Details about the number of events in each region and the specific boundaries will be provided in this section.

Region 1 contains portions of North Carolina, and South Carolina primarily between the Appalachian Mountains and the Atlantic coast; this area is also known as the Piedmont and will

be referred to hereafter as such. The Piedmont region has a maximum average F-scale value of 3.4 and is the geographically smallest of the chosen regions. Also, this region has the least number of severe tornado events (48). It should be noted that this region is not typically part of popular notions for "tornado alleys" which is ironic considering that the Piedmont region has one of the highest average tornado intensities for severe tornado events in the U.S (Fig 2.4.1e)

Moving west, region 2 is roughly the same area that popular nomenclature refers to as "Dixie Alley" which consists of portions of Alabama, Mississippi, Arkansas, Louisiana, Tennessee, and in this case, extreme southern Missouri, Illinois, and Kentucky. This region will hereafter be known as the Dixie Alley region. This Dixie Alley region is both the largest in area and contains the largest number of events of all the regions (256). One caveat of the size of this region is the inclusion of portions of Southern Mississippi which, in this dataset does not stand out as relatively high in average F-scale, but is commonly known as being the location of a significant portion of known violent U.S. tornadoes on record. Southern Mississippi is the only known historically significant region which is not manifest as above average in this 30 year period, and is thus included within the Dixie Alley region. Moreover this area while not standing out in average F-scale does have a local maximum in frequency of both F3 and F4 tornadoes. Again, this is the only local maximum to not be collocated with a local maximum in average F-scale; reasons for the absence of F5 tornadoes in this area over the 30 year period is beyond the scope of this study but worthy of future work.

Central Kansas and Oklahoma comprise region three in what is commonly known as the heart of the world famous "tornado alley." As this misleading title does not suit the goals of this study it will be referred to from here on as the K/O region for Kansas and Oklahoma. The K/O region is the home to the majority of study on tornadoes of all kinds. Prior work on

tornadogenesis and atmospheric conditions in this region creates a large body of material for comparison with other regions in later chapters. It should also be mentioned that this region is home to the most powerful tornado on record, the May 3rd, 1999 F5 which tracked near Norman, Oklahoma. Fortunately this event is part of the dataset for this work and the environmental conditions responsible for its creation factor into the rest of the data. The number of events in the K/O region is 187.

Region 4 is comprised of almost the entire state of Iowa, Eastern Nebraska, extreme Northern Missouri, Southern Minnesota, and western Wisconsin and has 128 events. For simplicity it will be hereafter referred to as the Iowa region. Severe tornadoes in the Iowa region are also extremely well documented. As mentioned earlier, it is possible- due to the geographical proximity of the local maxima and relative homogeneity of terrain- that this region may not necessarily be independent of the K/O region in terms of pre-tornadic atmospheric conditions.

Region 5 is made up of Much of Illinois, Wisconsin, and Indiana and has a peak near the city of Chicago. Relating to its proximity to the Great Lakes, it will be from here on known as the Great Lakes region. The Great Lakes region is the second smallest in number of events at 78 total severe tornadoes. While this area is not as well known for its prominence of severe tornadic activity, the maximum of average F-scale in this region is the largest of all the other regions (Fig. 2.4.1e). Apart from these five regions there are two other semi-closed regions in figure 2.4.1g: one in Western Pennsylvania, and another in central Texas. Due to very small comparative sample sizes of severe tornado events, these regions were not chosen as focus areas for this work. However, is possible that similar analysis could be effectively applied to these regions given a larger dataset.

2.5 Methods of Analysis

A main goal in this study is to assess pre-tornadic atmospheric conditions in these regions for severe tornado events and to perform a comparison in order to elucidate possible significant differences in the presence of key convective and dynamic variables. Toward accomplishing this goal several methods are utilized in the following chapters. Skew-T plots derived from CFSR data are one lens through which a comparison can be viewed. For every F3+ tornado event in each region the skew-Ts are calculated at the closest possible grid point at the closest synoptic time (0000, 0600, 1200, 1800) preceding the initial reported tornado touchdown. Given the temporal resolution of the reanalysis data, the maximum error in time is just less than 6 hours. If instead the sounding was calculated at the closest synoptic time either before or after the event, the maximum error would be only approximately three hours. However, it is beneficial to hold the criteria for closest synoptic time preceding the event in order to remove the possibility of large biases in atmospheric variables due to extremely quick moving systems or frontal passages. Since many tornadoes are often shortly anteceded by passages of fronts, this would seem to be a sound condition. Also, even with a maximum temporal error of approximately 6 hours, this is much less than the maximum error of observed soundings which is around 12 hours (except for rare instances when they are 6 hourly). The main use of these CFSR soundings is to observe the vertical structure of pre-tornadic environments with respect to vertical wind profiles, and features of temperature and dew points at various levels. Although CAPE, helicity, CIN and other relevant variables may also be derived from the CFSR soundings, these variables are in the CFSR data which will be utilized instead for the statistical analysis portion of this work.

Hodographs are computed along with the skew-Ts following the same protocol for using the closest synoptic time preceding the event and the closest grid point. Hodographs are used for

examining the key kinematic aspects from the wind profile of an atmospheric sounding. The particular pertinence to tornadoes is that hodographs enable an examination of helicity and the cyclonic tendencies of the atmosphere. On the hodograph, points are plotted from the surface upward at increasing heights; the angle reflects the direction of the wind and the length of the vector specifies the speed. When a hodograph curves counterclockwise, anti-cyclonic storms are favored, while a clockwise curvature favors cyclonic storms. Since the vast majority of tornadoes are cyclonic, this is relevant. It is especially useful to examine this condition in the lowest kilometers of the atmosphere, where tornadogenesis occurs.

A skew-T chart with accompanying hodograph is plotted for each severe tornado event in each of the specified regions. All of the fields within the reanalysis data which are used to compute the skew-Ts and hodographs within a single region are averaged and a composited skew-t and hodograph are created to picture typical pre-tornadic atmosphere in that region. Compositing the skew-Ts and hodographs with estimates of variability allows for a concise, comparable representation of the local atmosphere. It is important to mention here that all compositing in this work assumes that tornado events are independent of each other. However, this is not reality since some tornadoes may have occurred close to the same grid point, meaning that multiple tornadoes could provide the same data to the calculations multiple times. It is rare though, for tornadoes of F3 and greater intensity to occur very close to each other in space and time.

Following Brooks et al. (2003a), individual variables relevant to tornadogenesis (as specified in chapter 1.2) are composited in order to elucidate what the typical presence of each variable is in each region prior to a severe tornado event. Specifically, the variables examined in this manner are: surface based CAPE, 0-1km helicity, vertical wind shear at various levels,

specific humidity at various levels, LCL height, wind speed and direction at various levels, lapse rates at various levels, surface parcel CIN, and pressure at various levels (see chapter 1). For every event, each variable is temporally composited as a field over the entire region and plotted. Further, the values of each variable at the closest grid point to the tornado touchdown point are also taken for statistical analysis purposes detailed in the next section. This method of compositing fields and specific points leads to a partial picture of the both thermodynamic and dynamic conditions present in the typical pre-tornadic atmosphere in each region.

Another analysis tool used in this work is composited surface analysis charts calculated from reanalysis data. These charts are similar to the surface analysis charts commonly used in forecasting and show the 10m above ground winds, temperature, dew point, and pressure. Instead of data being plotted at weather stations as is done in forecasting, data is plotted at each reanalysis grid point, resulting in much finer resolution compared to analysis based only on upper-air observations. One of the main uses in surface analysis is to observe the passing of synoptic and meso-scale features, specifically those that would be useful in providing convective triggers such as drylines and other fronts. For this reason, the composite surface analysis charts are plotted not just at the closest synoptic time to the tornado event, but for several time steps leading up to the event to better observe the motions of said features. Analysis of fronts is conducted by hand from the composited surface analysis charts.

2.6 SigTor Parameter

The Significant Tornado Parameter (STP or SigTor) was developed by the Storm Prediction Center (SPC) as a tool in the efforts to discriminate between storms with the potential to produce significant tornadoes (F2 and greater) and those which do not have that potential

(Thompson et al. 2002). Another parameter, the Supercell Composite Parameter (SCP), was developed in tandem with STP with a similar aim of distinguishing between areas with potential for supercell development and those without that potential. Other parameters which preceded the development of STP such as the Energy-Helicity Index (Hart and Korotky, 1990) serve as part of the foundation for STP. Previous works including Markowski et al. (1998) identify which specific variables or "ingredients" pertain specifically to storm environments producing significant tornadoes. Much work has been conducted toward distinguishing which atmospheric variables are relevant to distinguish tornadic conditions from normal thunderstorm conditions (Rasmussen and Blanchard, 1998; Thompson et al. 2003). The development and integration of STP as a tool for operational forecasting of such storms is an attempt to combine all previously identified instability, wind shear, and moisture parameters into a concise, usable tool. Originally, STP was computed as follows:

Equation 1: STP = (MLCAPE / 1000 J kg^{-1}) * (0-6 km vector shear / 20m s^{-1}) * (0-1 km SRH / 100 m^2s^{-2}) * ((2000 - MLLCL) /1500m) * ((150 - MLCIN) / 125 J kg^{-1}

Where MLCAPE denotes the lowest 100mb mean parcel CAPE (CAPE in the lowest 100mb of the sounding from the ascent of the parcel), SRH is Storm-Relative Helicity, MLLCL is Mixed Layer Lifted Condensation Level, and MLCIN is Mixed Layer CIN. The MLCAPE and 0-6km vector shear terms serve as the supercell components of the parameter and the SRH and MLLCL terms are the tornado components. The MLCIN term is used to limit false positives and narrow the area of significant tornadic potential (Thompson et al. 2002). Inclusion of MLCIN is not always part of operational use of STP.

Since the original development of STP in 2002, it has been continuously updated and refined. Previous work has added much to our understanding on the performance of severe-predictive parameters (Rasmussen, 2003; Edwards et al. 2003; Craven and Brooks, 2002).

Currently there are two versions of the STP which are in use: the SigTor(CIN) and SigTor(Fixed). The difference between the two versions is that SigTor(CIN) incorporates effective layer values of atmospheric variables and SigTor(Fixed) does not. This study uses SigTor(Fixed) for the reason that its formulation uses more of the raw variables from the CFSR data rather than having to calculate effective layer values from a coarser than observed vertical profile. SigTor(Fixed) is calculated as such:

Equation 2: SigTor(Fixed)=(sbCAPE/1500J/kg)*(0-1kmSRH/150m^2/s^2)*(0-6km BWD/12m/s)*((2000-mlLCL)/1000)

The use of SigTor(Fixed) (from now on, "STF") allows for a look at how regional differences in forecast parameter tendencies could affect actual operational forecasts of severe tornado events. As stated in chapter 1, one of the main aims of this study is to examine how regional fluctuations of specific variables in such a parameter could result in biases in the typical magnitudes of the parameter between severe tornado alleys. STF is designed to evaluate potential for the development of F2 and greater tornadoes; given that the dataset used in this work includes only F3 and greater tornadoes, STF should be applicable to all these events. It should be noted though that the equation could possibly have been different if it was intended to exclude F2 tornadoes as well.

2.7 Statistical Analysis Methods

Toward understanding differences in pre-tornadic atmospheric conditions between regions, a specific analysis of atmospheric variables within the reanalysis data is conducted. The variables examined are 0-100km helicity, vertical wind shear (925-850mb, 850-700mb, 925-700mb), specific humidity at 925, 850, 700 and 500mb, lapse rates across various layers, CIN,

and surface-based CAPE. Each variable is taken from reanalysis at the closest synoptic time preceding the tornado event at the closest grid point. In order to analyze these variables, a Student T-test is performed. The steps in conducting said test are as follows: first the variance and mean of the sample are calculated, second the standard deviation and standard error are calculated, and finally a confidence interval (CI) is determined. For this study a threshold of 95% is chosen to represent statistically significant differences in the data. In order to achieve a confidence interval at 95% significant difference a coefficient of 1.96 must be used in the formula

Equation 3: CI = mean ± (1.96)*standard error

Once, the confidence interval is established, the variables are compared to those in other regions to determine if significant differences exist. Significant differences at 95% confidence exist between two regions if there is overlap of CIs. Looking at certain variables over multiple atmospheric layers enables us to see if specific layers of the atmosphere stand out as having more significant differences than others, in order to identify a layer which may have crucial or unique features within a region.

Another way differences between the pre-tornadic environments regions can be evaluated is to quantify variances in the components of STF (see above). This method also has potential impact on forecast application if different regions have STF values that vary more or less with certain variables. For each region, STF and each of the variables within are calculated from the reanalysis data for every time step for every year in the dataset over a "peak season". Then, this analysis is performed at the lat/lon locations of every tornado touchdown with a specific region. The peak season is derived from performing a CI calculation, as described above, for the Julian days of every tornado event within all of the focus regions. The CI acts as the limits of the peak season. Here, it is found to be May 7th through May 22nd 1979-2009. Comparing atmospheric

conditions in the peak season analysis to atmospheric conditions in the analysis of the actual tornado events allows a look at how the atmosphere differs for the events and a mean atmospheric state. Covariances between each term in the STF equation are calculated and linear correlations between STF values and each variable in the STF equation are also calculated. Using covariance in this fashion allows us to examine how the individual terms in STF vary with STF values and to examine the tendency of that relationship to be linear. Hence, we will be able to see if any terms in STF effect to value of STF more than other terms. Also, we will be able to determine if there is a linear relationship between any of the terms in STF and STF values. This procedure is repeated for only the closest synoptic time step preceding and at the closest grid-point to, the event in order to examine how covariances and correlations of each to STF change during severe tornado events.

Scale	Wind Estimate (mph)	Damage
F0	<73	Light
F1	73-112	Moderate
F2	113-157	Considerable
F3	158-206	Severe
F4	207-260	Devastating
F5	261-318	Total

Table 2.1: The Fujita Scale. F-Scale rank (left), estimated wind speed (center), and damage description (right).

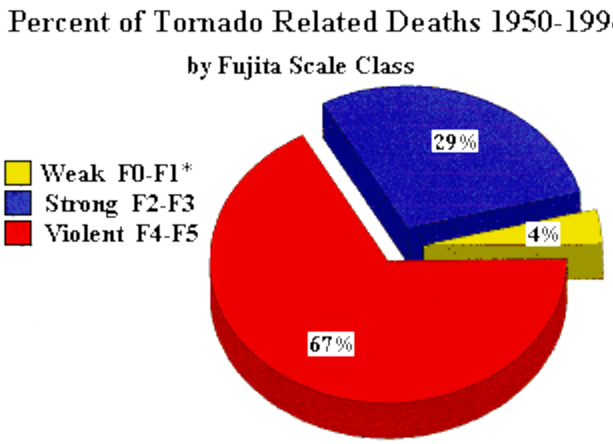

Figure 2.2: From www.tornadoproject.com. Percent of tornado related deaths broken down by classification.

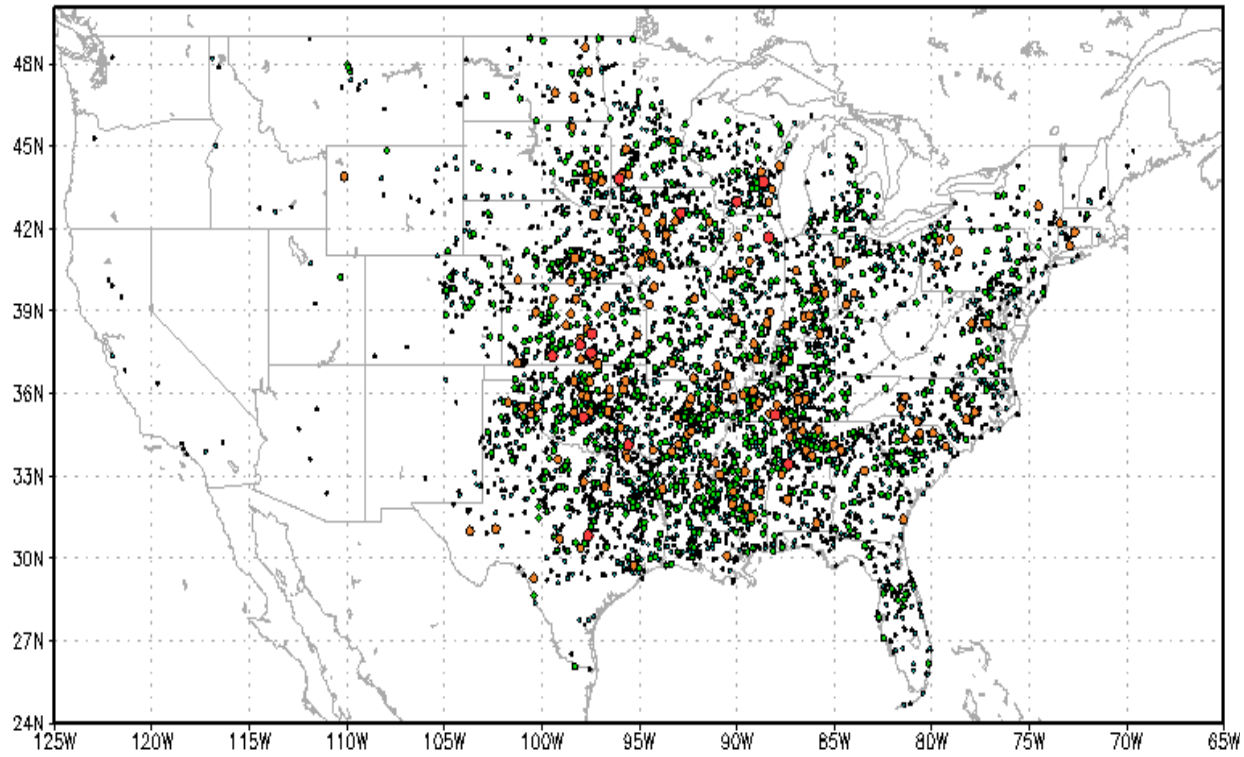

Figure 2.4.1a: Showing tornado touchdown point 1979-2009 of F2 (blue dots), F3 (green dots), F4 (orange dots), and F5 (red dots).

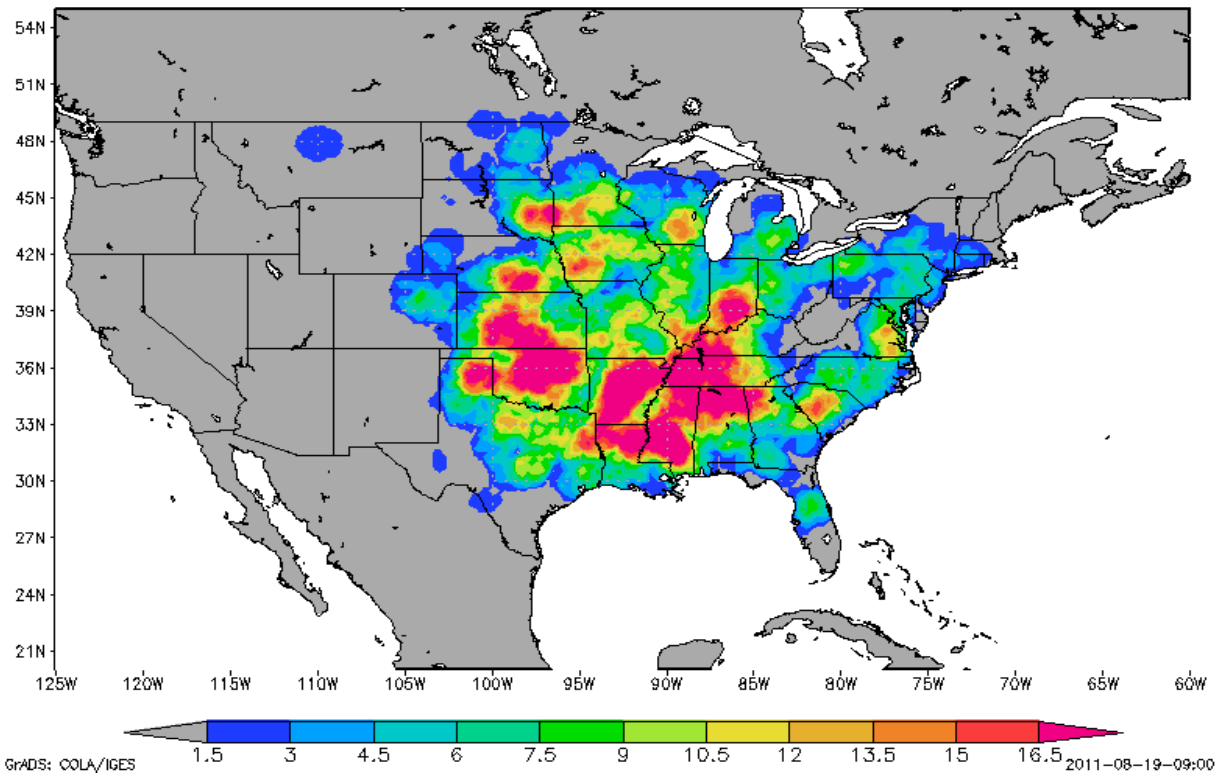

Figure 2.4.1b: F3+ tornado frequency 1979-2009. Maximums are noticeable over Kansas/Oklahoma, much of the south-east, parts of Nebraska, Iowa, South Dakota, Indiana, and South Carolina,

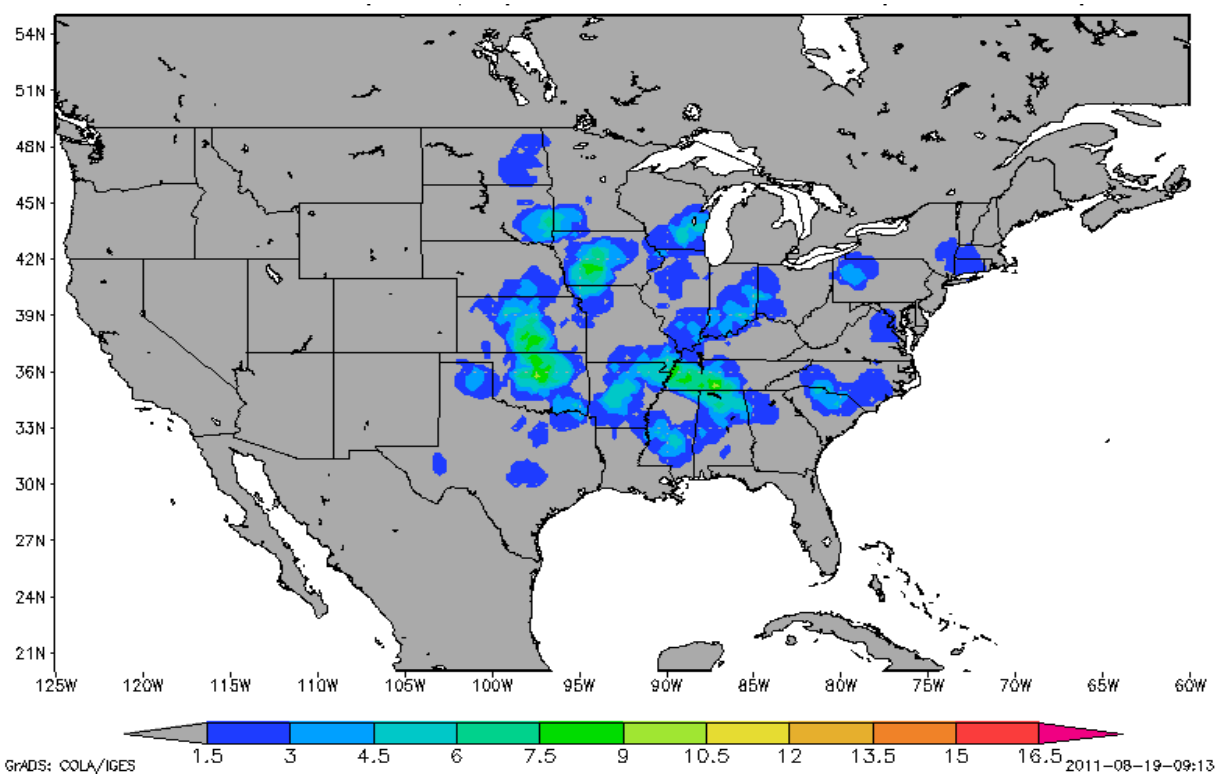

Figure 2.4.1c: As in 2.4.1b but for F4+ tornadoes. General locations of local maximums remain the same.

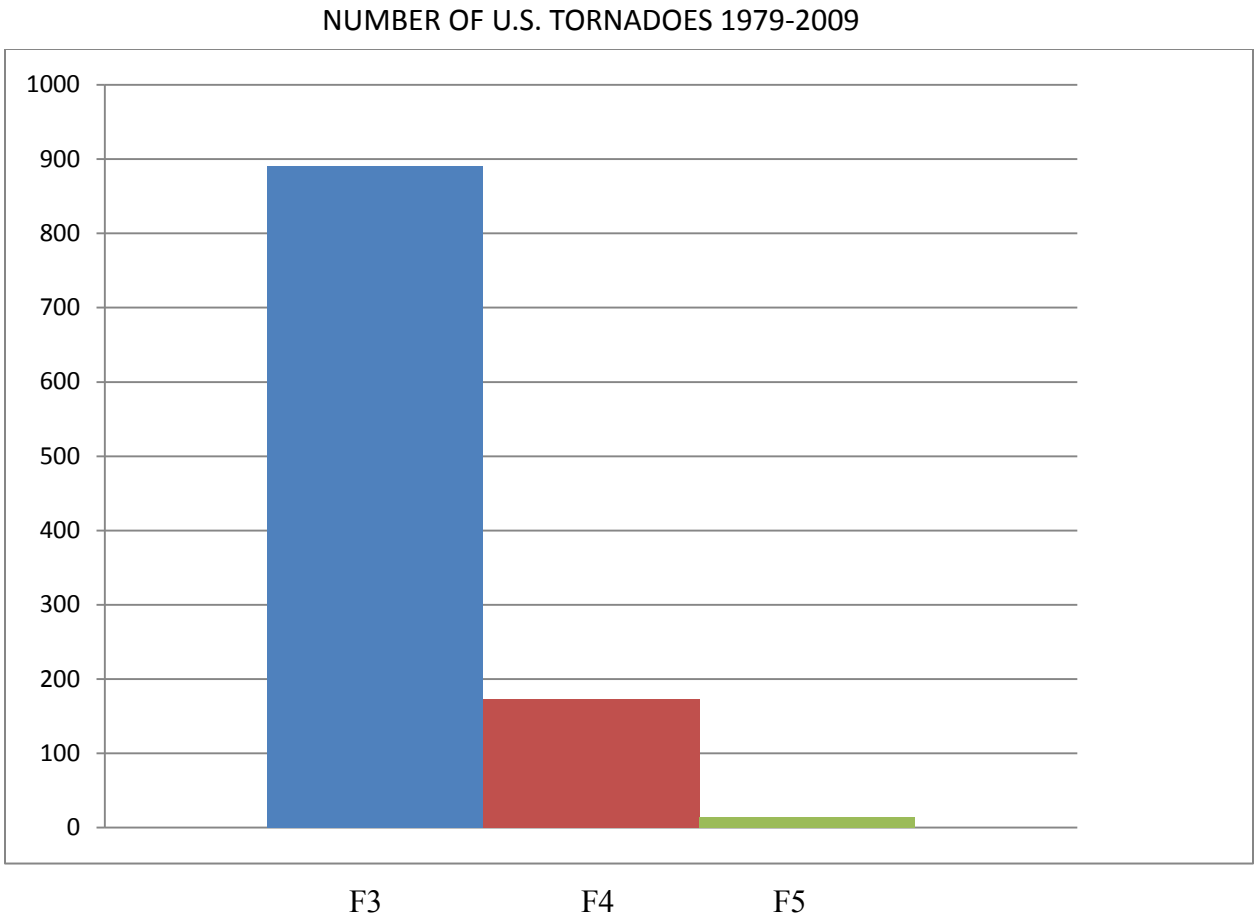

Figure 2.4.1d: Number of U.S. F3+ tornadoes 1979-2009. Y-axis is number of tornadoes, X-axis is tornado classification via F-scale.

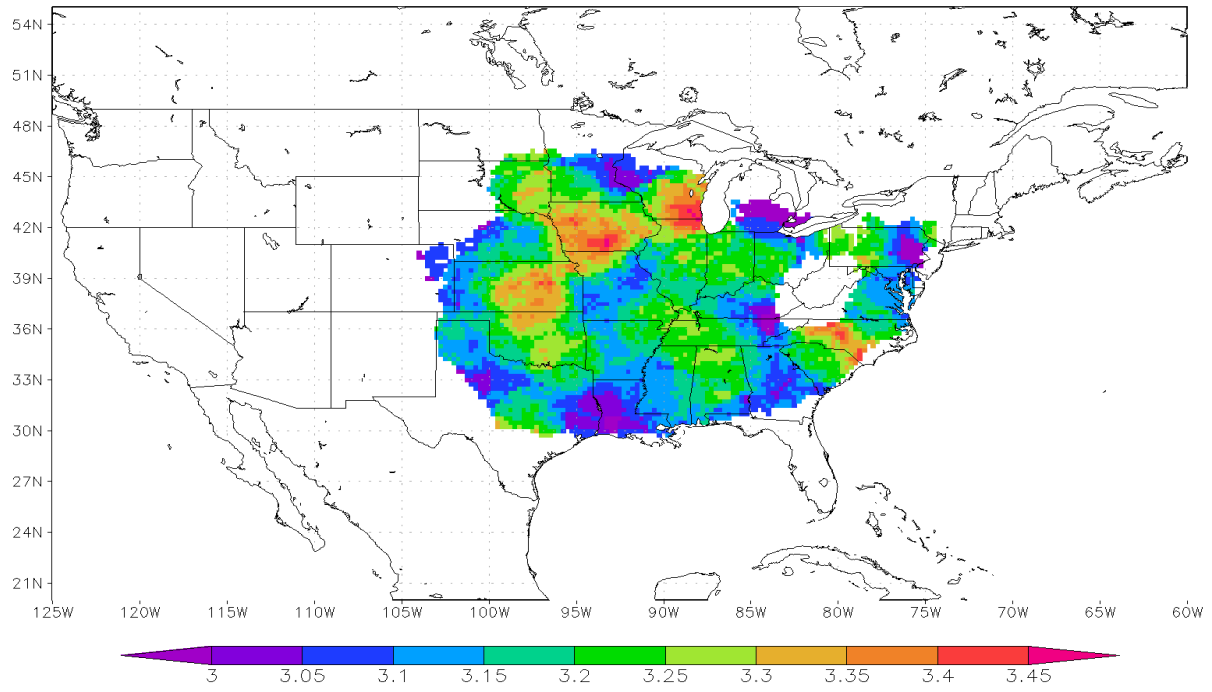

Figure 2.4.1e: Average F-scale shaded (F3+) 1979-2009. Data plotted only with 15+ events within 200km

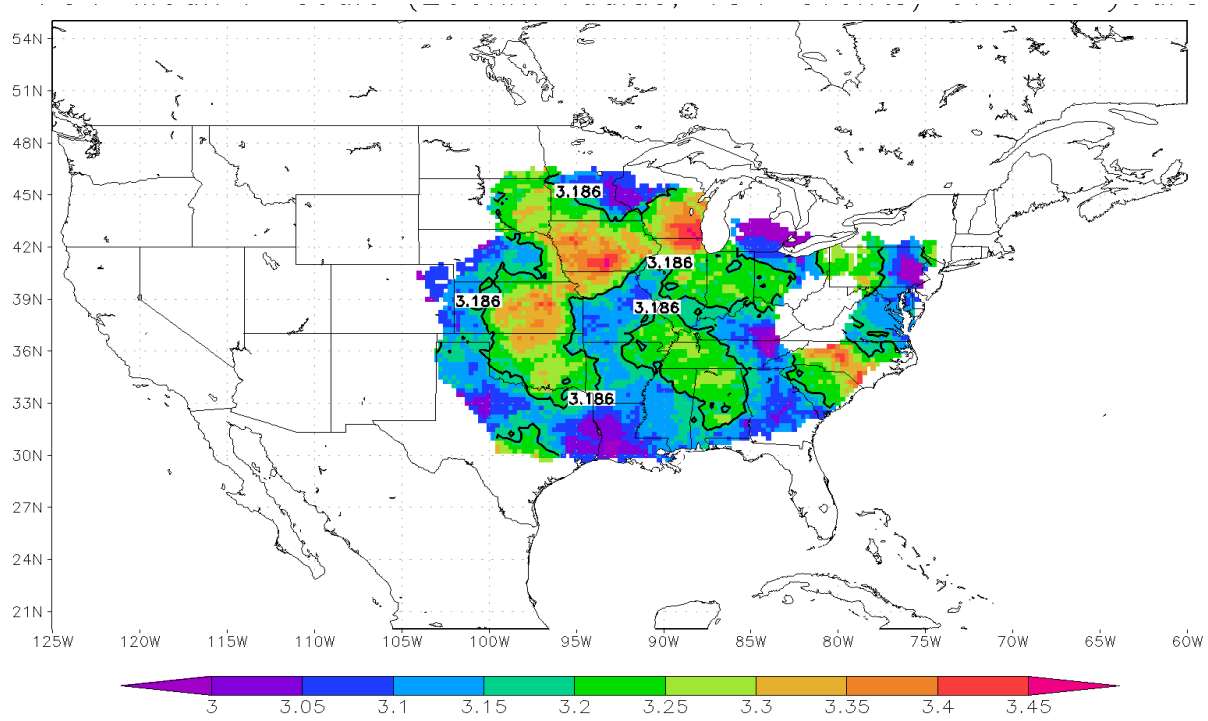

Figure 2.4.1f: As in 2.4.1e with average F-scale contoured. Contour value is 3.186, the average F-scale value for all F3+ events within the U.S. 1979-2009.

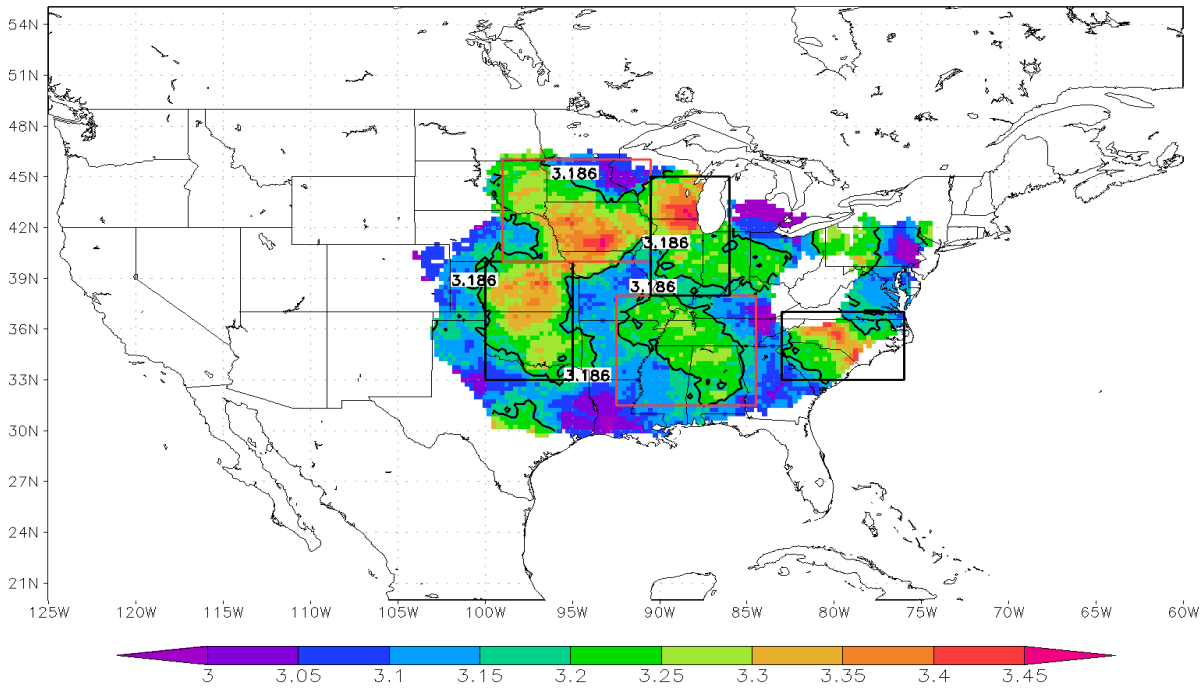

Figure 2.4.1g: As in 2.4.1e with average F-scale contoured and regions plotted (boxes). Contour value is 3.186, the average F-scale value for all F3+ events within the U.S. 1979-2009.

CHAPTER THREE

RESULTS

Results for this work are presented as follows: examination of case composites for each region, statistical analysis of atmospheric variables from reanalysis data, and finally analysis of STF. Case composites are examined from large scale (composite surface analysis plots), followed by composite variable plots, and finally local scale analysis (composite skew-T). Results from the STF analysis are presented in a similar fashion to the composite variable charts, then statistical analysis of the terms of STF are presented including covariances and correlations.

3.1 Piedmont Region Case Composites

Surface analysis charts for this region (Figs. 3.1a-c) display the composited at and near surface conditions at the time of the event (Fig. 3.1c), six hours preceding (Fig. 3.1b) and twelve hours preceding (Fig. 3.1a). Dew points in figure 3.1a are relatively constant across the Piedmont region with values between 17ºC and 20ºC. Near surface winds are blowing uniformly from the southwest between 5 and 10kts bringing in ever more moisture from the Gulf of Mexico. A broad 1007mb surface low is located over the region. A weak cold front is evident in the western portion of the region in eastern Georgia. Figure 3.1b shows that over the 6h time gap, dew point depression has decreased over much of South Carolina and eastern North Carolina, indicating an increase in surface moisture. Wind speeds remain similar between the two figures while the winds east of the region in Georgia and in northern South Carolina have taken on a more westerly component. Deepening of the surface low also occurs, with pressure at the center dropping from 1007mb to 1005mb, although the location of the center of the trough is remains

roughly the same. Increased temperature gradients along the cold front indicate a strengthening of the front, the northern reaches of which has moved into western South Carolina. At the time of the event (Fig. 3.1c) a general decrease in dew point depression is observable, indicating that the entire region experiences a moistening of the surface. Near surface wind speed has also increased in the western portion of the region from 10 to 20kts in some areas. As the trough has deepened, the winds also have a more southerly component throughout the entire area of the region. The center of the low pressure remains in almost exactly the same area but has intensified from 1005mb to 1002mb. Also, the front present in the previous two figures is now located well within the region (through the middle of South Carolina and southern North Carolina) and the magnitude of the temperature gradient is the same.

Composite field plots (Fig. 3.1b) show a maximum CAPE value of approximately 1000 J/kg located over extreme southern South Carolina. However, in much of the region, including most of North Carolina, southern Virginia, and northwest South Carolina, CAPE values are 400 J/kg or less; these values are much lower than what would be considered typical instability for an atmosphere preceding a severe tornado event. The helicity maximum is located over parts of southern Virginia and northern North Carolina with a max value of $300m^2/s^2$. Values of $200m^2/s^2$ and greater extend south through most of the region, with a minimum of $100m^2/s^2$ and less only in the extreme western portion of the Piedmont. Maximum values of specific humidity (about 1.3 g/kg) extend from southern Georgia into most of South Carolina. Moving north, there is a slight decrease in specific humidity through North Carolina and a more noticeable decrease near the southern border of Virginia. Composite 850mb winds show cyclonic flow about a low pressure centered in southern Ohio, resulting in flow from the southwest into the Piedmont. Further, a weak 850mb jet is located in the southeastern portion of the region, resulting in much of the

region residing in proximity to the left-exit area of the jet. Figure 3.1d shows the moisture advection into this region from the Gulf of Mexico and not the nearby Atlantic Ocean. Composite 250mb winds indicate a broad jet max over the Appalachian Mountains resulting in general divergence over much of the Piedmont region. Two local maximums of 925-700mb wind shear exist over northwest South Carolina and Southern Virginia at approximately 33kts respectively.

While the composite CFSR skew-T for the Piedmont region does not appear to be a typical pre-significant tornado sounding with very steep lapse rates and a well-defined capping inversion (elevated mixed layer) it should be noted that this is due to smoothing resultant from compositing. However, despite the smoothing of these features much can be gained from these composite soundings. Figure 3.1e exhibits a moist column throughout the troposphere with a precipitable water value of 3.58cm. In the near surface portion of the sounding, it is slightly drier than aloft. Above the moist area (approximately 925mb) the lapse rate becomes less steep and there is a separation between the temperature and dew point lines, indicating that a weak capping inversion is present in many of the events in the Piedmont region. The vertical wind profile indicates a slight veering with height through the entire troposphere. In the near surface portion of the profile, the veering is only a few degrees which would not typically be indicative of severe tornadogenesis (Brooks, 2008; Shaefer and Livingston, 1988). Sounding derived parameters indicate instability with lowest level CAPE at 643 J/kg, only 25 J/kg CIN and an LI of -2. Calculated from this sounding, LCL pressure is approximately 940mb, indicating a high cloud base pressure typical for severe tornado events in this region. The curvature of the hodograph supports cyclonic rotation (clockwise curvature), storm direction and speed of 258º at 39 kts respectively. Storm relative helicity (SRH) as calculated from the hodograph is $222 m^2/s^2$.

3.2 Dixie Alley Case Composites

Surface conditions twelve hours prior to severe tornado events (Fig. 3.2a) exhibit a very moist swath across most of Dixie Alley with dew point depressions of less than 5ºC and as small as 2ºC. Near surface winds are mostly southerly between 5 and 10kts. A broad surface low of 1008mb at its center is located to the northwest of the region over Missouri and Illinois. An associated cold front can be deciphered to the north and west of Dixie Alley. Figure 3.2b (composite of six hours before the tornado events) shows that the maximum area of surface moisture has expanded further north. Wind speeds stay the same but take on an even more southerly component throughout the region. The surface low remains stationary and does not deepen but the 1008mb isobar contracts to a slightly smaller area. Since the previous figure, the cold front has advanced eastward to the Mississippi River area with temperature gradients along it remaining more or less constant. By figure 3.2c the moisture through the region has not changed significantly, maintaining dew point depressions consistent with the previous figure. Near surface winds have become in almost perfectly meridional flow from the south. Furthermore the winds across all of Mississippi, Alabama, Tennessee, and Georgia have increased to 10kt uniformly. Having intensified slightly from the previous figure, the surface low is now 1007mb at its center and still remains in roughly the same place. The cold front however continues to advance west into central Mississippi and Tennessee, although it does not strengthen over the twelve hour period.

From the composite field charts (Fig. 4.2d) a maximum area of CAPE is centered over southwestern Mississippi at around 800 J/kg. All of Mississippi contains high values of CAPE (greater than 600 J/kg) with these values petering outward through Alabama and into Georgia

which has CAPE values between 200 J/kg and 400 J/kg. A broad helicity maximum with a value of $300m^2/s^2$ covers central Tennessee and northern Georgia, with a $250m^2/s^2$ contour closing northern Mississippi and Alabama as well. Almost all of Dixie Alley is contained within the $200m^2/s^2$ helicity contour line. Spatially, the specific humidity composite field follows the CAPE field with a maximum in Southern Mississippi and Alabama, decreasing northward from a value of 1.4g/kg to between 1.1 and 1.2g/kg at the farther reaches of the region. A strong 850mb jet centered over Mississippi and Alabama is present and pronounced in this composite field, indicating that this is a salient feature present for severe tornado events in Dixie Alley. This jet is consistently 40kt over much of the region and south-southwesterly, indicating strong moisture advection into the area. A broad 250mb jet is present to the northwest of the region, suggesting that if supercellgenesis here is affected by upper level convergence/divergence due to jet streak dynamics they are enhanced by the upper-level divergence typical with the right entrance (right rear) quadrant of the jet on average. Divergence and diffluence aloft over much of Mississippi and Alabama also imply convergence at the surface. A maximum area of 925-700mb vertical wind shear exists in northern Georgia (33kt) with slightly smaller values (24kt and greater) reaching into northern Alabama, Mississippi, and central Tennessee with the wind shear vectors turning from southwesterly to northwesterly across the region.

Figure 3.2e, the composite skew-t for this region, shows strong veering winds in the lower troposphere, suggesting a cyclonically favorable atmosphere. A slightly drier surface below the LCL (approximately 950mb) underneath a moist mixed layer indicates the presence of a capping inversion present prior to severe tornado events in this region. While an actual inversion does not manifest in the composite sounding, this is likely due to the closeness in temporal proximity to the tornado event, which would require the capping inversion to already

have broken - or to be breaking - within the maximum temporal error of less than 6h. Thus, the shape of this sounding says more about a broken cap than an actual cap being in place this close to the event. Most of the vertical column remains relatively moist within the troposphere with a column precipitable water value of 3.41cm. The hodograph exhibits clockwise curvature, indicating a cyclonically favorable atmosphere. Also from the hodograph, storm direction is calculated at 253º and at 43kts, with SRH calculated at $302m^2/s^2$. Overall, this is a convectively unstable profile with a CAPE value of 864 J/kg and CIN only 20 J/kg as well as a lifted index of -3. From the surface to about 600mb, the lapse rates are conditionally unstable (between dry and moist adiabatic).

3.3 K/O Region Case Composites

Composite surface analysis for the K/O region shows the surface moisture through the region dropping off sharply to the west from central Kansas, Texas, and Oklahoma via dew point depressions in figure 3.3a. These depressions have a gradient of about 5º to about 20º (moving from east to west) over a horizontal distance of about 100 miles. As documented in prior works (see chapter 2) this feature is likely the dryline front, which provides an additional lifting mechanism for severe weather events in this region. Here, we can see that the dryline is located though western Kansas, Oklahoma, and Texas. The near surface winds are largely meridional through the region, between 5 and 10kt. A center of low pressure is located in western Kansas and eastern Colorado at 1004mb. The cold front associated with this trough trails the dryline, located in the western extreme of the K/O region. Figure 3.3b shows that the dryline has not changed much in location or strength as noted through dew point depressions. The winds are still very much meridional and with speeds of 5 and 10kt. Also, the location and strength of the

trough does not appear to change over this time step. At the closest synoptic time to the tornado events, the dryline seems to advance slightly further west into the region (Fig. 3.3c). Dew points seem to remain mostly the same through all of the time steps, but the dew point depression seems to move eastward. Near surface winds remain the same. There is a deepening of the trough from 1004mb to 1002mb and it can be seen to have moved slightly to the southeast from its prior location. The cold front seems to have moved eastward as well, but remains behind the location of the dryline front. Since tornadoes in this region typically occur in the afternoon, the unchanging location of the dryline in these composite images is not unexpected, due to the nature of the dryline. The dryline follows a diurnal progression and recession much like a sea breeze front since they are both density currents. During the daytime, the dryline forges eastward and then ebbs back toward the west after the land begins to cool at night.

An area of maximum of CAPE is present over north-central Texas and south-central Oklahoma (Fig. 3.3d). The shape of this region in very narrow and long, with CAPE values sharply weakening outward from 1800 J/kg at the center to 200 J/kg on the outer fringes of the K/O region. Two local maxima of helicity exist: one in western Oklahoma and eastern Arkansas at $260 m^2/s^2$, and another broader region of $240 m^2/s^2$ over northern Kansas and its bordering states to the west and north. Composite specific humidity shows that a swath of maximum moisture (1.4 g/kg) extends up from south central Texas into Oklahoma, and then decreasing gradually to the east and very sharply to the west. Almost exactly meridional flow is shown with a weak jet max of about 30kt over Texas and Oklahoma. Here we can also see a very well defined low located over northwest Kansas. At 250mb, a jet max is centered right over the north-central Kansas with maximum speed of 50kt blowing from the southwest to the northeast. The combination of divergence at this level and proximity to the right entrance region of the jet streak

likely add to the potential for the creation of supercells. Further, there is apparent veering with height between the 850mb level and the 250mb level, yielding an even more cyclonically favored atmosphere. A broad area of 24kt and greater vertical 925-700mb wind shear is located over the majority of the region, extending from southern Oklahoma through Kansas to Northern Missouri and even southern Iowa. A small local maximum of wind shear (greater than 27kt) is located in south-central Kansas. The wind shear vectors through the region are roughly zonal, turning more southerly in the northern portions of the K/O region.

Figure 3.3e, the composite sounding for the K/O region, shows an 8ºC dew point depression at the surface and this is maintained throughout much of the troposphere except for a slightly moister section in the mixed layer; reasons for the relative dryness at the surface will be discussed in the following chapter. Strong veering is present in the vertical wind profile in the lowest 600mb, with the strongest veering with height in the near surface portion. From the hodograph clockwise curvature can be noticed yielding a cyclonic favoring atmosphere. The storm direction is 246º, the storm speed is 34kt, and the SRH is 217m^2/s^2 as also calculated from the composite hodograph. Steep lapse rates near dry adiabatic in the lower troposphere and a CAPE value of 2469 J/kg with only 60 J/kg of CIN depict a very convectively unstable atmosphere - a fact bolstered by a LI value of -7. The LCL is located at approximately 925mb. Like the two regions discussed prior to this one, the K/O composite skew-T does show evidence of a breaking or broken capping inversion per the moister elevated mixed layer.

3.4 Iowa Region Case Composites

Composite surface analysis at twelve hours preceding the events (Fig. 3.4a) shows much of the region having dew point depressions of between 9 and 15 with a steep gradient to the west

of the region, possibly indicating a dryline front. Near surface winds are at between 5 and 10kt out of the south-southwest. A broad low pressure area of 1006mb lies over much of Nebraska and Kansas. Evidence of a weak cold front can be seen just east of the low pressure center. Figure 3.4b does not seem to display any sort of evolution or progression of the dryline front or any change in moisture throughout the region. Near surface winds seem to have remained the same as well in terms of both direction and speed. The center of low pressure has expanded slightly into the Dakotas and Colorado but remains of the same intensity at 1006mb. As nothing else seems to have changed in the composite surface, the cold front as well seems to remain stationary. Over the next 6 hours, the dry line front advances slightly to the east (Fig. 3.4c) and the winds take on a more easterly component, now south-southeasterly across the region with speeds of 5kt uniformly across Iowa and into Minnesota and Nebraska. The low pressure experiences a slight deepening of 2mb to 1004mb and advances slightly eastward into central Nebraska. The cold front as well moves eastward into the Iowa/Nebraska border area.

The composite field in figure 3.4d shows a broad area of maximum CAPE at 1300 J/kg centered over much of Iowa, and parts of Nebraska, Missouri, and Kansas and another much smaller local maximum located in western Illinois. West of this area there is a steep decreasing gradient of CAPE, dropping from 1100 J/kg or more in only 100mi. Most of the region lies between the $160m^2/s^2$ and the $220m^{2/}s^2$ iso-lines while a maximum of $260m^2/s^2$ is centered in northern Iowa. Maxima of composite specific humidity exist south of the regional boundaries at 1.5g/kg while the entire state of Iowa shows a value of 1.3g/kg. North and west of Iowa however, the specific humidity rapidly drops off to 0.7 in central Nebraska and North Dakota. 850mb winds flow from the southwest, turning north around a well-defined low located in eastern North Dakota at speeds ranging from 20 to 30kt through the region. At the 250mb level a

composite jet max of 40kt is visible above Minnesota, and the Dakotas. The best chance for effects of upper-level jet dynamics to bolster supercellgenesis would likely be in northern Iowa and Nebraska due to proximity to the right rear quadrant and divergence aloft. No diffluence is observable over the region. Three maxima of 925-700mb vertical wind shear (24kt) can be seen in close proximity to each other over Iowa, Minnesota, and Wisconsin respectively, with the rest of the region largely encompassed by the 18kt shading line. The wind shear vectors turn from southwesterly to northwesterly over the range of the region.

Examining the composite sounding for the Iowa region (Fig. 3.4e), there is a dew point depression of 7º at the surface. This depression remains relatively constant throughout the vertical profile except for a slight moistening near 850mb in the mixed layer. Significant veering exists in the lowest 800mb of the troposphere indicating that the atmosphere favors the cyclonic. Near surface lapse rates are near dry adiabatic and conditionally unstable until about 400mb. Again, this is a sounding exhibiting many features of convective instability. Calculated from the sounding, there is 1909 J/kg CAPE, 67 J/kg CIN and a LI of -6. From the hodograph, which favors cyclonically rotating storms via the clockwise curvature, storm direction is calculated at 242º, with storm speed of 30kt and an SRH value of $193 m^2/s^2$. The LCL in this skew-T is located at 925mb.

3.5 Great Lakes Region Case Composites

Composite surface analysis of conditions twelve hours preceding the tornado events (Fig. 3.5a) shows that the region is relatively moist with dew point depressions between 6ºC and 3ºC across the majority of the area. Near surface winds are out of the southwest at 5kt everywhere in the region except for in Indiana, where they are 10kt. A trough at 1006mb is centered over

Wisconsin; no cold front is visible in this image. 6 hours into the future (Fig. 3.5b) and the northern portions of the Great Lakes region experiences a slight decrease in dew point depression, with the rest of the region remaining the same. The 1006mb isobar has expanded and advanced eastward through central Illinois. Winds through the region remain mostly the same. A warm front can be observed in northern Illinois, and it is the only front manifest at the time of this image. Figure 3.5c shows that by the time closest to the events, the moisture at the moisture at the surface level has remained largely the same from the previous time step. Near surface winds as well have remained the same in terms of direction with a slight increase in speed from 5 to 10kt over Illinois. The surface tough increases from 1006mb to 1004mb and remains stationary. The warm front from the previous time step remains in the same area, implying that perhaps isentropic lifting along the warm front boundary may be a player in severe tornadogenesis in this region.

In figure 3.5d, the composite CAPE shows a maximum of 1200 J/kg far south of the region (near Arkansas) leaving the region to be in a decreasing CAPE gradient of 1100 J/kg (a small local max) in southern Illinois to 300 J/kg in central Wisconsin. A maximum area of helicity is centered over northern Indiana at 300 J/kg. Specific humidity values across the Great Lakes region range from 1.3 in southern Illinois and Indiana to 0.8 in central Wisconsin. A low pressure center is visible in the 850mb wind field in central Minnesota with winds blowing from the southwest through the region varying in speed from 40kt in southern Illinois to 15kt in Wisconsin. A 55kt jet at 250mb is centered over central Wisconsin, thus the majority of the region is in the right entrance region of the jet streak. Furthermore, upper-level diffluence and divergence combine to add to severe weather potential. Wind shear (925-700mb) is maximum over the Wisconsin/Illinois border and the Indiana/Michigan border at 24-27kt. Much of the rest

of the region shows values of 18kt and above. Wind shear vectors show diffluence over the region from southwesterly to south-southwesterly in the northern portion of the region, and from southwesterly to northwesterly in the southern portion of the region.

A dew point depression of 3.5ºC can be seen at the surface of the composite skew-T for the Great Lakes region (Fig. 3.5e). Slight veering in the lowest 800mb of the vertical profile suggests a cyclonic favoring atmosphere. Lapse rates through 600mb are conditionally unstable with a small stable area above the mixed layer (850mb). Strong clockwise curvature in the hodograph also suggests a cyclonically favored atmosphere, with a storm direction of 253º, storm speed at 38kt, and SRH at 262m^2/s^2. This sounding, like all of the others discussed earlier, represents a convectively unstable atmosphere with a LI value of -5, CAPE at 1205 J/kg and only 23 J/kg CIN.

3.6 Statistical Analysis of Atmospheric Variables

Thermodynamic variables assessed in this work are displayed in table 3.6a. Regions differ from each other at 95% confidence with respect to a variable if the two region's CIs for that variable do not overlap. The K/O region shows the highest mean CAPE value and the Piedmont region shows the lowest. One notable feature is that CAPE values in the Piedmont region are significantly different (smaller) than all of the other regions before severe tornado events since the CIs do not overlap. In terms of CAPE, a significant difference between the eastern two regions and the two mid-west regions is apparent, with the Great Lakes region lying between the extremes of the Piedmont and K/O regions and not significantly different from either Iowa or Dixie Alley.

Moving on to lapse rates, we can again see a similar difference between the eastern and western regions with the western regions exhibiting significantly steeper lapse rates at all levels. While significant differences exist between regions at all examined levels, the Great Lakes region remains not significantly different from any region until the 700mb and higher levels. Over all, the most significant differences in lapse rates exist for the highest portions of the atmosphere examined (700-500mb) between the regions. For CIN, the K/O region shows the highest mean and Dixie Alley shows the lowest. Here, the difference between the eastern and western regions in terms of pre-severe tornadic thermodynamic variables is again manifest; Dixie alley and the Piedmont region are both significantly different from both the Iowa region and K/O regions with the Great Lakes region falling in the middle. These results suggest that geography is possibly a big factor in determining the thermodynamic environments of severe tornadoes.

Table 3.6b shows significant differences in 0-1km helicity and vertical wind shear at different levels. The highest mean helicity is revealed to be in Dixie Alley with the lowest mean in the Piedmont region. Furthermore, these are the only regions which are significantly different from each other in terms of helicity. With vertical wind shear in the lowest examined level (925-850mb) it is much the same. The Piedmont region and Dixie alley are found to have the lowest and highest means respectively. At the 850-700mb level, Dixie alley has the lowest mean however, and the K/O region has the highest. No discernible geographical pattern of significant differences can be observed at this level between regions. For vertical wind shear at the 900-700mb level, there is not much difference since the 850-700mb vertical wind shear seems to mass the majority of the total wind shear up to 700mb.

In terms of the moisture related variables examined (LCL height and specific humidity) the only real significant differences seem to exist in LCL heights. Table 3.6c shows that most of

the regions are significantly different from each other. The only places which aren't significantly different from each other are the Piedmont and Great Lakes regions and the Piedmont and Dixie Alley regions. The K/O region has the highest mean LCL of all of the regions and the Piedmont region has the lowest mean, however it does have the largest CI. It is interesting to note only two significant differences in terms of specific humidity: between the K/O region and Piedmont region at 700mb and between the K/O region and Dixie Alley at 600mb. The lack in significant differences with respect to this variable is not surprising since a moist atmosphere is required not only for tornadogenesis, but also for convection in general.

Calculations for peak tornado season within each region show zero significant differences. In fact, the means for each region are all within three days of each other. Late April to Mid-Late June seems to be the severe tornado season for all of the regions within the CI. The same calculation was done for all F3 and greater tornadoes within the U.S. for the same time interval; table 3.6d shows that the severe tornado season for the entire U.S. is May 7th through May 22nd. Therefore, severe tornado alleys show a broader severe tornado peak season than the rest of the United States. Moreover, previous work has shown that a general tornado season moves north throughout the year (Brooks et al. 2003b). This work was not specific to Intensity of tornadoes. It is shown in table 3.6d that severe tornado season is geographically static.

3.7 STF Analysis.

Table 3.7a shows the CI calculation for severe tornado events within each region. For every region except the Piedmont region, the CI only includes values greater than 1, which is indicative of potential for genesis of F2 and higher twisters; that the Piedmont region has a CI partially below that threshold for severe (F3+) tornadoes is noteworthy. Many significant

differences exist for STF between regions with the individual components calculated at the closest synoptic time preceding the tornado event, which would be the most relevant time for forecasting. Only the Great Plains region and Dixie Alley, the Iowa region and the Great Plains region, and the K/O and Iowa regions are not significantly different from each other. The Piedmont region is has by far the lowest mean, and the K/O has the highest mean.

For every time step for every grid-point within the regions it is shown that variables within the K/O region change the most with STF and furthermore that the variables within the K/O region are correlated the highest with STF of all of the regions. Dixie Alley is the second highest correlated for all variables except for CAPE where the Iowa region is second highest. Covariances and correlations of variables to STF within other regions are much lower. Table 3.7b shows that the CAPE term within STF is by far the largest contributor to the STF value within each region, followed by SRH, then LCL, then BWD uniformly. It is interesting that the terms of STF contribute in approximately the same way between each region even though variables within each region show different correlations with STF. Average components of STF show that in Dixie Alley and the Piedmont region, LCL values are typically favorable of severe tornadogenesis (values higher than 1) regardless of whether a severe tornado event is occurring or not. In the K/O region, BWD component values are in the same way typically favorable of severe tornadogenesis while in the Great Lakes and Iowa regions, both LCL and BWD component values are on average higher than 1.

Examining component covariances and correlations at the actual events in each region, there are indeed variations of the individual components relevant to STF when compared to the peak season analysis (Table 3.7c). In all regions, the BWD, Helicity, and LCL terms show average values higher than 1 which would be indicative of severe tornadogenesis; only in the

K/O region is the CAPE term also greater than 1. In the Piedmont region, correlations for all components are greater except for the LCL term, which actually becomes negatively correlated. In Dixie Alley, the results are similar to those in the Piedmont region except with a lesser increase from the peak season analysis - correlations between the LCL term and STF decrease but remain positive. In the K/O region correlations between STF and CAPE and LCL remain nearly the same. However, correlations between STF and the helicity term increase significantly, and increase to a lesser extent between STF and BWD. Results are very similar in the Iowa region, except correlation of the LCL term to STF actually decreases. The Great Lakes region shows a uniform increase in correlations of CAPE, BWD, and helicity terms for the events of between .11 and .16 with LCL correlation decreasing by .2.

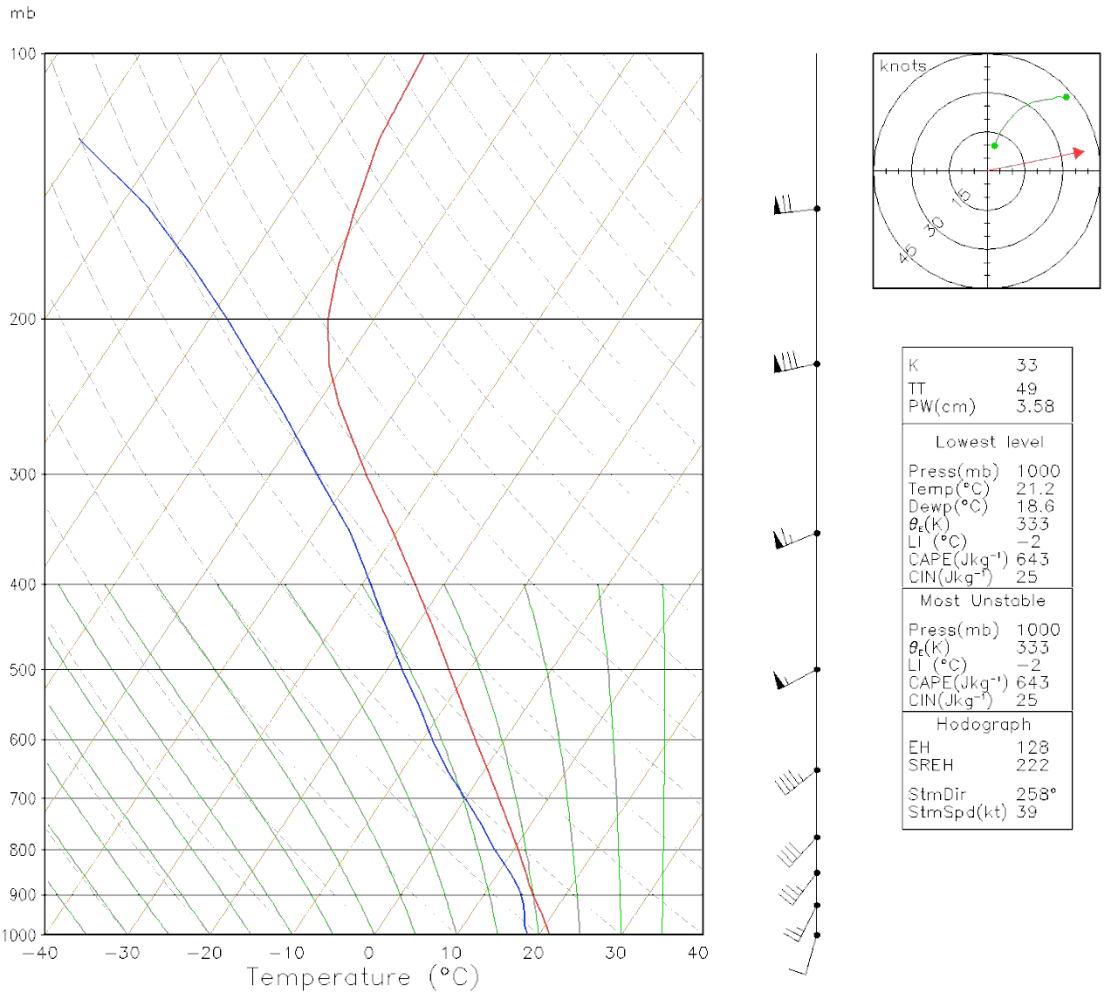

Figure 3.1e: Composite skew-T for the Piedmont region calculated from CFSR variables at closest synoptic time preceding tornado events within this region; wind profile, hodograph, and skew-T derived parameters to the right of the sounding.

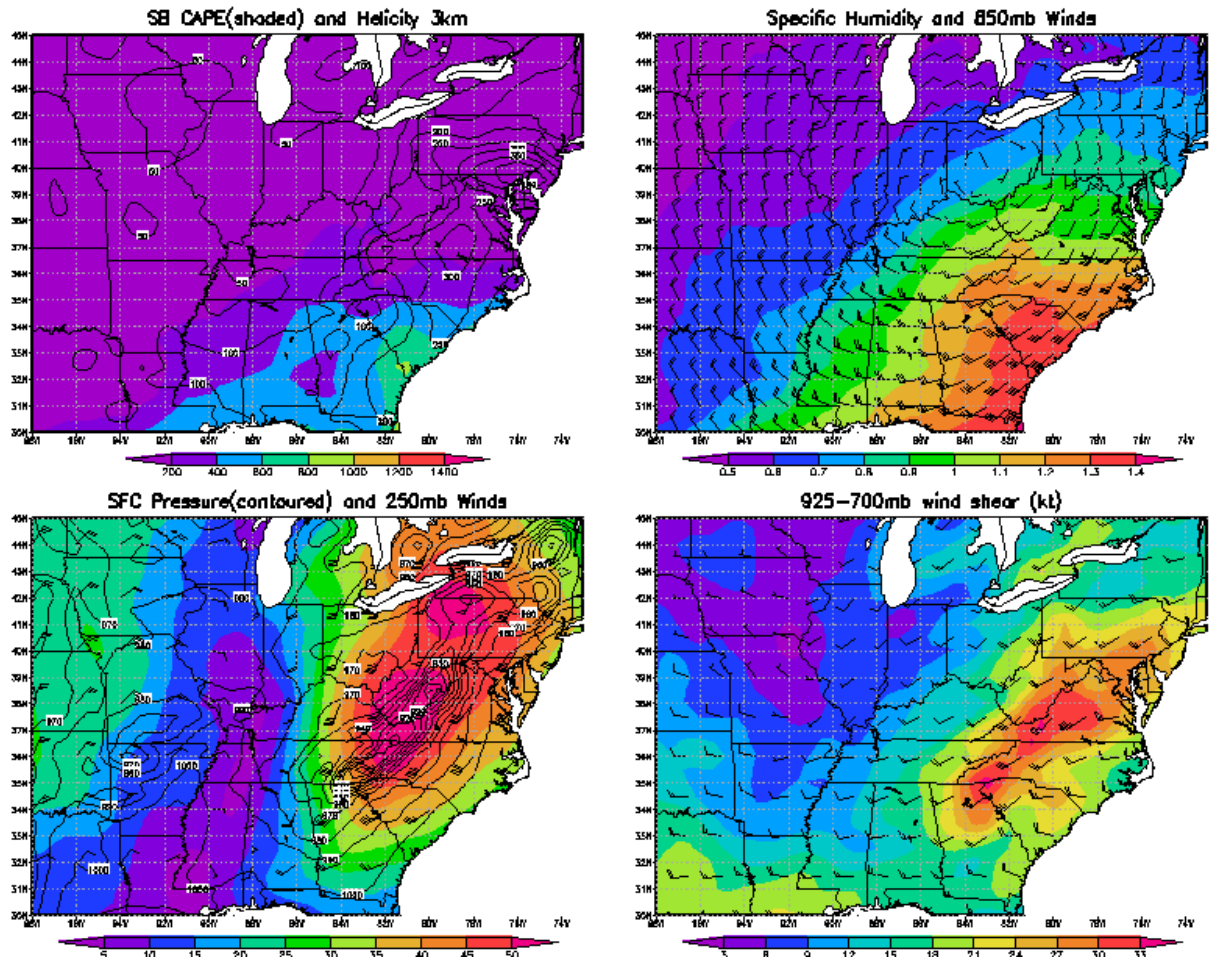

Figure 3.1d: Composite field charts for the Piedmont region from CFSR variables at the closest synoptic time preceding tornado events. Upper left - Surface-based CAPE (shaded) and 0-3km helicity (contoured). Upper right - Surface specific humidity (shaded) and 850mb winds (barbed). Bottom left - surface pressure (contoured) and 250 winds (shaded and barbed). Bottom right - 925-700mb wind shear (shaded and barbed).

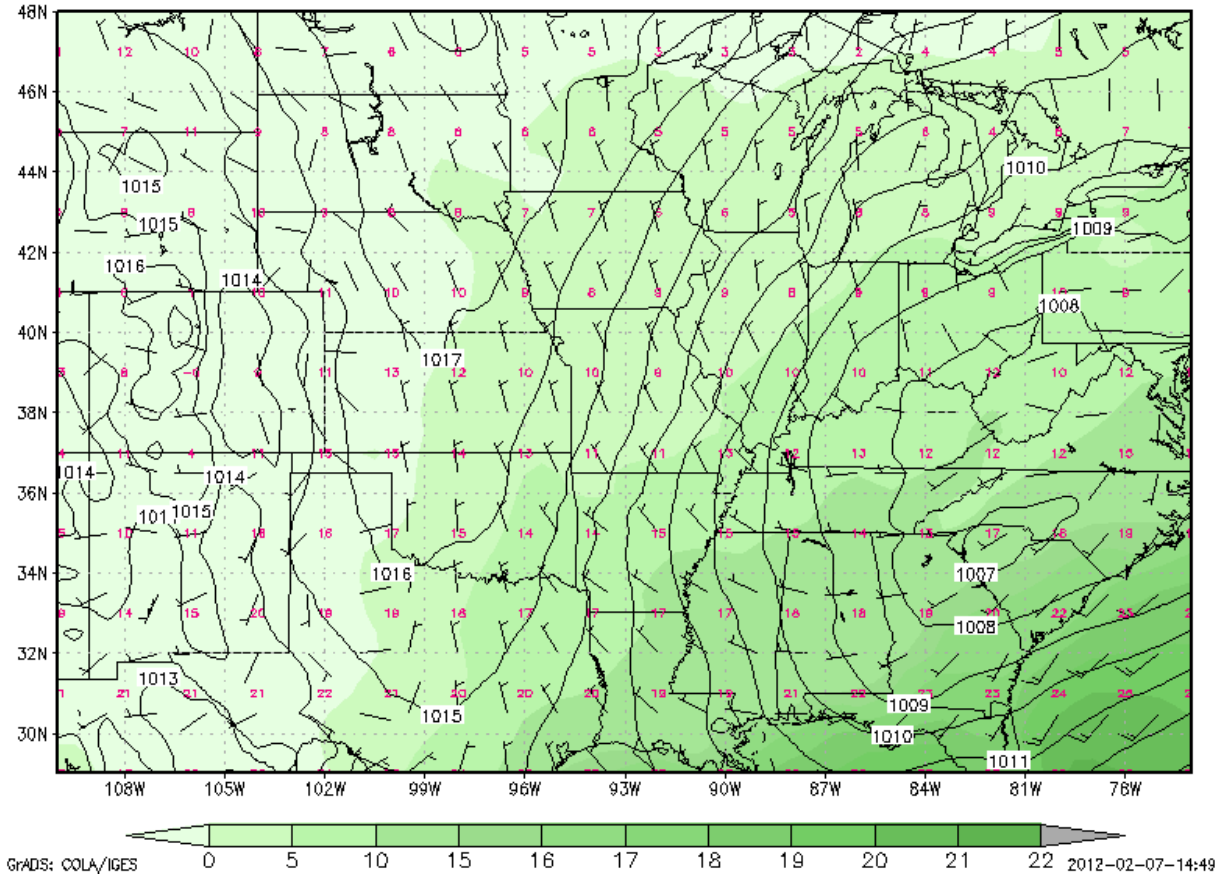

Figure 3.1a: Composite surface analysis chart for severe tornado events within the Piedmont region from CFSR variables. Variables averaged 12 hours prior to (2 time-steps) events. Surface pressure (shaded), 10m above ground winds kt (barbed), surface Temperature Celcius (printed at grid-points in red), surface dewpoint temperature Celcius (shaded).

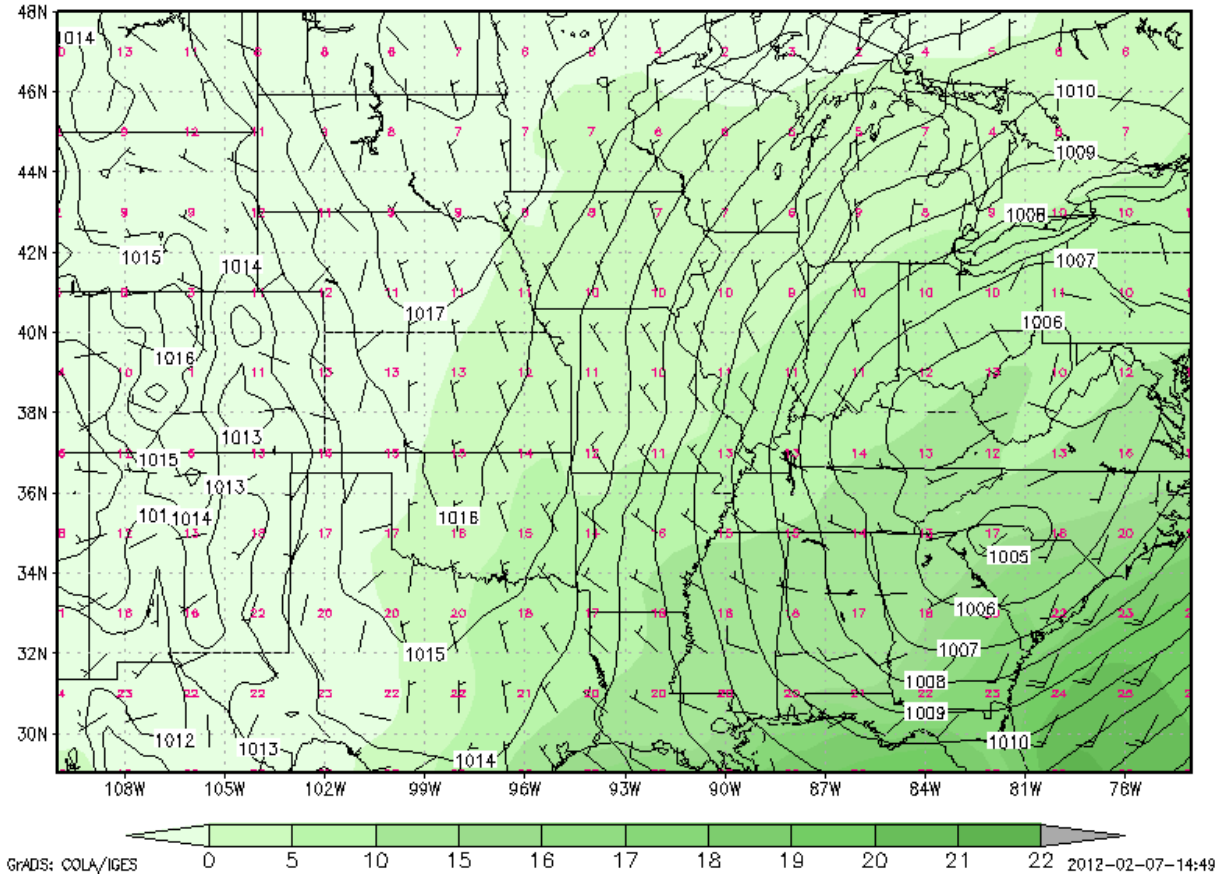

Figure 3.1b: As in 3.1a but variables averaged at 6 hours (1 time-step) before closest synoptic time to event.

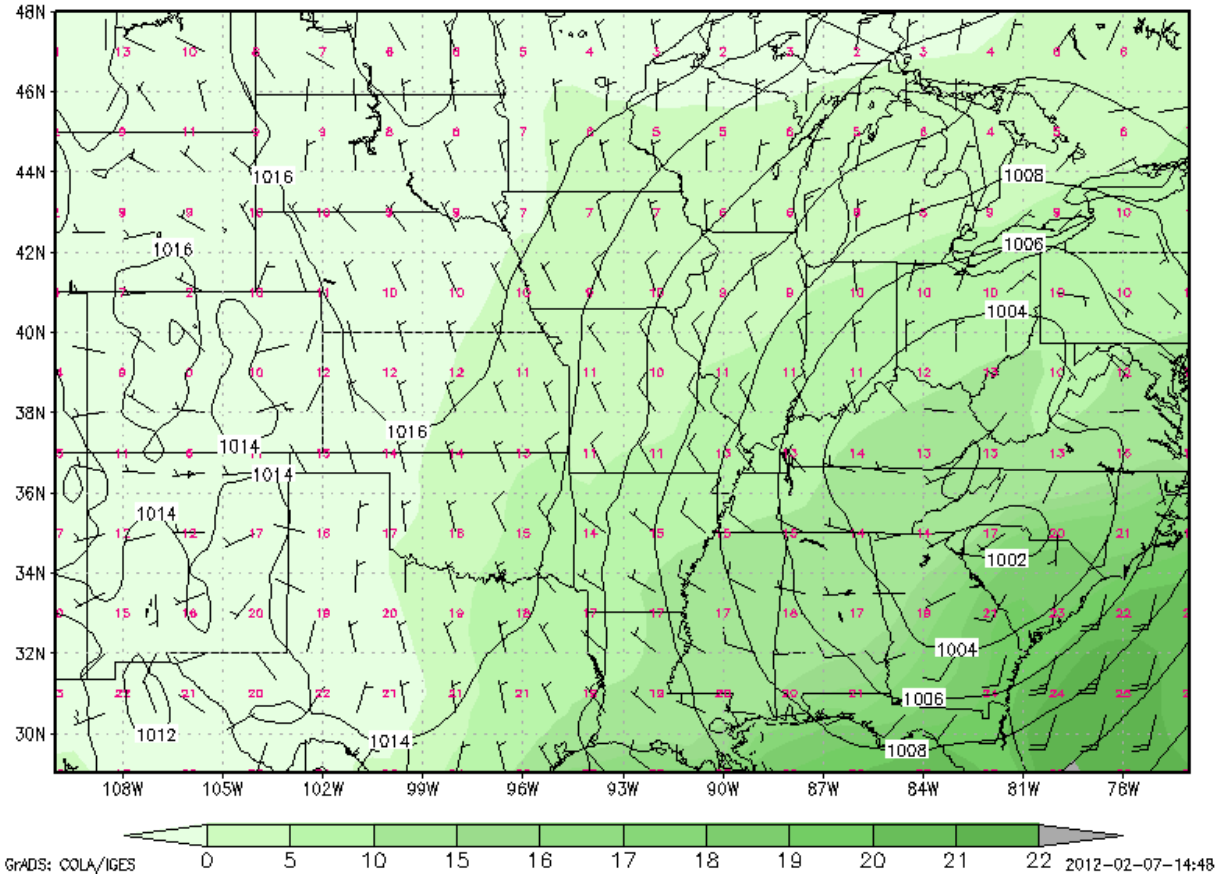

Figure 3.1c: same as 3.1a but variables averaged at the closest synoptic time to event.

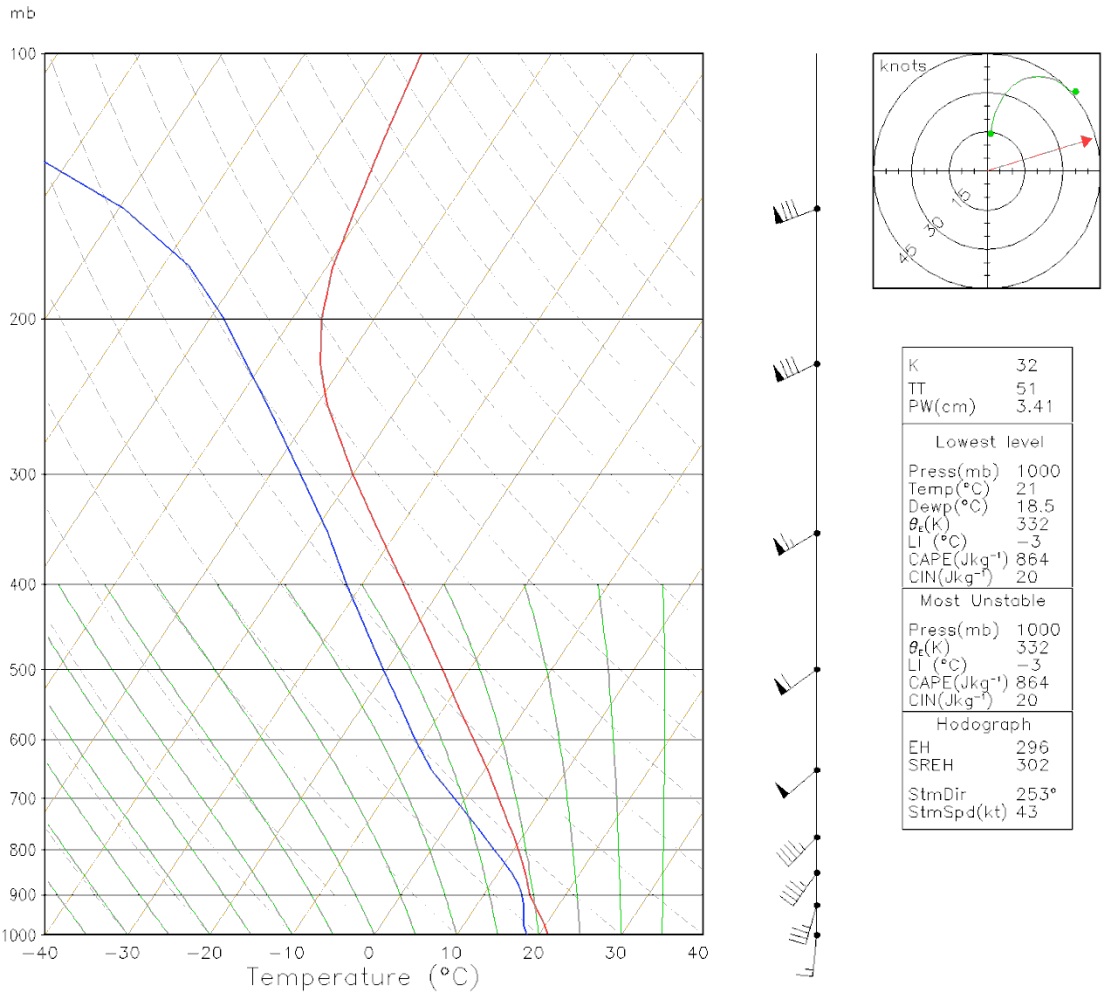

Figure 3.2e: Composite skew-T for Dixie Alley; wind profile, hodograph, and skew-T derived parameters to the right of the sounding.

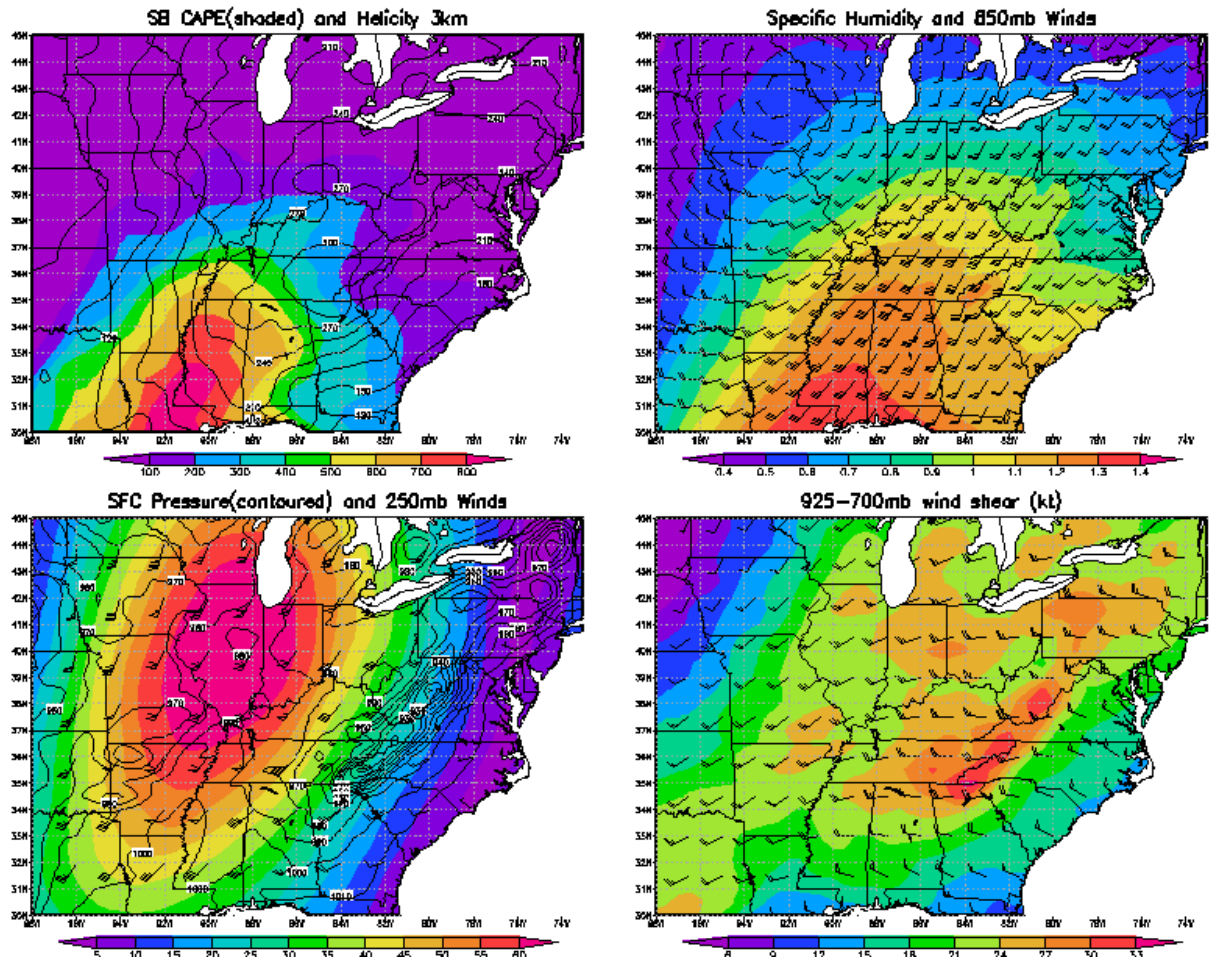

Figure 3.2d: Composite field charts for Dixie Alley. Upper left - Surface-based CAPE (shaded) and 0-3km helicity (contoured). Upper right - Surface specific humidity (shaded) and 850mb winds (barbed). Bottom left - surface pressure (contoured) and 250 winds (shaded and barbed). Bottom right - 925-700mb wind shear (shaded and barbed).

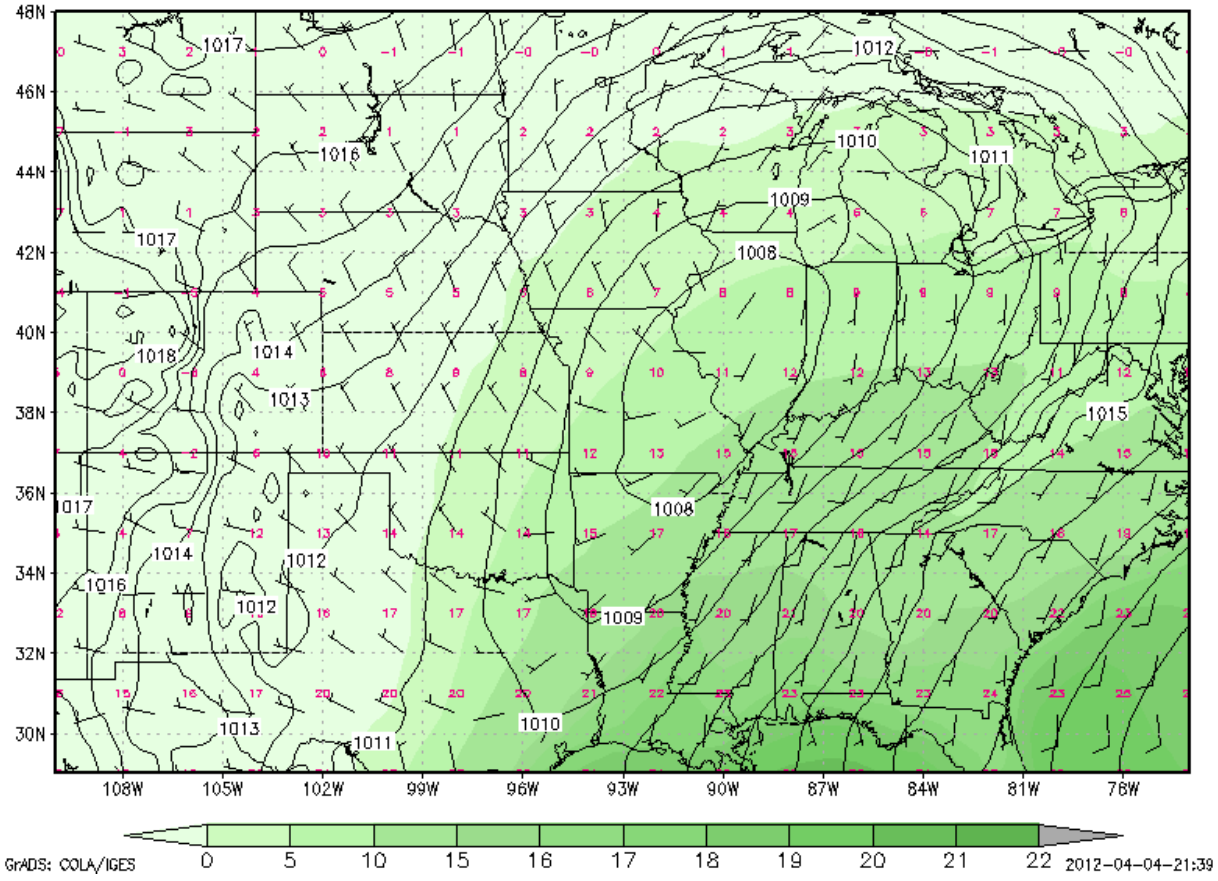

Figure 3.2a: Composite surface analysis chart for severe tornado events within Dixie Alley. Variables averaged 12 hours prior to (2 time-steps) events. Surface pressure (shaded), 10m above ground winds kt (barbed), surface Temperature Celcius (printed at grid-points in red), surface dewpoint temperature Celcius (shaded).

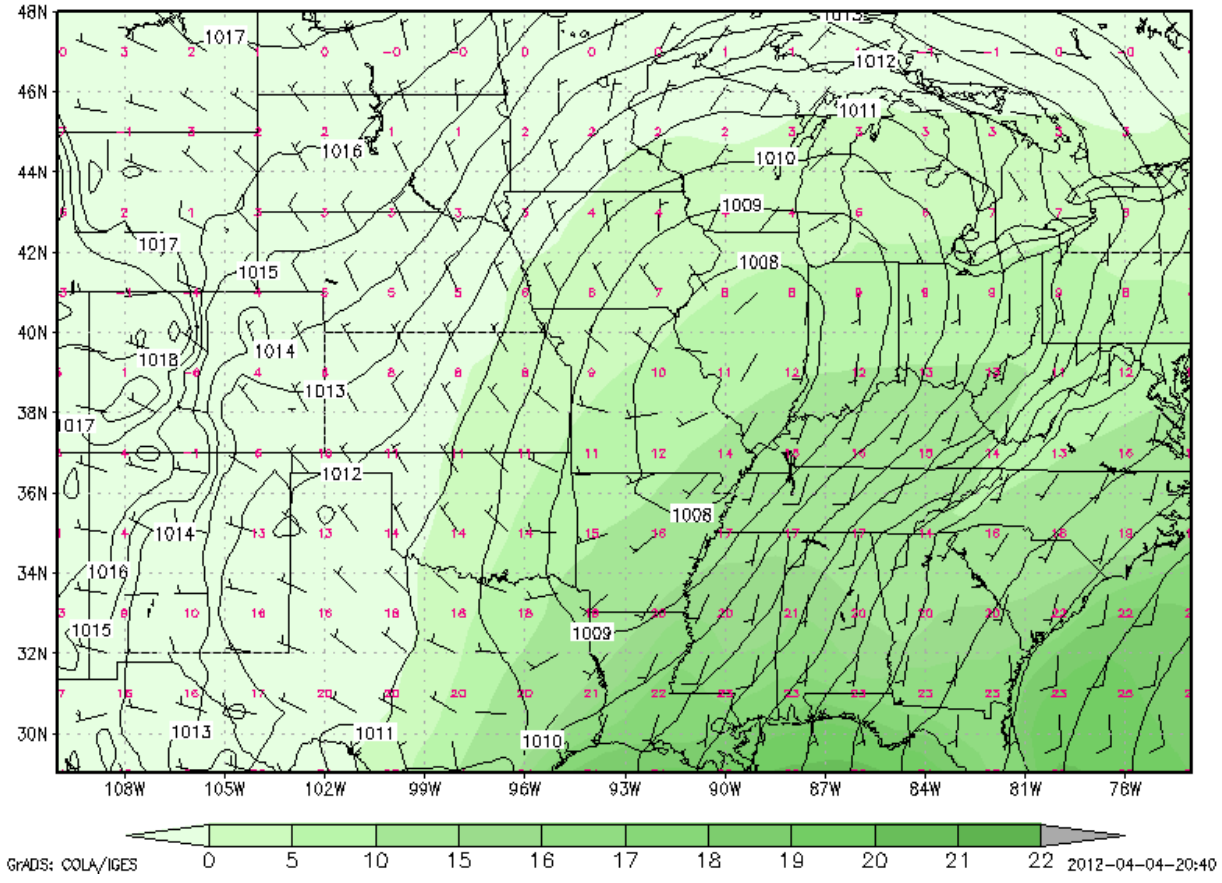

Figure 3.2b: As in 3.2a but variables averaged at 6 hours (1 time-step) before closest synoptic time to event.

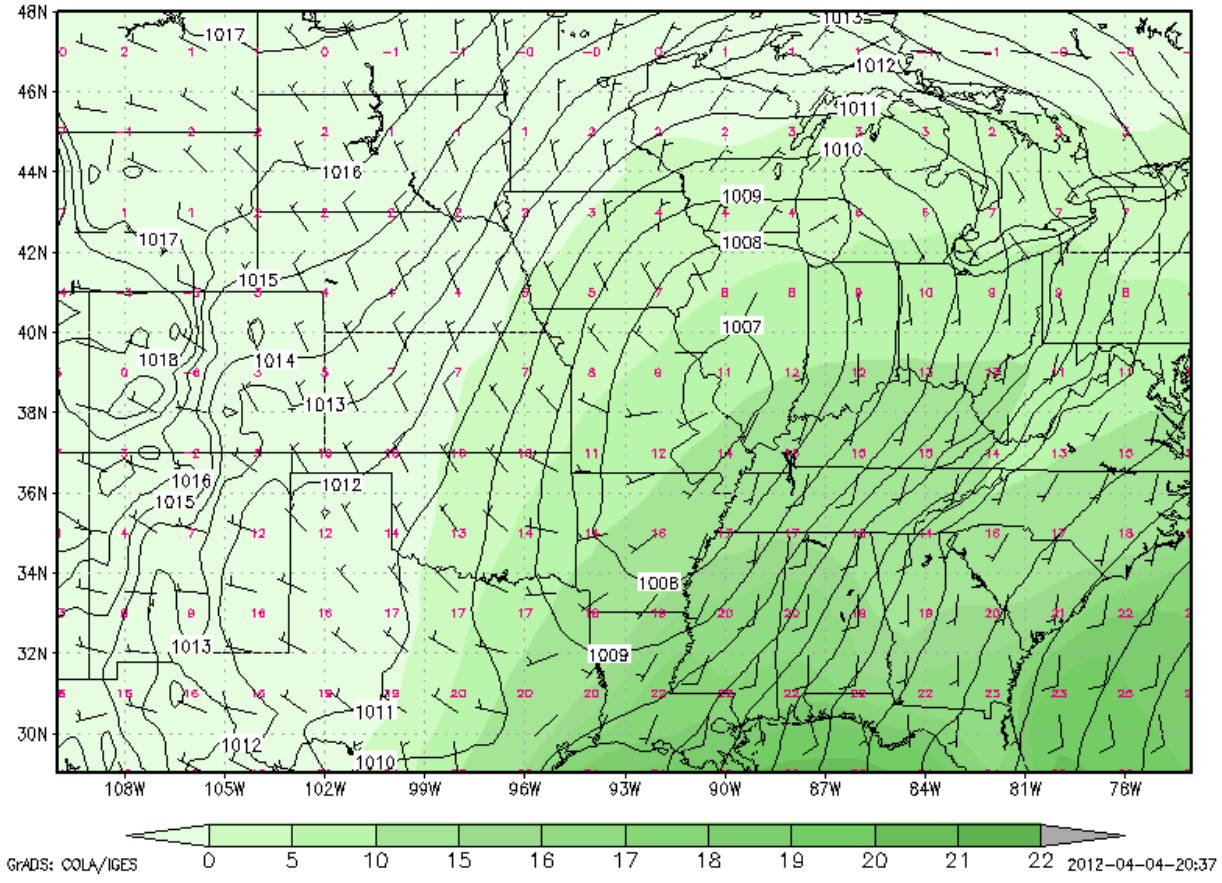

Figure 3.2c: As in 3.2a but variables averaged at closest synoptic time to event.

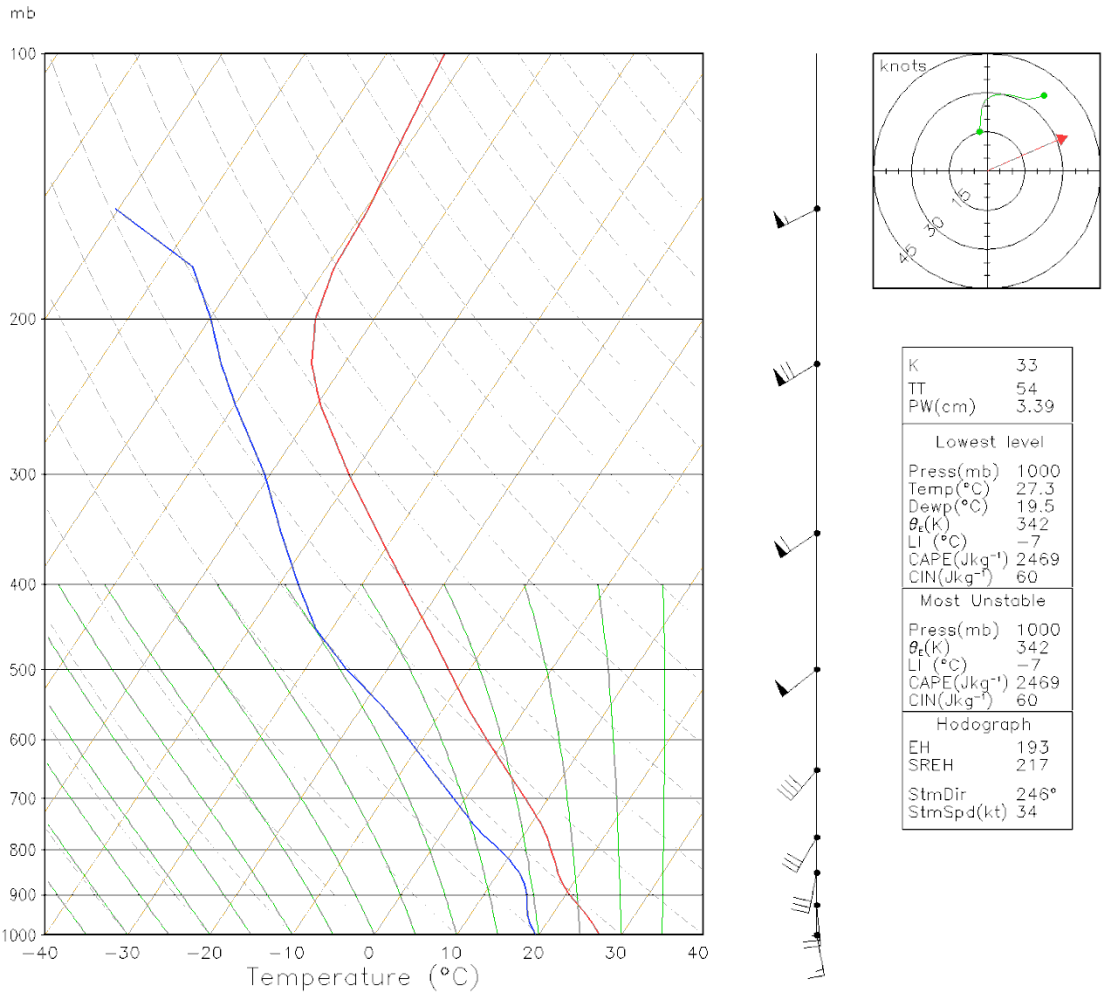

Figure 3.3e: Composite skew-T for the K/O region; wind profile, hodograph, and skew-T derived parameters to the right of the sounding.

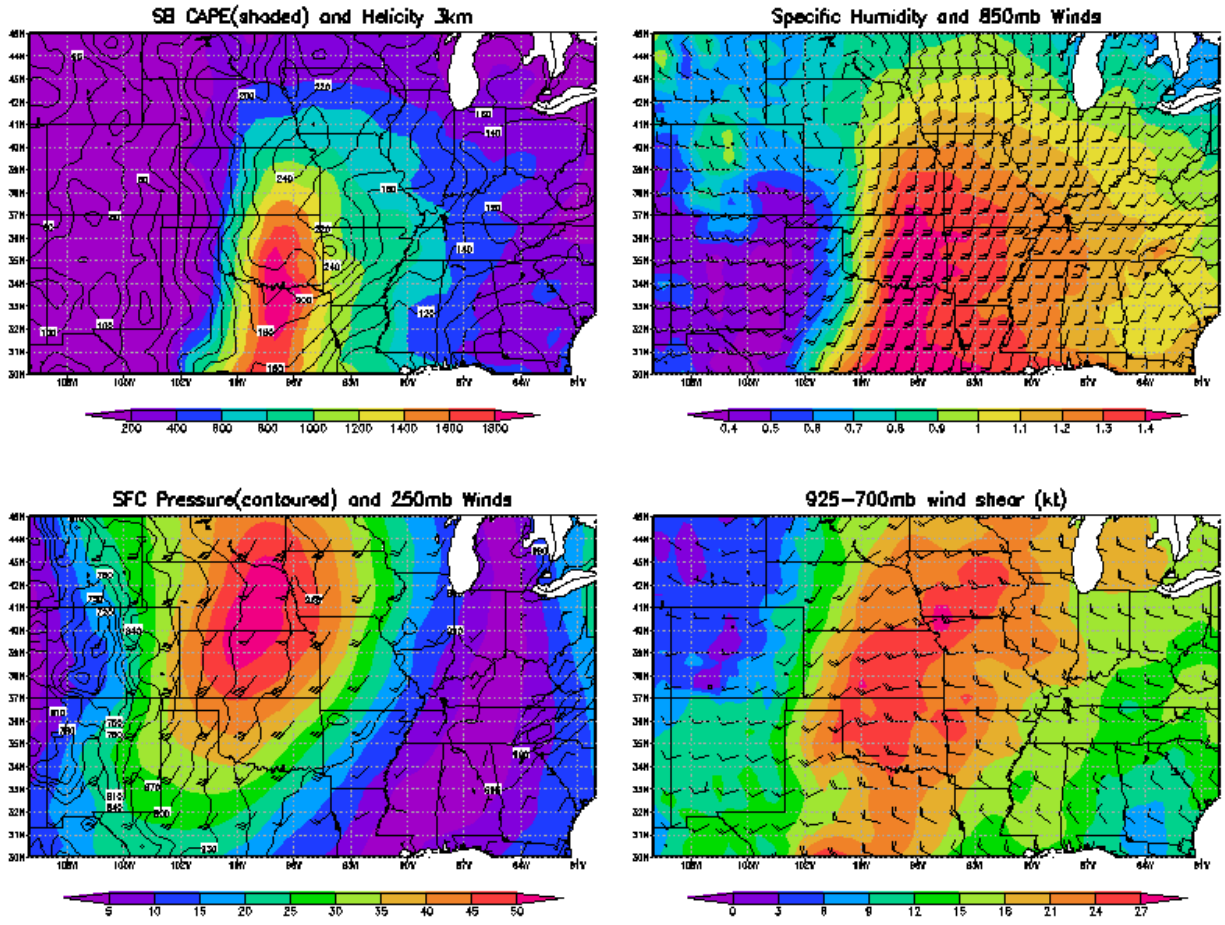

Figure 3.3d: Composite field charts for the K/O region. Upper left - Surface-based CAPE (shaded) and 0-3km helicity (contoured). Upper right - Surface specific humidity (shaded) and 850mb winds (barbed). Bottom left - surface pressure (contoured) and 250 winds (shaded and barbed). Bottom right - 925-700mb wind shear (shaded and barbed).

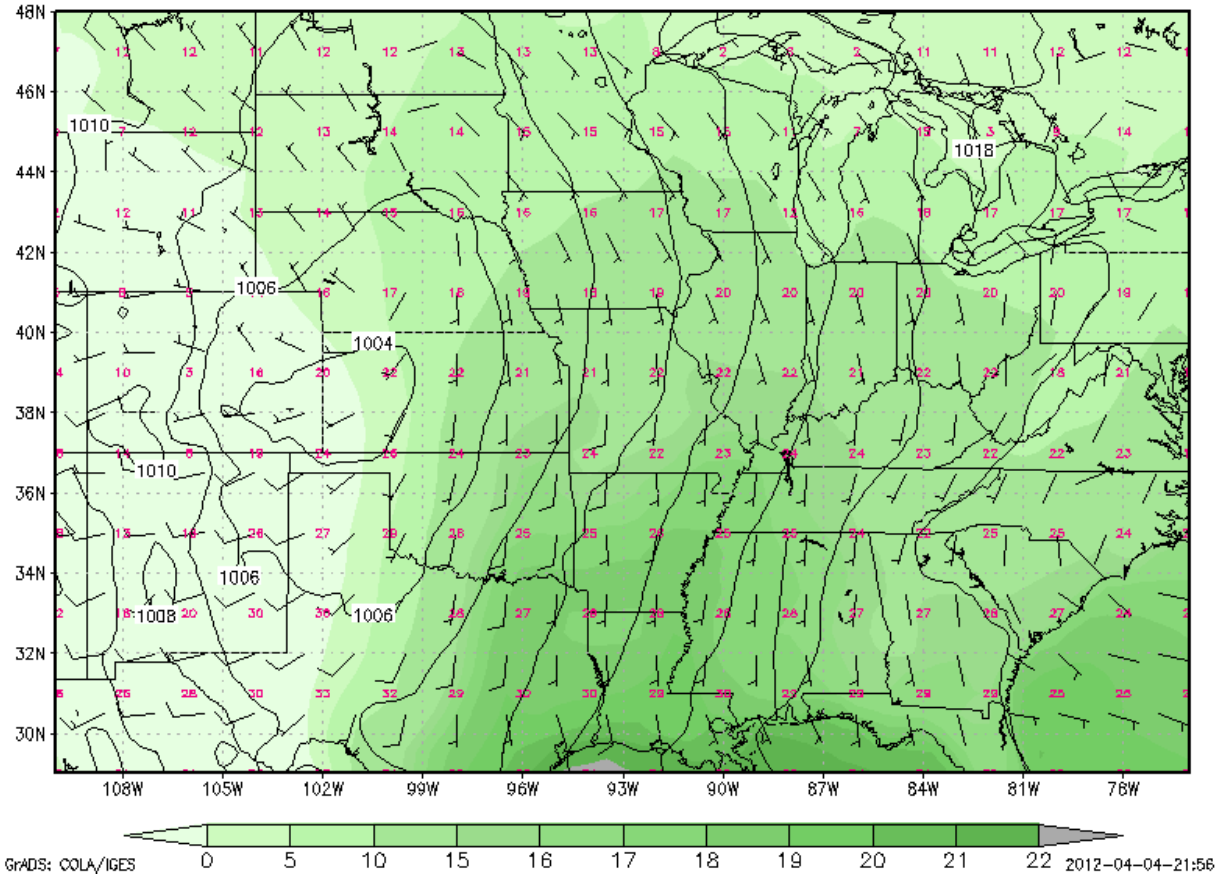

Figure 3.3a: Composite surface analysis chart for severe tornado events within the K/O region. Variables averaged 12 hours prior to (2 time-steps) events. Surface pressure (shaded), 10m above ground winds kt (barbed), surface Temperature Celcius (printed at grid-points in red), surface dewpoint temperature Celcius (shaded).

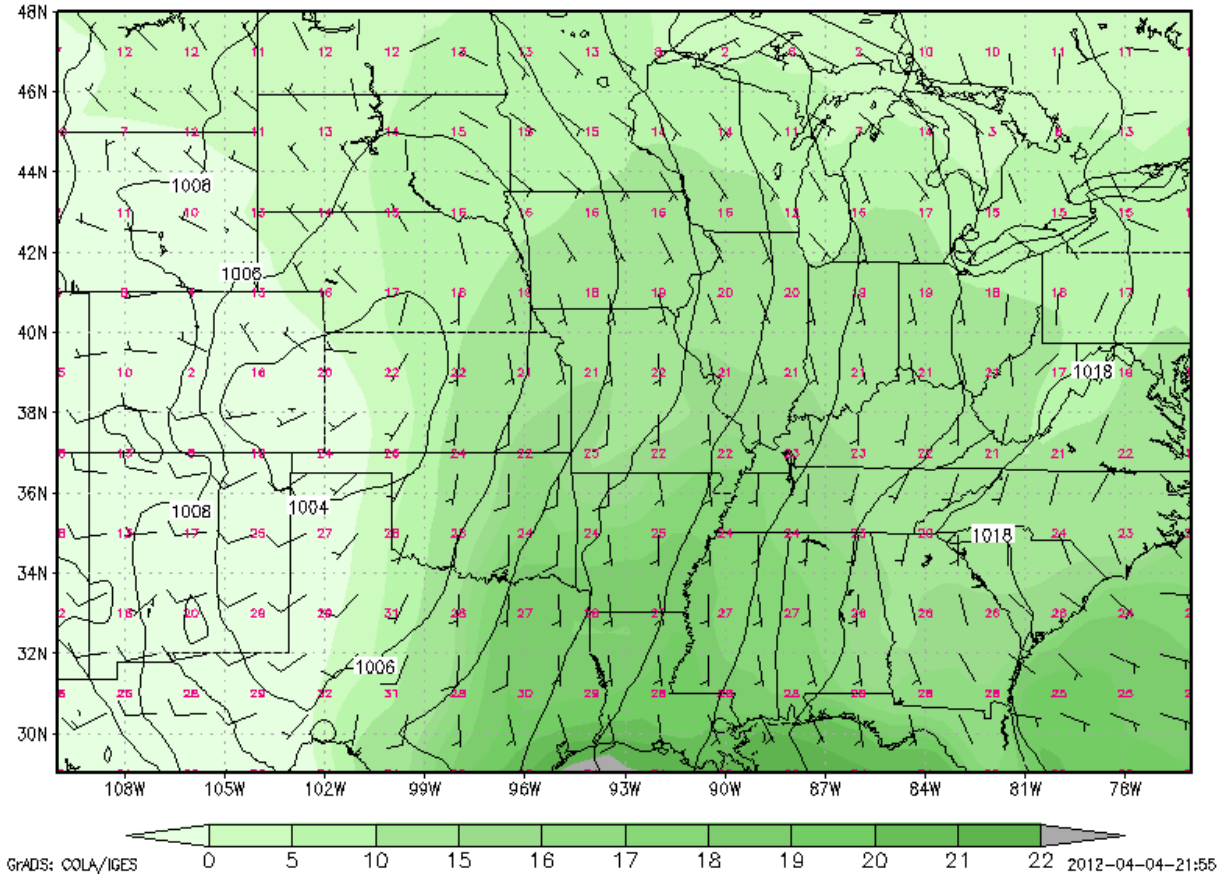

Figure 3.3b: As in 3.3a but variables averaged at 6 hours (1 time-step) before closest synoptic time to event.

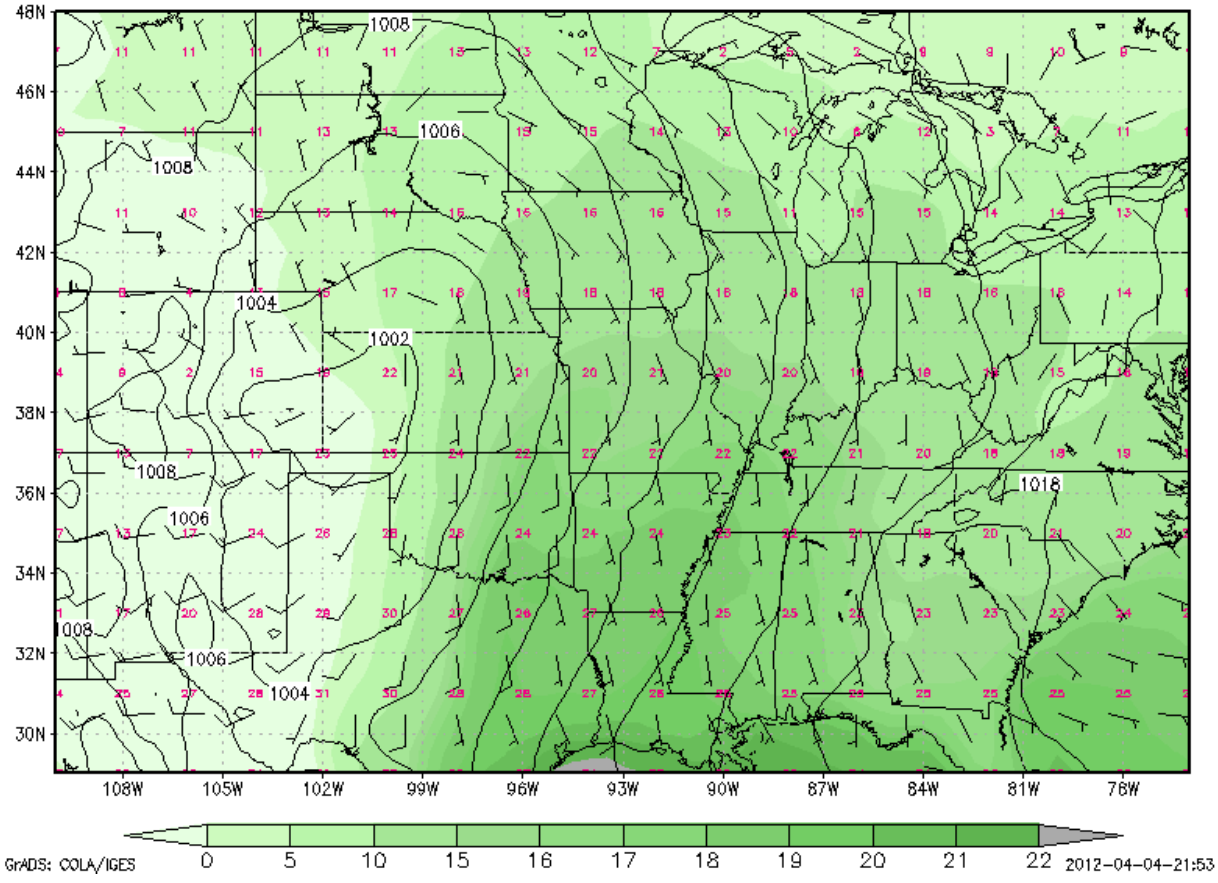

Figure 3.3c: As in 3.3a but variables averaged at closest synoptic time to event.

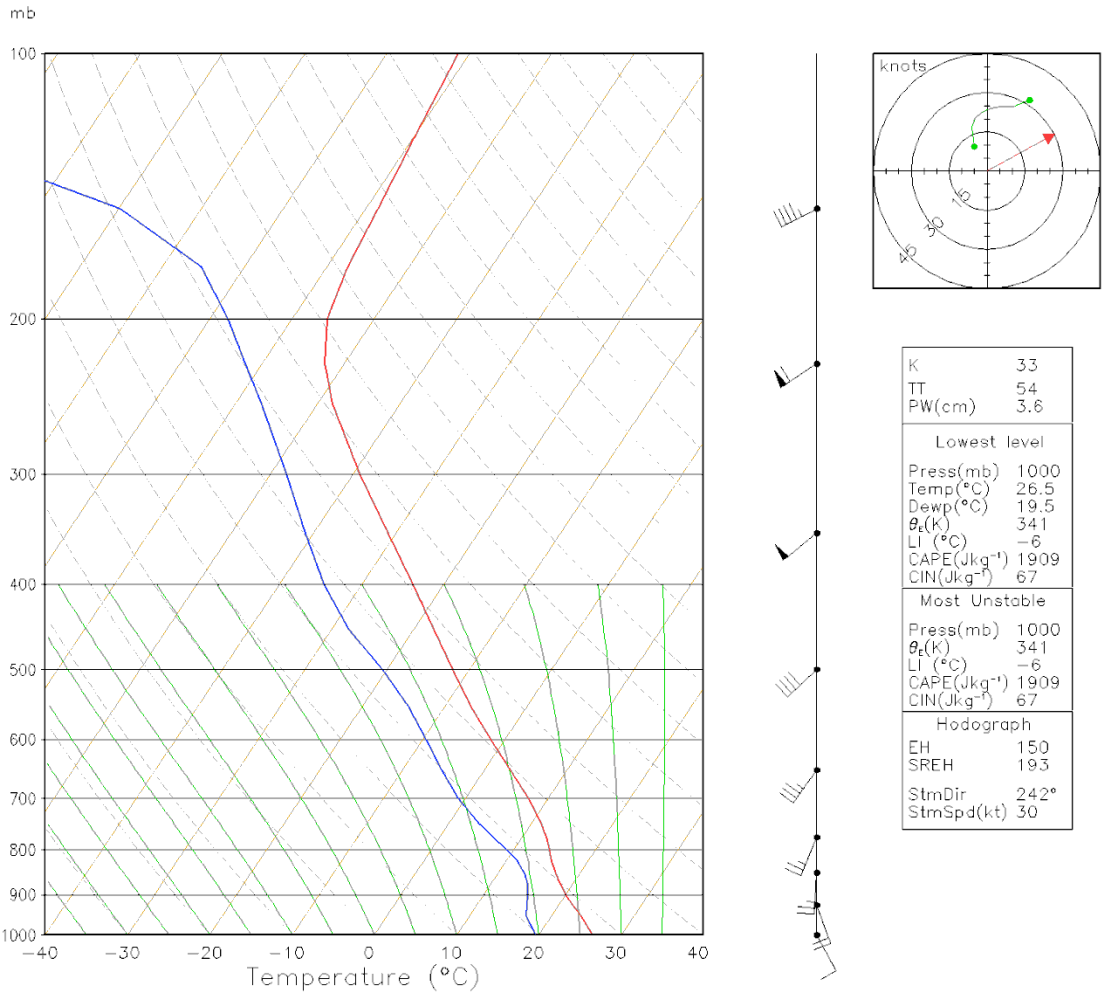

Figure 3.4e: Composite skew-T for the Iowa region; wind profile, hodograph, and skew-T derived parameters to the right of the sounding.

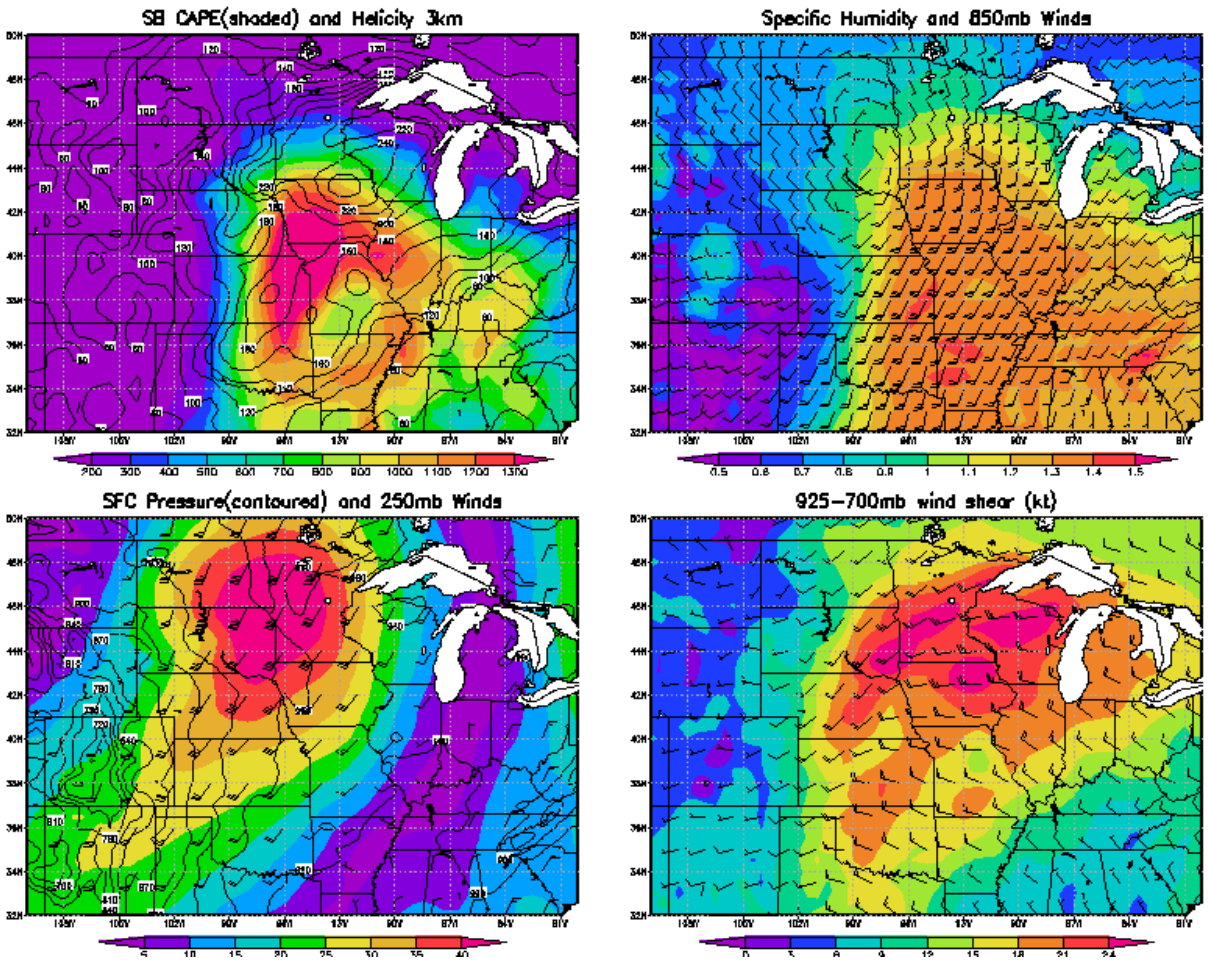

Figure 3.4d: Composite field charts for the Iowa region. Upper left - Surface-based CAPE (shaded) and 0-3km helicity (contoured). Upper right - Surface specific humidity (shaded) and 850mb winds (barbed). Bottom left - surface pressure (contoured) and 250 winds (shaded and barbed). Bottom right - 925-700mb wind shear (shaded and barbed).

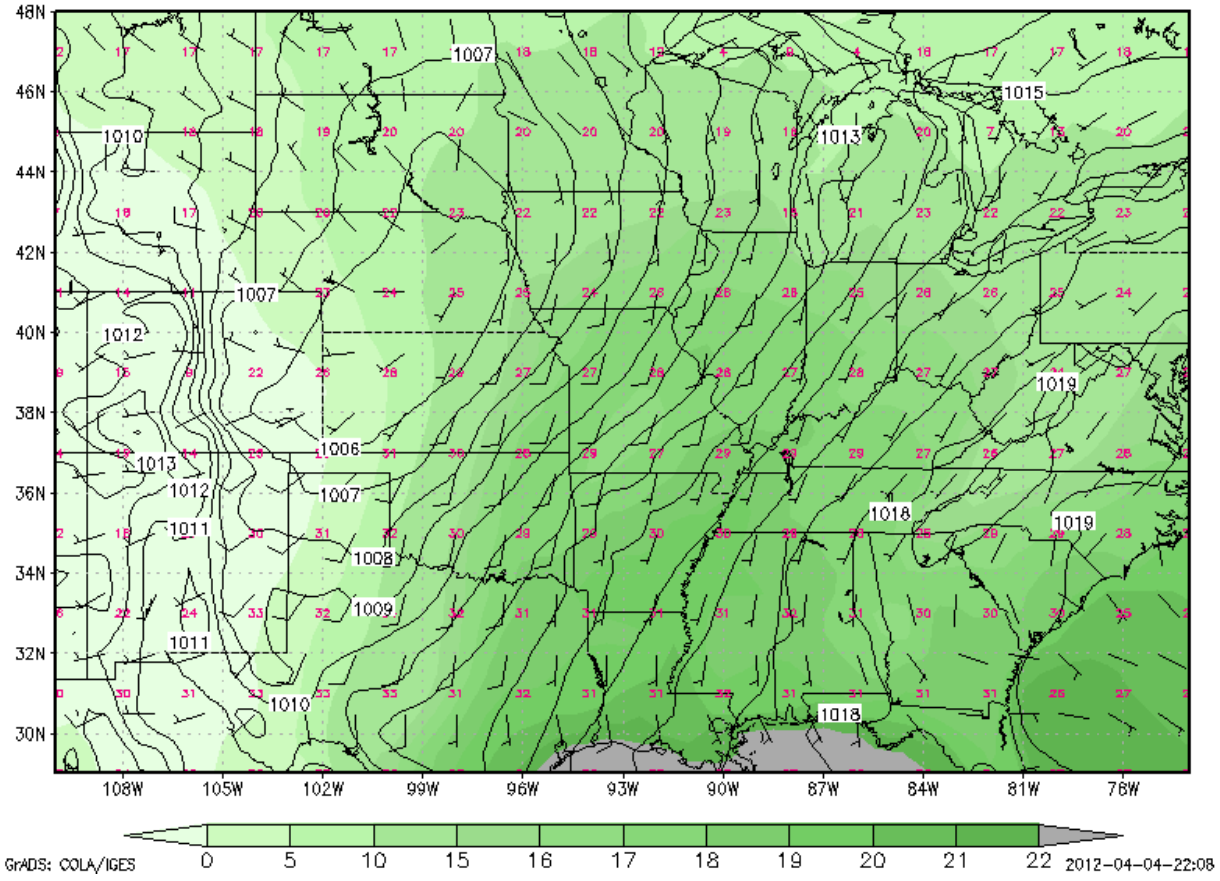

Figure 3.4a: Composite surface analysis chart for severe tornado events within the Iowa region. Variables averaged 12 hours prior to (2 time-steps) events. Surface pressure (shaded), 10m above ground winds kt (barbed), surface Temperature Celcius (printed at grid-points in red), surface dewpoint temperature Celcius (shaded).

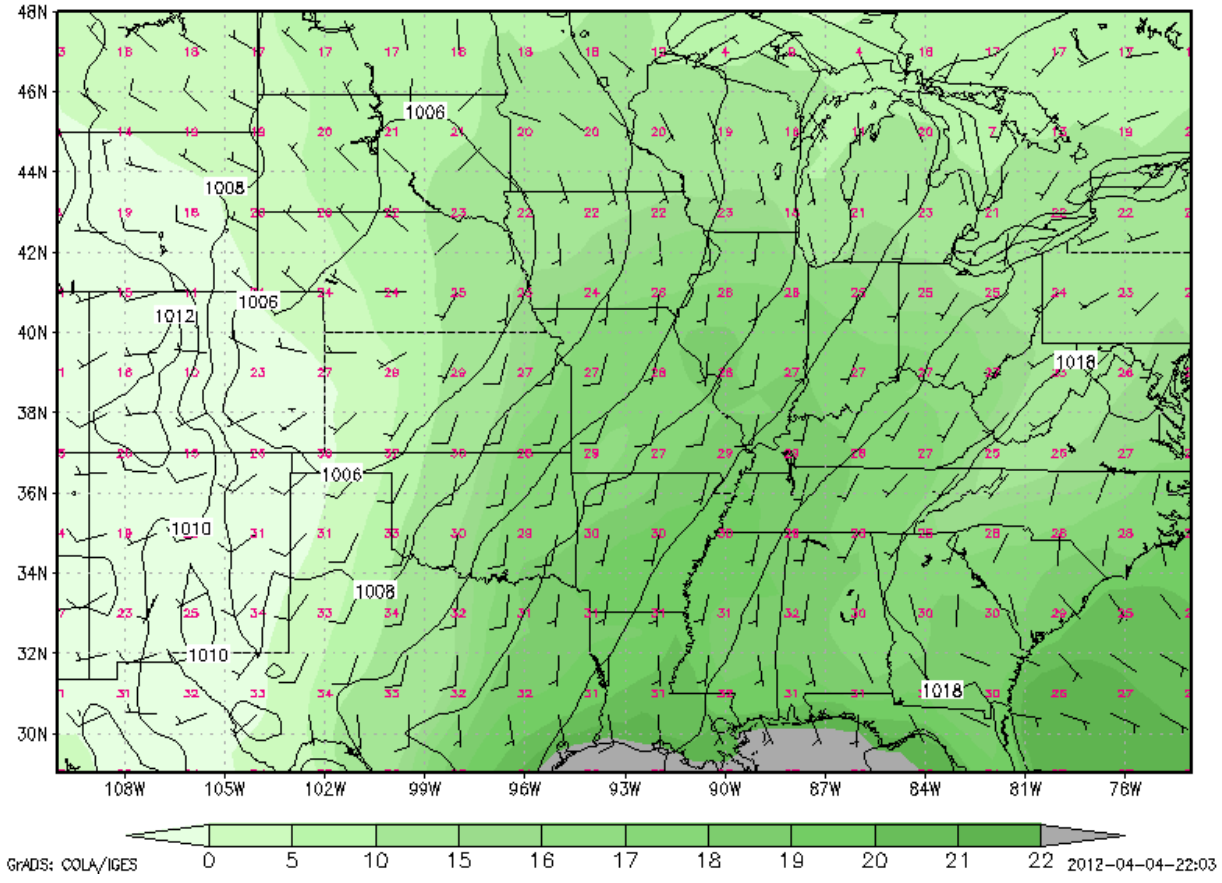

Figure 3.4b: As in 3.4a but variables averaged at 6 hours (1 time-step) before closest synoptic time to event.

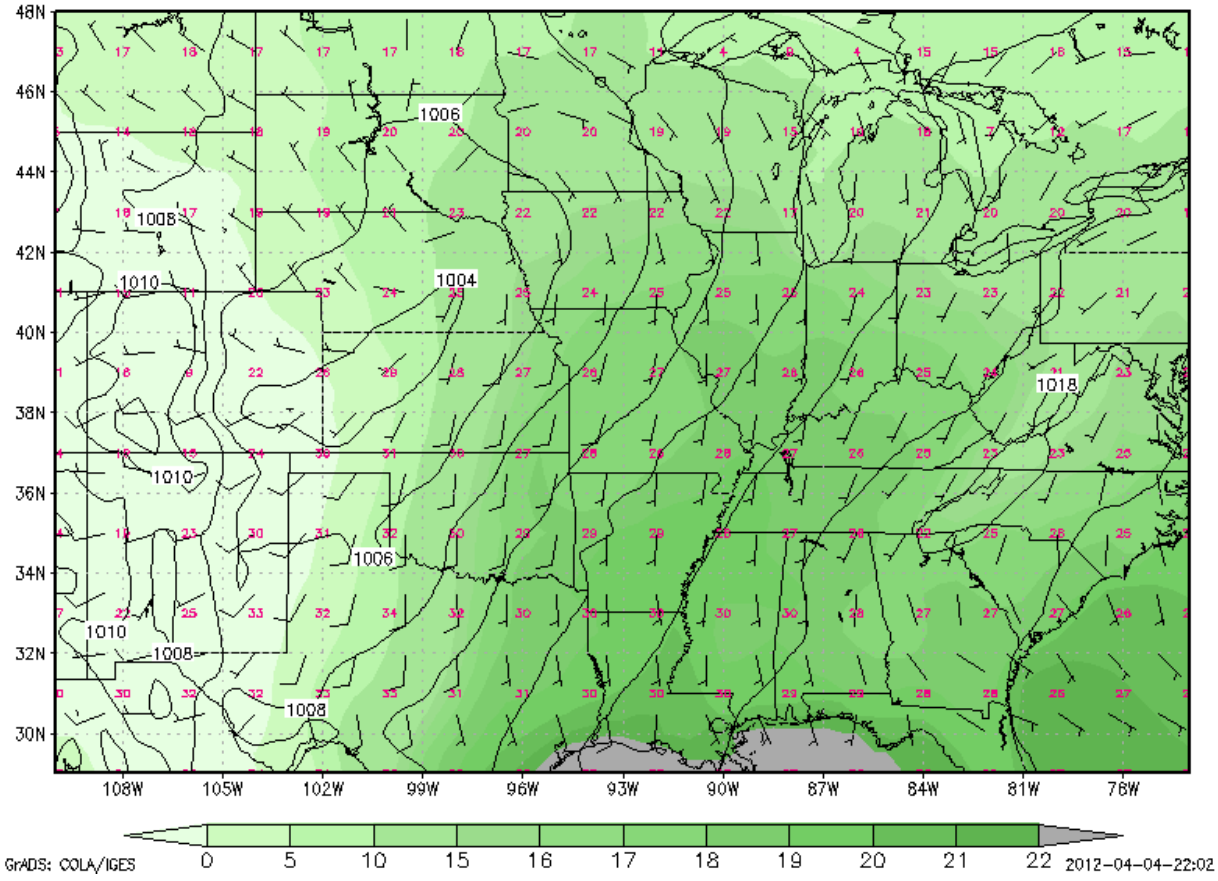

Figure 3.4c: As in 3.4a but variables averaged at closest synoptic time to event.

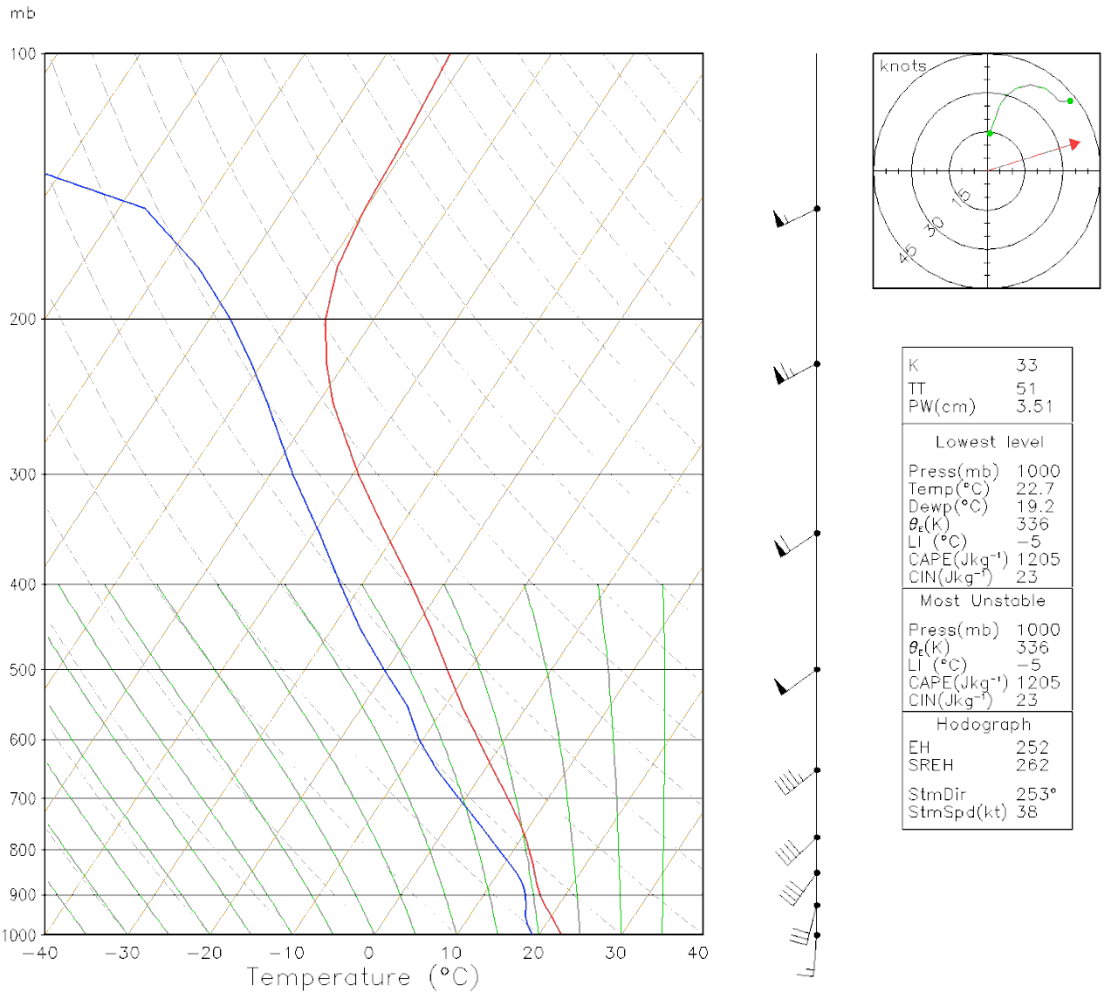

Figure 3.5e: Composite skew-T for the Great Lakes region; wind profile, hodograph, and skew-T derived parameters to the right of the sounding.

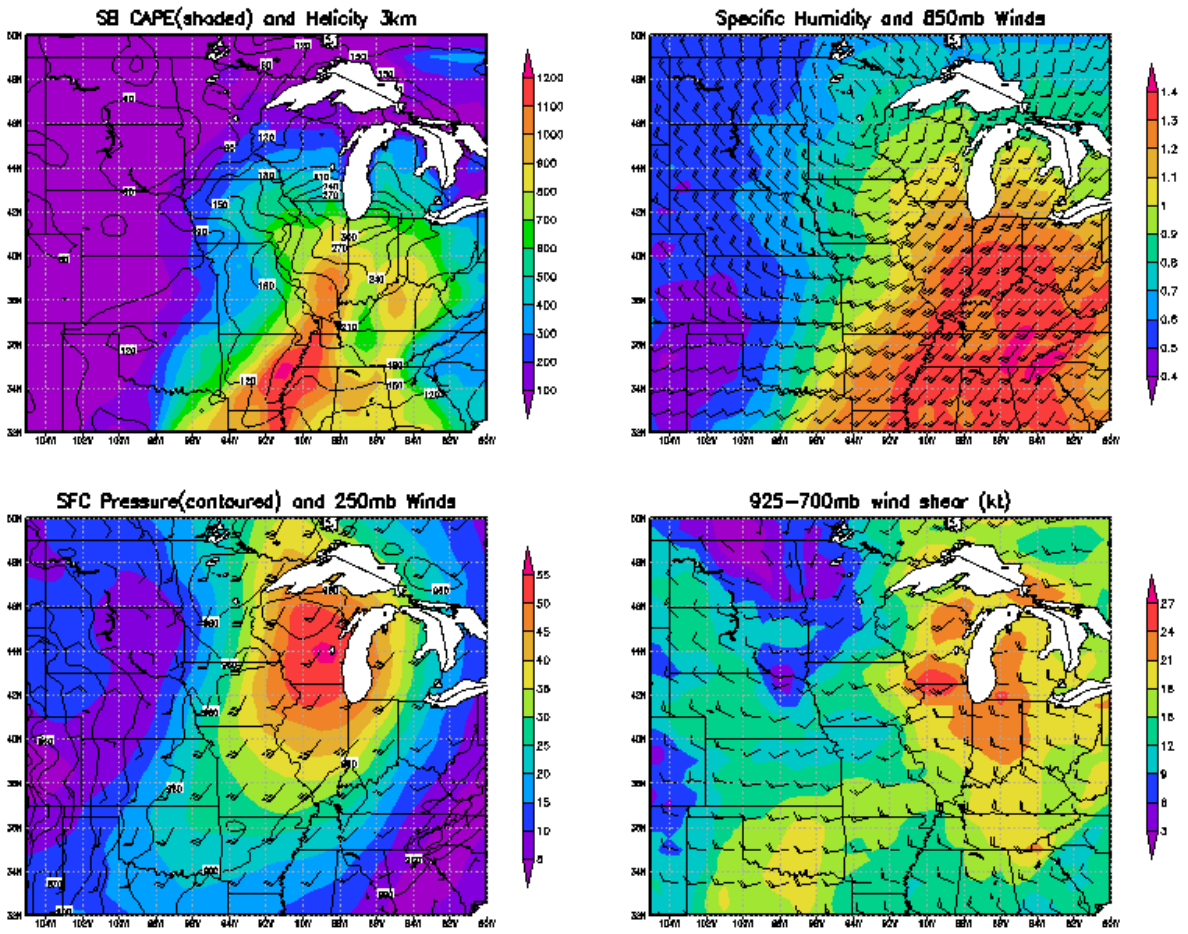

Figure 3.5d: Composite field charts for the Great Lakes region. Upper left - Surface-based CAPE (shaded) and 0-3km helicity (contoured). Upper right - Surface specific humidity (shaded) and 850mb winds (barbed). Bottom left - surface pressure (contoured) and 250 winds (shaded and barbed). Bottom right - 925-700mb wind shear (shaded and barbed).

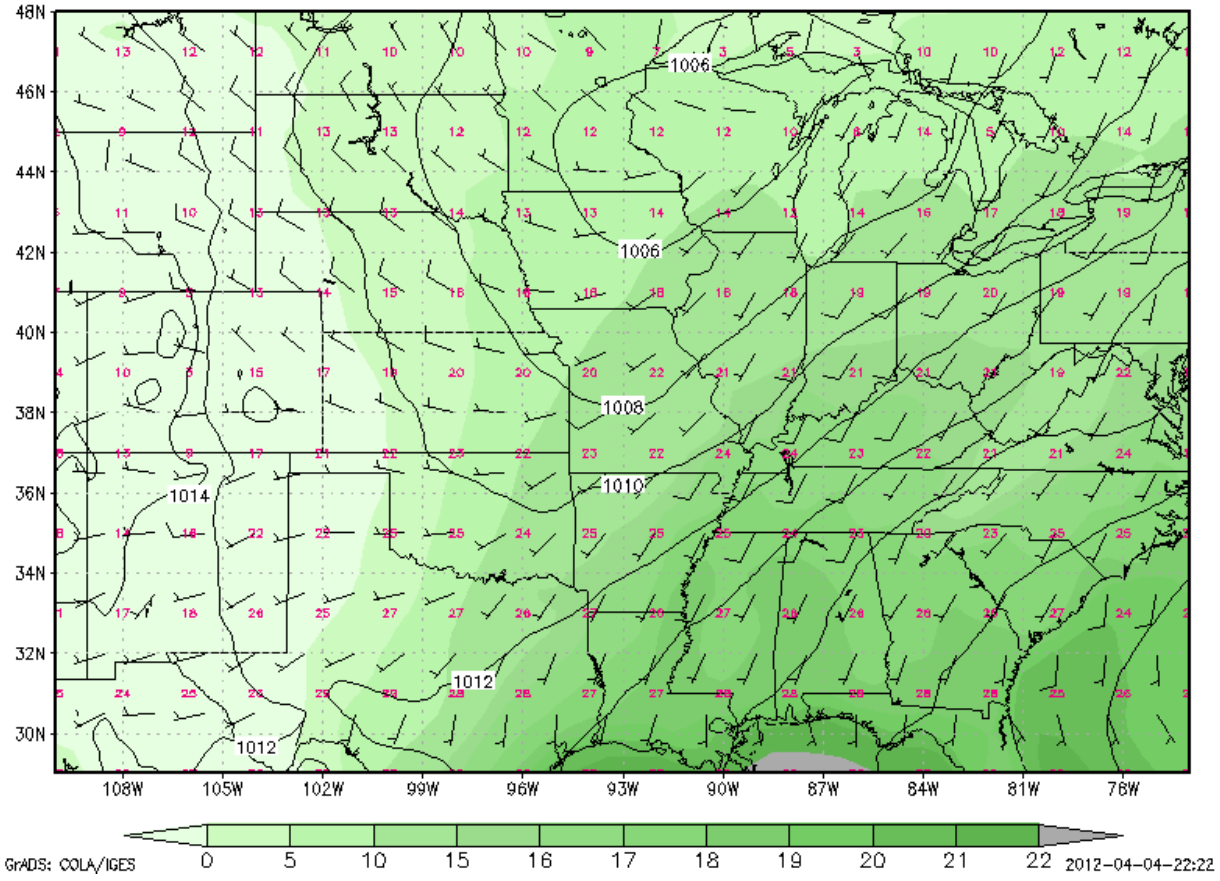

Figure 3.5a: Composite surface analysis chart for severe tornado events within the Great Lakes region. Variables averaged 12 hours prior to (2 time-steps) events. Surface pressure (shaded), 10m above ground winds kt (barbed), surface Temperature Celcius (printed at grid-points in red), surface dewpoint temperature Celcius (shaded).

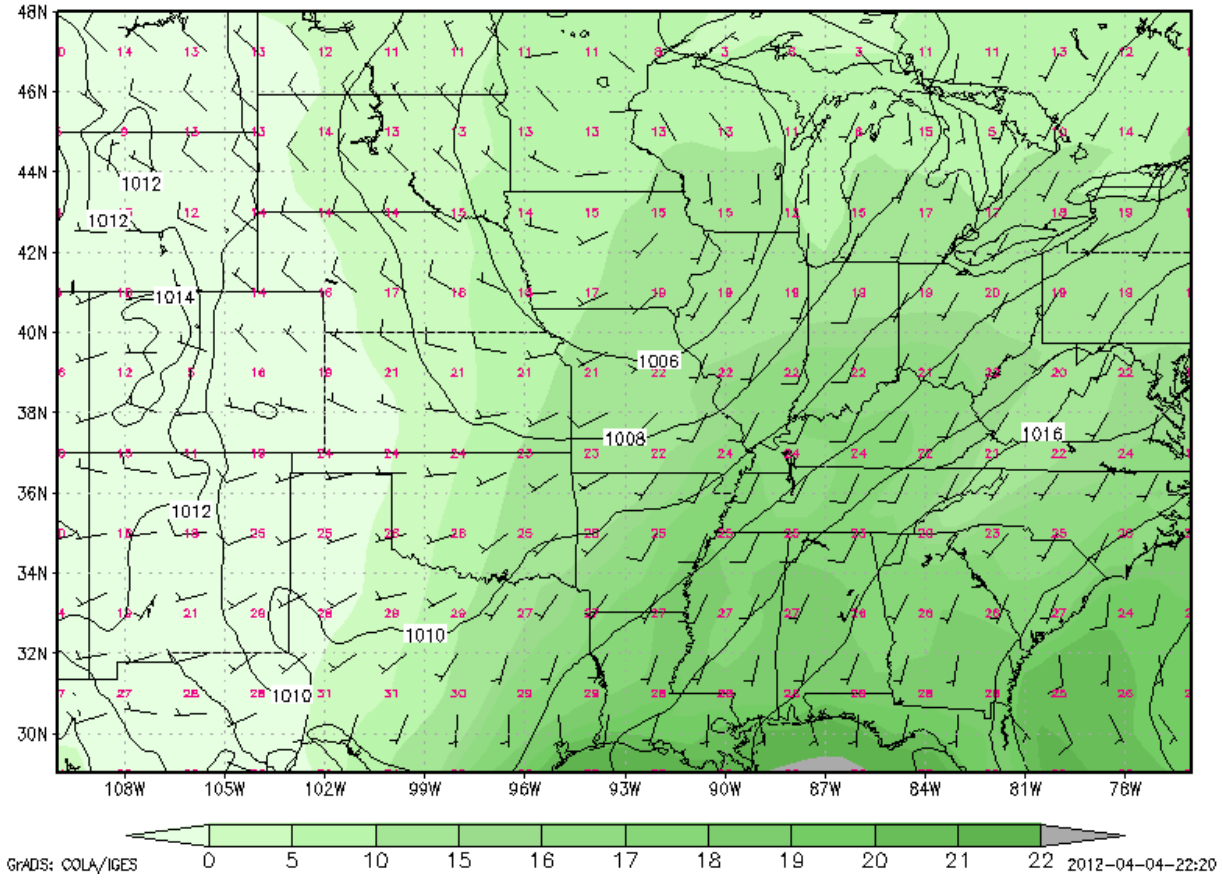

Figure 3.5b: As in 3.5a but variables averaged at 6 hours (1 time-step) before closest synoptic time to event.

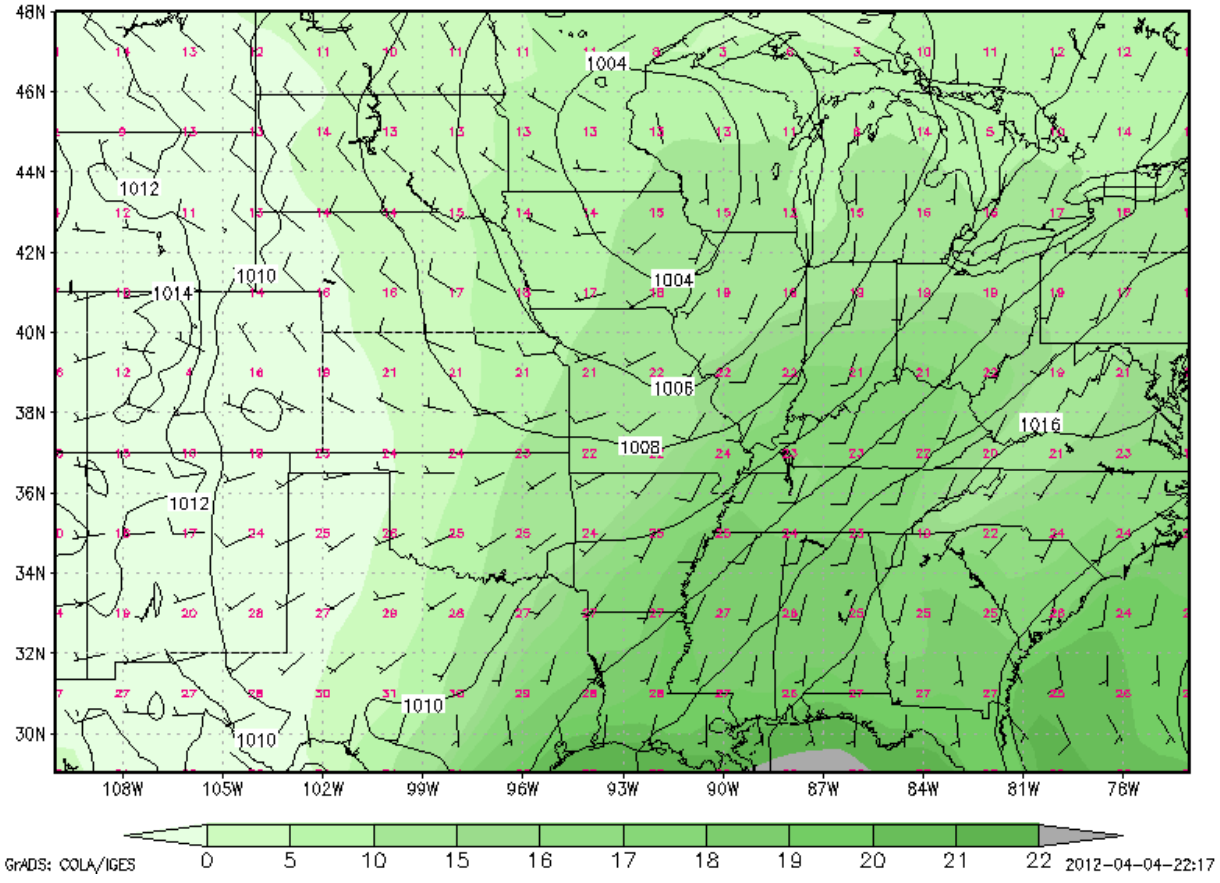

Figure 3.5c: As in 3.5a but variables averaged at closest synoptic time to event.

Thermodynamic Variables	*Piedmont N=48*	*Dixie N=256*	*K/O N=187*	*Iowa N=128*	*Great Lakes N=78*
CAPE (J/kg)					
Mean	*574.1*	*855.6*	*1762.3*	*1412.6*	*1135.6*
Confidence Interval	*420-727*	*776-934*	*1612-1911*	*1230-1594*	*896-1375*
CIN (- J/kg)					
Mean	*38*	*30.5*	*66.6*	*76.8*	*47.3*
Confidence Interval	*54.3-21.7*	*35.7-25.2*	*77.8-55.4*	*93.5-60.1*	*62.2-32.5*
Lapse Rate (K/mb)					
925-850mb Mean	*5.7*	*5.4*	*6.9*	*6.4*	*6.0*
Confidence Interval	*5.25-6.12*	*5.21-5.67*	*6.53-7.28*	*5.88-6.85*	*5.58-6.42*
850-700mb Mean	*5.8*	*5.9*	*6.6*	*6.5*	*6.1*
Confidence Interval	*5.56-6.06*	*5.79-5.97*	*6.34-6.79*	*6.29-6.75*	*5.9-6.38*
925-700mb Mean	*5.8*	*5.7*	*6.7*	*6.5*	*6.1*
Confidence Interval	*5.52-6.03*	*5.64-5.85*	*6.46-6.88*	*6.23-6.72*	*5.58-6.32*
925-500mb Mean	*5.9*	*6.1*	*7.0*	*6.8*	*6.2*
Confidence Interval	*5.77-6.05*	*6.0-6.14*	*6.88-7.14*	*6.64-6.91*	*6.06-6.35*

Table 3.6a: Thermodynamic variables (left column) in each region (top row). Both the mean and confidence interval are shown as calculated from the closest synoptic time preceding tornado events in each region.

Dynamic Variables	*Piedmont*	*Dixie*	*K/O*	*Iowa*	*Great Lakes*
Helicity 0-1km (m^2/s^2)					
Mean	*213*	*261*	*257*	*238*	*228*
Confidence Interval	*182-243*	*246-276*	*237-277*	*212-264*	*205-250*
Vertical Wind Shear (kt)					
925-850mb Mean	*13.2*	*16.2*	*14.9*	*15.0*	*14.6*
Confidence Interval	*11.9-14.6*	*15.4-16.9*	*13.9-15.9*	*13.7-16.3*	*13.1-16.0*
850-700mb Mean	*17.1*	*14.7*	*23.2*	*21.0*	*16.0*
Confidence Interval	*14.2-19.9*	*13.7-15.7*	*21.8-24.6*	*19.35-22.6*	*14.1-17.9*
925-700mb Mean	*25.7*	*26.7*	*32.9*	*30.6*	*28.0*
Confidence Interval	*22.7-28.7*	*25.7-27.8*	*31.4-34.4*	*28.5-32.6*	*25.7-30.2*

Table 3.6b: Dynamic variables (left column) in each region (top row). Both the mean and confidence interval are shown as calculated from the closest synoptic time preceding tornado events in each region.

Moisture Variables	Piedmont	Dixie	K/O	Iowa	Great Lakes
LCL (gpm)					
Mean	465	492	923	686	467
Confidence Interval	438-491	486-497	917-929	676-696	454-479
Specific Humidity (g/kg)					
925mb Mean	12	12	11.9	12	12
Confidence Interval	11.7-12.5	11.8-12.3	11.5-12.2	11.5-12.5	11.5-12.8
850mb Mean	10	10.1	10.4	10.9	10.3
Confidence Interval	9.7-10.5	9.9-10.3	10.0-10.8	10.5-11.4	9.7-10.9
700mb Mean	5.7	5.3	4.9	5.6	5.1
Confidence Interval	5.5-6.2	5.1-5.6	4.6-5.2	5.2-6.0	4.6-5.6
600mb Mean	3.4	2.9	2.5	3.1	2.7
Confidence Interval	2.9-3.8	2.8-3.1	2.3-2.8	2.8-3.4	2.4-3.1

Table 3.6c: Moisture related variables (left column) in each region (top row). Both the mean and confidence interval are shown as calculated from the closest synoptic time preceding tornado events in each region.

Peak Season	Piedmont	Dixie	K/O	Iowa	Great Lakes	U.S.
Peak Season (Julian)						
Mean	136	133	134	136	134	135
Confidence Interval	102-170	119-148	115-153	115-156	106-161	127-142
Days	Apr12-Jun19	Apr29-May28	Apr25-Jun2	Apr25-Jun5	Apr16-Jun10	May7-May22

Table 3.6d: Peak season calculation using the confidence interval procedure for Julian Days. Mean, Confidence Interval, and Days are shown (left column) for each region (top row)

STF	*Piedmont*	*Dixie*	*K/O*	*Iowa*	*Great Lakes*
Mean	*1.51*	*2.51*	*4.36*	*3.60*	*2.83*
Confidence Interval	*.88-2.13*	*2.19-2.82*	*3.74-4.98*	*2.92-4.28*	*2.16-3.49*

Table 3.7a: Mean and confidence interval are calculated for STF parameter values (left column) for each region (top row) from the closest synoptic time preceding tornado events in each region.

STF Peak Season Analysis	**Average**	**Covariance /w/ STF**	**Correlation /w/ STF**
Piedmont			
Cape(J/kg)	.146	.057	.544
BWD(kt)	.992	.020	.100
Helicity (0-1km)	.578	.034	.182
LCL(gpm)	1.41	.002	.156
Dixie			
Cape(J/kg)	.226	.139	.511
BWD(kt)	.990	.064	.173
Helicity (0-1km)	.561	.114	.296
LCL(gpm)	1.42	.005	.229
K/O			
Cape(J/kg)	.244	.295	.635
BWD(kt)	1.29	.114	.179
Helicity (0-1km)	.928	.282	.317
LCL(gpm)	.991	.012	.267
Iowa			
Cape(J/kg)	.101	.128	.675
BWD(kt)	1.26	.034	.082
Helicity (0-1km)	.804	.104	.199
LCL(gpm)	1.23	.005	.173
Great Lakes			

Cape(J/kg)	.135	.125	.619
BWD(kt)	1.13	.029	.077
Helicity (0-1km)	.700	.081	.195
LCL(gpm)	1.44	.004	.156

Table 3.7b: Average, covariance, and correlation with STF value (top row) of the components of STF - CAPE, BWD, Helicity, and LCL - for each region (left column). Values are calculated from every time step over the peak severe tornado season of the U.S. May 7 - May 22 at each grid-point within each respective region.

Event-Specific STF Analysis	**Average**	**Covariance /w/ STF**	**Correlation /w/ STF**
Piedmont			
Cape(J/kg)	.38	.58	.73
BWD(kt)	1.52	.43	.30
Helicity (0-1km)	1.42	1.11	.71
LCL(gpm)	1.53	-.02	-.12
Dixie			
Cape(J/kg)	.57	.79	.71
BWD(kt)	1.60	.36	.31
Helicity (0-1km)	1.74	1.10	.52
LCL(gpm)	1.50	.003	.03
K/O			
Cape(J/kg)	1.17	1.53	.63
BWD(kt)	1.82	.70*	.37
Helicity (0-1km)	1.71	2.42	.74
LCL(gpm)	1.07	.03	.25
Iowa			
Cape(J/kg)	.94	1.90	.69
BWD(kt)	1.72	.56	.24
Helicity (0-1km)	1.58	2.02	.52

LCL(gpm)	1.31	.01	.06
Great Lakes			
Cape(J/kg)	.75	1.57	.78
BWD(kt)	1.65	.45	.23
Helicity (0-1km)	1.52	.59	.31
LCL(gpm)	1.53	-.01	-.06

Table 3.7c: Average, covariance, and correlation with STF value (top row) of the components of STF - CAPE, BWD, Helicity, and LCL - for each region (left column). Values are calculated from the closest synoptic time-step and grid-point to each tornado event within each respective region.

CHAPTER FOUR

DISCUSSION

From the results in chapter 3, there seem to be many similarities and differences among the regions on terms of the pre-tornadic atmosphere. The aim of this chapter is to discuss those differences and some of the potential reasons for them. First, the results from the case composites (composite surface analysis, variable plots, and skew-T) are compared, then a discussion of the statistical analysis results and finally, the STF analysis results discussion. By looking at the composite pre-tornadic atmosphere in each region we are able to determine what similarities and differences exist among the regions at the synoptic and meso-scales.

4.1 Comparison of Case Composite Results

Synoptic composite analysis shows that each region is in some manner different than each other region with respect to the presence of atmospheric variables in pre-tornadic environments. While it is known that conditions for convection and even severe convection can vary geographically, this analysis provides a detailed quantification of atmospheric conditions for 30 years of severe tornadoes. Characterizations of general severe tornadogenesis conditions such as this bring many useful implications for forecasting and furthermore provide a reliable background for future case studies within specific regions.

Composite soundings and field plots show that in general, the Piedmont region and Dixie alley exhibit weaker instability than western regions before severe tornado events. However, these two regions seem to make up for weaker instability by a generally higher moisture content

and vertical wind shear in the lowest levels (surface to 850mb). Discussion of Dixie Alley and the Piedmont region in tandem makes sense due to the similarity of these two regions in geography, forcing mechanisms, and pre-tornadic atmospheric environments. Severe tornado events in both regions are found to occur, in general, ahead of strong cold fronts and furthermore preceded by strong moisture advection along a low-level jet; this jet is likely responsible for some of the vertical wind shear. Interactions with low and upper level jets can combine to aid in severe convection (Uccellini et al. 1979). Upper level dynamics such as divergence and diffluence also seem to be a semi-permanent feature in these regions, as well as proximity to the right entrance region of the 250mb jet streak, causing enhanced vertical motion at the surface. In both regions, the SRH maximum lies well to the north of the CAPE maximum. Examining the position of the severe tornado touchdown locations, it can be discerned that the tornadoes occur in close proximity to either one maximum or the other, leading to the conclusion that very high presence of a certain variable may suffice for severe tornadogenesis without a more balanced mix of severe-indicative variables. Several differences though should also be noted between these two regions: the Piedmont region exhibits the highest vertical wind shear values of all the regions, yet has the lowest CAPE values, while Dixie Alley has relatively much higher CAPE and lower vertical wind shear.

The K/O and Iowa regions share much in common as well. Both regions seem to favor severe tornadogenesis along dryline fronts ahead of cold fronts, which is not surprising given previous studies in these regions. While both regions show the highest instability of all of the regions in terms of both proximity soundings and composite fields, the K/O region is substantially more unstably than the Iowa region. The K/O region is bar far the most thermodynamically unstable with an LI value of -7, steep lapse rates, and relatively high CAPE

values. Also the K/O region shows the strongest upper-level divergence of all the regions and very strong veering with height. Some caveats do exist here though, in that this region also shows the highest LCL, and exhibits more mid-level shear than low-level shear. Both the Iowa and K/O region have composite CAPE and helicity maximums collocated with areas of highest density of tornado occurrence. Also, both the K/O and Iowa regions show close proximity to the right entrance region of jest streaks, indicating enhanced vertical motion in the lower levels.

Primary forcing in the Great Lakes region seems to be isentropic lifting along a warm front boundary, as shown in composite surface analysis. Previous work document tornadogenesis in this region from similar mechanisms and suggests severe tornadoes in this region may occur from isentropic lifting with positive vorticity advection (Jungbluth, 1993). This region shows less presence of thermodynamic variables than the two western regions but more than the two southeastern regions, and vice versa for moisture and helicity values. Severe tornadoes in this region don't show any spatial pattern relevant to positions of either CAPE or helicity maxima. Similar to the other regions, there is strong divergence aloft and close proximity to the right entrance region of an upper level jet streak.

4.2 Comparison of Statistical Results

Statistical analysis of atmospheric variables shows that all of the prescribed regions are significantly different from each other with respect to certain variables in the pre-tornadic atmosphere. Regions geographically closer to each other tend to have overall less significant differences than those further apart. Still, regions as close as Dixie Alley and the Piedmont region show significant differences in dynamic variables in the lowest 850mb of the atmosphere (0-3km helicity and 925-850 vertical wind shear). The Iowa and K/O regions differ significantly

in terms of LCL heights and CAPE. Between these two sets of regions, there are many significant differences in terms of thermodynamic, moisture, and dynamic variables. The southeastern two regions have lower LCL heights, more low-level wind shear, less CAPE and less steep lapse rates than the K/O and Iowa regions. The Great Lakes region can arguably be considered distinct from the greater "tornado alley" area of the two western regions and distinct from the two southeastern regions in terms of CAPE, LCL height, vertical wind shear at certain levels, and lapse rates between certain levels. Specifically, at the 850mb and higher levels, The Great Lakes region is different from the K/O and Iowa regions.

4.3 Discussion of STF Analysis

While the previous section shows that there are significant differences in the presence of atmospheric variables in the pre-tornadic environments in each of these regions, even though severe tornadogenesis is relatively common (when compared to the rest of the U.S), further examination is warranted to include forecast specific application. Finding that a commonly utilized forecast parameter can vary geographically as discussed in chapter 4 has significant implications for forecasting. Understanding exactly how the different components of the STF parameter vary as indicative of severe tornadogenesis is crucial for future studies and said forecasting application. Moreover, these results show that STF is generally a useful tool in forecasting severe tornadoes since it is obviously much larger (and typically greater than 1) for severe tornado events with a relatively small number of false positives.

Among the regions, significant differences at 95% confidence in STF value are shown. The difference between STF values for the two Mid-West regions and the Piedmont region is enormous. It is also important to note that the Piedmont region contains values less than 1 in the

95% CI. Since 1 is the threshold value for STF which is indicative of the potential for severe tornadogenesis, it is concerning that values of STF as low as .88 exist within 95% confidence for the Piedmont region. This suggests that STF cannot be used in the same manner among all the regions in the U.S.

In every region, for the peak season analysis, the CAPE term is the most highly correlated variable with STF values. However, this correlation decreases, and in one region is even surpassed (K/O region with helicity), when examining only severe tornado events. In the Piedmont region, where the LCL term is shown to be generally favorable for severe tornadogenesis (value >=1) for the entire peak season, correlation with the LCL term becomes negative for severe tornado events and correlations of all other variables increase. Specifically, the helicity and CAPE terms greatly increase for severe tornado events in this region, meaning that for severe tornado events, an anomalously high presence of these variables manifests. In Dixie Alley the results are very similar, only with a lesser increase in correlations with the CAPE, BWD, and helicity terms, and a lesser decrease of correlation with the LCL term, which still remains positive. This is not surprising since CAPE, BWD, and helicity are shown in previous chapters to be present in higher magnitudes in Dixie Alley compared to the Piedmont region while the LCL height is lower (more favorable for severe tornadogenesis) in the Piedmont region. Furthermore, these findings are consistent with synoptic analysis in that an approaching cold front coupled with warm moist air advection from the Gulf of Mexico would likely cause an increase in local helicity and CAPE values.

Likewise, the K/O region shows an increase in correlations of the helicity and BWD terms from peak season analysis to the event-specific analysis. Again, it follows that the other two terms, CAPE and LCL are shown to be present and favorable for severe tornadogenesis on

average throughout the peak season, and remain relatively the same. Therefore, severe tornado events in this region are characterized by anomalously high BWD and helicity. The Iowa region follows with similar increases in correlations of BWD and helicity to STF, but of a higher magnitude than in the K/O region. Further, correlation of the LCL term actually decreases. The relationship between these two regions is similar to that of the previous two regions where similar dynamics exist with a generally greater presence of the STF terms in the K/O region. To compare with the synoptic analysis for these regions, specifically the dryline forcing mechanism, it makes sense that CAPE and LCL values remain similarly correlated between total peak season and event specific analysis since the dryline front would not pass until very near the actual time of the event, thus changing CAPE and LCL values later than is considered in the closest synoptic time preceding analysis. Like the other regions, the Great Lakes region shows an increase in correlations from the peak season analysis to the event specific analysis of all terms but LCL which is favorable for severe tornadogenesis on average in the peak season. No discernible connection with the synoptic analysis can be seen from this data alone.

Increases in covariances of terms in the STF equation to the STF values from the peak season analysis to the event-specific analysis support the notion that certain variables become are more indicative of severe tornadogenesis in each region. For example, STF values in the K/O region, while the highest in correlation and covariance with respect to the CAPE term in the peak season analysis, are shown to be most affected by the helicity term. Perhaps the most important finding of these results is that STF values, and each of the terms therein, significantly vary with respect to geography for the small subset of severe tornadoes. Therefore, STF values cannot be understood uniformly across the U.S. in terms of predictability of severe tornadogenesis and

regional biases in presence of tornado-relevant atmospheric variables must be taken into consideration by forecasters.

CHAPTER FIVE

CONCLUSIONS AND FUTURE WORK

Accurately forecasting severe tornadoes remains a great challenge for forecasters despite advances in predictive tools and real-time observable data. More importantly, any increase in forecast skill for these types of events can lead to immediate and permanent decrease in loss of life and property. Toward that goal, the areas of the U.S. which experience the highest density and frequency of severe tornadoes are examined to gain insight into not only what the pre-tornadic environments look like in each region, but to accrue a regional comparison of these conditions. A new metric for defining severe tornado alleys is presented, which uses average f-scale values over a certain area in the U.S. for a 30-year period (1979-2009).

Reanalysis data allows for a close and reasonably accurate look at atmospheric variables spatially and temporally near severe tornado events. Thus, reanalysis data is used in this work, specifically NCEP CFSR, to obtain approximations of pre-tornadic atmospheric conditions. Using reanalysis data as a base, composite skew-Ts, composite field charts, and composite surface analysis are created to elucidate a full picture of what the atmosphere would look like on average preceding a severe tornado event in each region. Further, statistical analysis of tornado relevant atmospheric variables, such as CAPE and helicity, is conducted to establish whether the presence of these variables differ significantly from region to region. Finally, a commonly used tornado forecast parameter, STF, is utilized to connect the results directly with forecasting application. Terms in STF are calculated from reanalysis data for every time-step of the "peak severe tornado season" (as defined using a statistical analysis of Julian days where severe tornadoes occurred) of the U.S. over every grid point within each defined region, and also for

only event-specific times and locations. Correlations and covariances of the terms in STF are calculated from this procedure to illustrate what roles are played by the individual terms of STF between each region and how they change with respect to total peak season analysis to event-specific analysis.

Major findings of this study include illustration of the typical synoptic set-up for severe tornado events with each region, both spatially and vertically. Therein, major forcing mechanisms, synoptic and meso-scale features such as jet streaks, and general presence of atmospheric variables associated with severe tornadogenesis are presented specific to each region and compared. Significant differences at the 95% confidence level of atmospheric variables are documented between regions. It is significant to note that each region is significantly different from each other region with respect to more than one variable at different levels. The most significant differences are shown to be between the two eastern regions and the two western regions. Moreover, analysis of STF within each region as prescribed above yields major differences in how STF is affected by regional biases in the presence of atmospheric variables. Hence, STF values cannot be homogeneously utilized across different regions from a forecasting perspective and these biases must be taken into consideration by forecasters. This work quantitatively outlines those biases by analyzing how the individual terms of STF correlate to STF values within each region. Overall, the STF parameter seems to favor the mid-western regions in terms of predictability of severe tornado events (via higher values).

Following the metric for defining regions, this work could easily be expanded to both severe hail and wind events. Also, where data is available, other regions of high severe tornado occurrence around the globe could be analyzed with the same procedure. This type of analysis could be especially useful in regions where real-time data is more scarce. With global reanalysis

data like CFSR, this type of extension would be a logical next step in developing a complete global severe tornado database. Another possible use of this work is to develop regionally specific tornado forecast parameters. Hopefully, as the tornado database increases over the years, statistics will become more robust, and further relations and differences between regions can be discovered. Finally, studies of future tornado outbreaks over longer time periods can be examined against this work to elucidate the possible existence of climatological trends in severe tornado occurrence.

REFERENCES

Brooks, H. E., and C. A. Doswell III, 2000: Some Aspects of the International Climatology of Tornadoes by Damage Classification. NOAA/National Severe Storms Laboratory Norman, Oklahoma, USA. J. Atm. Res. August, 2000.

------, Charles A. Doswell, Michael P. Kay, 2003a: Climatological Estimates of Local Daily Tornado Probability for the United States. Wea. Forecasting, 18, 626–640.

------, J. W. Lee, and J. P. Craven, 2003b: The Spatial Distribution of Severe Thunderstorm and Tornado Environments from Global Reanalysis Data. Atmos. Res., 67–68, 73–94.

------, 2009: Proximity Soundings For Severe Convection For Europe and the United States From Reanalysis Data. Atmos. Res., 93, 546–553.

Broyles, C. and C. Crosbie, 2004: Evidence of Smaller Tornado Alleys Across the United States Based on Long-Track F3 to F5 Tornado Climatology Study from 1880 to 2003. 22nd Conference on Severe Local Storms, 2004

Concannon, P.R., H.E. Brooks and C.A. Doswell III, 2000: Climatological Risk of Strong and Violent Tornadoes in the United States. Preprints, 2nd Conf. Environ. Applications, Amer. Meteor. Soc., Long Beach, CA.

Craven, J.P., 2001: A Baseline Climatology of Sounding Derived Parameters Associated With Deep, Moist Convection. Unpublished manuscript. 56 pp. [Available from Storm Prediction Center, 1313 Halley Circle Norman, OK 73069 U.S.A.].

------, Brooks, H.E., Hart, J.A., 2002. Baseline Climatology of Sounding Derived Parameters Associated With Deep, Moist Convection. Preprints, 21st Conference on Severe Local Storms, San Antonio, Texas, USA, Amer. Meteorol. Soc., pp. 643 – 646.

David, C. L., 1976: A Study of Upper Air Parameters at the Time of Tornadoes. Mon. Wea. Rev., 104, 546–551.

Davies-Jones, R., R. J. Trapp, and H. B. Bluestein, 2001: Tornadoes and Tornadic Storms. Severe Convective Storms, Meteor. Monogr., No. 50, Amer. Meteor. Soc., 167–222.

Doswell, C. A. III, and D. W. Burgess, 1988: On Some Issues of United States Tornado Climatology. Mon. Wea. Rev., 116, 495–501.

Dotzek, N., 2000: Tornadoes in Germany. Atmos. Res.

Edwards, R., J. A. Hart, K. L. Elmore, and P. Markowski, 2003: Close Proximity Soundings Within Supercell Environments Obtained from the Rapid Update Cycle. Wea. Forecasting, 18, 1243–1261.

Feuerstein, Bernold, Nikolai Dotzek, Jürgen Grieser, 2005: Assessing a Tornado Climatology from Global Tornado Intensity Distributions. J. Climate, 18, 585–596.

Gensini, V. A., and H. E. Brooks, 2008: Regional Variability of CAPE and Deep Shear from the NCEP/NCAR Reanalysis. Presented, 12th Annual Severe Storms and Doppler Radar Conference, Des Moines, IA, Central Iowa Chapter of the National Weather Association.

Grams, Jeremy S., Richard L. Thompson, Darren V. Snively, Jayson A. Prentice, Gina M. Hodges, Larissa J. Reames, 2012: A Climatology and Comparison of Parameters for Significant Tornado Events in the United States. Wea. Forecasting, 27, 106–123.

Grazulis, T.P. 1993: Significant Tornadoes 1880 – 1991. St. Johnsbury, VT: Environmental Films.

Hart, J. A., and W. Korotky, 1991: The SHARP workstation v1.50 users guide. National Weather Service, 30 pp. [Available from NWS Eastern Region Headquarters, 630 Johnson Ave., Bohemia, NY 11716.]

Higgins, R. W., V. E. Kousky, V. B. S. Silva, E. Becker, P. Xie, 2010: Intercomparison of Daily Precipitation Statistics over the United States in Observations and in NCEP Reanalysis Products. J. Climate, 23, 4637–4650.

Johns, R. H., J. M. Davies, and P. W. Leftwich, 1993: Some Wind and Instability Parameters Associated With Strong and Violent Tornadoes. Part II: Variations in the Combinations of Wind and Instability Parameters. The Tornado: Its Structure, Dynamics, Prediction, and Hazards, Geophys. Monogr., No. 79, Amer. Geophys. Union, 583–590.

Kelly, D. L., J. T. Schaefer, R. P. McNulty, C. A. Doswell, R. F. Abbey, 1978: An Augmented Tornado Climatology. Mon. Wea. Rev., 106, 1172–1183.

Klemp, J. B., R. B. Wilhelmson, P. S. Ray, 1981: Observed and Numerically Simulated Structure of a Mature Supercell Thunderstorm. Journal of the Atmospheric Sciences, 38, 1558-1580

Kounkou, R., G. Mills, and B. Timbal, 2009: A Reanalysis Climatology of Cool-Season Tornado Environments over Southern Australia. International Journal of Climatology. V29, pp.2079-2090.

Lee, J.W., 2002. Tornado Proximity Soundings from the NCEP/NCAR Reanalysis Data. MS Thesis, University of Oklahoma.

Lemon, L. R., and C. A. Doswell III, 1979: Severe Thunderstorm Evolution and Mesocyclone Structure as Related to Tornadogenesis. Mon. Wea. Rev., 107, 1184–1197.

Lileo, S. and O. Petrik, 2010: Investigation on the Use Of NCEP/NCAR, MERRA and NCEP/CFSR Reanalysis Data in Wind Resource Analysis. EWEC Proceedings.

McDonald, JR, 2001: T. Theodore Fujita: His Contribution to Tornado Knowledge through Damage Documentation and the Fujita Scale. Bull. Amer. Meteor. Soc., 82, 63–72.

Markowski, Paul M., Erik N. Rasmussen, Jerry M. Straka, 1998: The Occurrence of Tornadoes in Supercells Interacting with Boundaries during VORTEX-95. Wea. Forecasting, 13, 852–859.

------, and Y.P. Richardson, 2009: Tornadogenesis: Our Current Understanding, Forecasting Considerations, and Questions to Guide Future Research. Atmos. Res., 93, 3–10.

National Climate Data Center (NCDC), 2001: The Fujita Tornado Scale. NOAA, Asheville, NC. http://www.ncdc.noaa.gov/ol/satellite/satelliteseye/educational/fujita.html (accessed 7/25/02).

National Weather Service: A Recommendation for an Enhanced Fujita Scale (EF-Scale) Submitted to The National Weather Service and Other Interested Users October 10, 2006 Revision 2 Wind Science And Enginering Center Texas Tech University Lubbock, Texas 79409.

Passe-Smith, M., 2006: Exploring Local Tornado Alleys for Predictive Environmental Parameters. Department of Geography University of Central Arkansas. ESRI Conference Proceedings.

Potvin, C. K., K. L. Elmore, and S. J. Weiss, 2010: Assessing the Impacts of Proximity Sounding Criteria on the Climatology of Significant Tornado Environments. Wea. Forecasting, 25, 921–930.

Rasmussen, E.N., and D. O. Blanchard, 1998: A Baseline Climatology of Sounding-Derived Supercell and Tornado Forecast Parameters. Wea. Forecasting, 13, 1148–1164.

------, 2003: Refined Supercell and Tornado Forecast Parameters. Wea. Forecasting, 18, 530–535.

Romero, R., Gaya, M., and C. A. Doswell III 2005: European Climatology of Severe Convective Storm Environmental Parameters: A Test for Significant Tornado Events. J. Atm. Res. v.83 389-404.

Saha, S., et al. 2010: The NCEP Climate Forecast System Reanalysis, Bull. Am. Meteorol. Soc., 91(8), 1015–1057, doi:10. 1175/2010BAMS3001.1.

Schaefer, J. T., and R. Livingston, 1988: The Typical Structure of Tornado Proximity Soundings. Journal of Geophysical Research, Vol. 93, No. d5, pp. 5351-5364.

------ and R. Edwards, 1999: The SPC Tornado/Severe Thunderstorm Database. Preprints, 11th Conf. on Applied Climatology, Dallas, TX, Amer. Meteor. Soc., 603–606.

Thompson, R.L., R. Edwards and J.A. Hart, 2002: Evaluation and Interpretation of the Supercell Composite and Significant Tornado Parameters at the Storm Prediction Center. Preprints, 21st Conf. Severe Local Storms, San Antonio TX.

------, Roger Edwards, John A. Hart, Kimberly L. Elmore, Paul Markowski, 2003: Close Proximity Soundings within Supercell Environments Obtained from the Rapid Update Cycle. Wea. Forecasting, 18, 1243–1261.

Tippett, M. K., Sobel, A. H., and S. J. Camargo, 2012: Association of U.S. tornado occurrence with monthly environmental parameters. Geophysical Research Letters, Vol. 39, L02801, 6 PP.

Wakimoto, Roger M., James W. Wilson, 1989: Non-supercell Tornadoes. Mon. Wea. Rev., 117, 1113–1140.

Wicker, Louis J., Robert B. Wilhelmson, 1995: Simulation and Analysis of Tornado Development and Decay within a Three-Dimensional Supercell Thunderstorm. Journal of the Atmospheric Sciences, 52, 2675-2703

Williams, R. J., Surface Parameters Associated with Tornadoes. Mon. Wea. Rev., 104, 540–545 1976.

BIOGRAPHICAL SKETCH

Grayum Michael Vickers was born in Tampa on April 17th, 1988 to D. Grayum Vickers and Laura Vickers. It was in Tampa that he grew up with older brother James W. Vickers. Grayum graduated from Hillsborough High School in 2006 with a International Baccalaureate Diploma and afterwards attended Florida State University and earned a BS in Meteorology. Thereafter Grayum began working on his Masters of Science in Meteorology with Drs. Hart and Chassignet at COAPS. Grayum enjoys playing music and has put out several studio albums with multiple acts and has toured internationally. Currently, Grayum lives in Brooklyn, New York and teaches high school level Earth Science as a New York City Teaching Fellow.